

# ABSTRACT

Title of Dissertation:      COHERENT DYNAMICS IN ATOM-FIELD  
INTERACTIONS

Sanjiv Shresta, Doctor of Philosophy, 2003

Dissertation directed by:   Professor Bei-Lok Hu  
Department of Physics

This dissertation treats quantum open system dynamics, focusing on the coherent evolution of a two-level atom (as the system) interacting with an electromagnetic field (as the bath), for purposes relevant to quantum computing. In order to maintain the quantum correlations that develop between the system and bath throughout the evolution path integral formalisms such as the influence functional and closed time path formalisms are used. Predictions of effects due to the quantum correlations in the composite interacting system are computed.

Conventional treatments using Schrödinger-master equation and Heisenberg-Langevin approaches usually ignore system+bath quantum correlations as a technical simplification. It is argued that although neglect of system+bath correlations is generally a good approximation when the bath has a large continuous set of degrees of freedom, a residual coherence effect remains due to the non-zero bath correlation time. Though small, these effects are

becoming more relevant as, with the advent of ultra cold atom sources, atom optics experiments are reaching levels at which such residual effects are becoming measurable.

Three specific problems are investigated in this thesis: First is a self-dressing rederivation of the Casimir-Polder retardation force. The well known stationary atom result is reproduced and a result for a slowly moving atom is obtained which is up to twice the stationary atom correction. Second is the entangled evolution of a qubit with an *initially* thermal low temperature bath. The diagonal matrix elements are found to thermalize and the off-diagonal elements to decohere as expected, however they do so non-exponentially due to the quantum correlations that develop between the qubit and bath. Third is a calculation of qubit dynamics in the presence of quantized atomic motion as well as zero point fluctuations of the electromagnetic field. The decoherence rate of the qubit is found to increase slightly in that case due to the additional degree of freedom.

COHERENT DYNAMICS IN ATOM-FIELD  
INTERACTIONS

by

Sanjiv Shresta

Dissertation submitted to the Faculty of the Graduate School of the  
University of Maryland, College Park in partial fulfillment  
of the requirements for the degree of  
Doctor of Philosophy  
2003

Advisory Committee:

Professor Bei-Lok Hu, Chair  
Professor Wendell T. Hill, III  
Professor Steven L. Rolston  
Dr. Carl J. Williams  
Professor Victor M. Yakovenko

© Copyright by

Sanjiv Shresta

2003

## DEDICATION

I dedicate this work to my parents.

## ACKNOWLEDGMENTS

In the graduate studies which have led me to the completion of this dissertation I have received valuable assistance from many sources. That includes stimulating discussions with my collaborators Charis Anastopoulos, Adrian Dragulescu, and Nicholas Phillips, and morale support from family and friends, among whom I would especially like to acknowledge Lubna Rana, Sabina Khadka, and Projjwal Khadka. Most of all, I acknowledge and thank my thesis advisor, Bei-Lok Hu, without whose guidance the work in this dissertation would not exist. His example of how to be a physicist has been, and continues to be, a model for me to follow.

# TABLE OF CONTENTS

List of Figures	viii
List of Abbreviations	ix
1 Introduction	1
1.1 Summary of Research . . . . .	3
1.1.1 Casimir-Polder retardation force . . . . .	3
1.1.2 Qubit in an initially thermal bath . . . . .	7
1.1.3 Qubit with quantized center of mass motion . . . . .	9
1.2 Organization of Dissertation . . . . .	12
2 Review of open system dynamics	13
2.1 Review of Schrödinger-master equation approach . . . . .	16
2.1.1 Fixed bath assumption . . . . .	19
2.1.2 Coarse graining approximation . . . . .	24
2.2 Review of Heisenberg-Langevin approach . . . . .	26
2.3 Review of influence functional approach . . . . .	32
2.3.1 General overview . . . . .	33

2.3.2	Coherent state path integrals . . . . .	38
2.3.2.1	coherent state representation . . . . .	38
2.3.2.2	Evaluation of Grassmann path integrals . . . . .	41
3	Casimir-Polder Retardation Force	46
3.1	Model and Approach . . . . .	49
3.1.1	Hamiltonian . . . . .	50
3.1.2	Transition amplitude . . . . .	52
3.1.3	Momentum expectation and force . . . . .	54
3.2	Results . . . . .	56
3.2.1	Stationary atom . . . . .	56
3.2.2	Adiabatic motion . . . . .	60
3.2.2.1	Adiabatic evaluation . . . . .	60
3.2.2.2	Force and potential . . . . .	65
3.3	Discussion . . . . .	66
3.3.1	Physical interpretation . . . . .	66
3.3.1.1	Stationary atom . . . . .	68
3.3.1.2	Moving atom . . . . .	69
3.3.2	Prospects for experimental observation . . . . .	70
3.3.2.1	Reflection from an evanescent laser . . . . .	70
3.3.2.2	Transmission between parallel plates . . . . .	71
3.3.3	Conclusion . . . . .	72

4	Thermal Bath	73
4.1	Model and Approach . . . . .	75
4.1.1	Hamiltonian . . . . .	75
4.1.2	Transition amplitude . . . . .	77
4.1.3	Reduced propagator . . . . .	81
4.2	Results . . . . .	81
4.2.1	Low temperature . . . . .	82
4.2.2	Zero temperature limit . . . . .	83
4.3	Discussion . . . . .	84
4.3.1	Decoherence . . . . .	84
4.3.2	Relaxation . . . . .	85
5	Motional Decoherence	88
5.1	Transition amplitude . . . . .	92
5.1.1	EMF path integral . . . . .	96
5.1.2	COM path integral . . . . .	96
5.1.3	Qubit path integral . . . . .	98
5.2	Evolutionary operator . . . . .	100
5.3	Discussion . . . . .	104
6	Discussion	106
A	Simple examples of Grassmann path integrals	113

A.1	Spin- $\frac{1}{2}$ in a general time-dependent classical magnetic field . . . . .	113
A.2	Single mode Jaynes-Cummings . . . . .	118
B	Recursive calculation of effective action	125
C	Momentum computation	131
D	Calculational details of qubit in a thermal bath	136
D.1	Approximated functional solutions . . . . .	136
D.2	Computation of density matrix elements . . . . .	139
E	COM functional integration	142
	Bibliography	144

# LIST OF FIGURES

3.1	Transient behavior in the atom-wall force at a fixed distance. . . . .	57
3.2	Snapshot of the transient behavior in the atom-wall force at a fixed time. . . . .	58
4.1	Decoherence rate of a qubit in a low temperature bath. . . . .	86
4.2	Relaxation of a qubit in a low temperature bath . . . . .	87
5.1	Decoherence rate of a qubit including quantized COM motion versus mass. . . . .	103

# LIST OF ABBREVIATIONS

AMO	Atomic, Molecular and Optical
COM	Center-of-Mass
CTP	Closed Time Path
DOF	Degree of Freedom
EMF	Electromagnetic Field
LHS	Left Hand Side
QED	Quantum Electro-Dynamics
RHS	Right Hand Side
RWA	Rotating Wave Approximation
TE	Transverse Electric
TM	Transverse Magnetic
vdW	van der Waals

# Chapter 1

## Introduction

This dissertation is focused on applying path integral techniques toward predicting effects due to system+bath correlations in atomic-molecular-optical (AMO) systems. At their core, correlation effects are due to interference in entangled system+bath evolution. Predicting them requires that the correlations between interacting subsystems be carefully maintained throughout their evolution. Path integral techniques are particularly well suited to this task because in computations of transition amplitudes, correlations between the interacting systems are naturally kept throughout the evolution. The resulting reduced dynamics is non-Markovian. The reason for choosing AMO systems in particular is first that the simplicity of the interactions and the delicate control attainable in experiments. Strongly motivated by the organized effort to build a working quantum computer and its requirement to maintain and use entanglement, current experiments are reaching a regime in which they can measure and apply effects due to maintained coherence. Second, since the Hamiltonian governing the dynamics is well understood, realistic situations can

be modelled theoretically.

The system of a two-level atom (qubit) interacting with the electromagnetic field (EMF) is used as a model to isolate and predict coherent back-action effects. Such systems offer simplicity and realism in analytic descriptions. The interactions are well known from the QED Hamiltonian, and since the EMF modes do not interact with each other except via the qubit, correlations that develop between the qubit and the field modes are not randomized by interactions within the environment. The net back-action of the EMF modes will then coherently accumulate to a nontrivial effect. We focus on two situations in which effects due to coherent back-action is the main goal and one situation which is related to it. The former include dynamic derivation of the Casimir-Polder (retardation van der Waals) force near a conducting wall [1] and coherent evolution of a qubit in an *initially* thermal EMF bath [2]. The latter is evolution of a qubit interacting with its own center of mass degree of freedom in addition to a zero temperature vacuum EMF [3]. Detailed summaries of the applications described in this dissertation are given in the next section.

In all three applications, the full system is evolved as a single entity, so that the entanglement between the subsystems is kept to a maximum throughout the evolution. Reduction of designated bath degrees of freedom then yields an effective dynamics for the subsystem of interest which includes fully coherent back-action from the bath. Path integral methods such as the influence functional formalism are used in order to maintain full coherence between the

atom, EMF, and the atom's center of mass motion. In addition, all three applications described above are computed in a resummed 2nd order vertex approximation, which allows non-perturbative results that include the effects of entangled evolution, but with the technical simplification of a small coupling approximation.

## 1.1 Summary of Research

### 1.1.1 Casimir-Polder retardation force

A well known situation in which the quantum correlations between two interacting systems is of critical importance is the Casimir-Polder retardation force between a polarizable atom and conducting wall. The retardation force is a quantum modification of the electrostatic attraction of an atom to its image in the wall [4]. In its usual interpretation the retardation force is understood physically to be a result of dressing of the atomic ground state by the vacuum EMF in the presence of a boundary. That is, the ground state of the atom-EMF interacting system is not a product of the separate free ground states, but is instead an entangled atom-EMF state. It is in that sense that the retardation force is an effect of system+bath correlations. Recent experiments have measured the presence of the Casimir-Polder retardation force [5, 6]. Since coherent effects are experimentally verifiable in this situation, it is a good choice in which to

confirm the coherence of the path integral approach as well as look for additional coherent effects. Using that approach we rederive the Casimir-Polder retardation force in terms of recoil associated with emission and reabsorption of virtual photons, rather than as the gradient of a spatially dependent dressed ground state. This mode of calculation allows extension to an atom that moves adiabatically, whereas the gradient calculation of the force assumes a stationary atom.

In the case of a stationary atom, our result is in exact agreement with the Casimir-Polder force. In the case of an adiabatically moving atom, we find a coherent retardation correction up to twice the stationary value. Since in both the stationary and adiabatically moving cases, the source of the retardation force can be thought of as being due to entanglement between the EMF and the atomic degrees of freedom, reproduction of the stationary atom result verifies that our calculation indeed captures coherent behavior. The additional correction for a moving atom can be understood in the energy gradient interpretation as indicating that the dressed ground states for stationary and moving atoms are not the same. The cause of the difference is due to the Doppler shift of the EMF modes with respect to the conducting wall. That is, a moving atom is in a Doppler shifted vacuum, so its dressed ground state is altered from the stationary one.

This work is relevant to applications in which atoms are trapped on the order of a resonant atomic wavelength near a surface. Examples include

evanescent wave gravito-optical [7], microlens array [8], and magnetic chip trapping [9]. Recent experiments have demonstrated the measurable effects of retardation on atomic motion near a surface [5, 6], and those effects will become more important as such applications become more refined. That is especially true when exacting control over the motion will need to be applied (e.g. to implement two qubit gates). In addition, what is usually pictured physically in terms of a gradient force is framed here in terms of the recoil associated with emission and absorption of virtual photons. It thus adds detail to a well known alternative interpretation of the dipole force [10]

The approach taken here is to allow an atom placed near a conducting wall in an initially factorizable state with the EMF vacuum to evolve according to the minimal coupling QED Hamiltonian in the dipole approximation. A path integral technique is used to compute the ground state-EMF vacuum transition amplitude of the evolved system, from which the expectation value of the momentum operator is computed. In the path integral, Grassmannian and bosonic coherent states are used to label the atomic and EMF degrees of freedom, respectively. The position and momentum basis are used for the atom's center of mass degree of freedom. The major approximation applied is a resummed 2nd order vertex approximation. The 2nd order vertex approximation allows the computation to be coherent at long and short times, as it is a partial resummation of all orders of the coupling. Only at the end of the calculation is the mass of the atom taken to infinity and its extension to a point, while

retaining finite terms due to their effect on the dynamics.

The extra correction from coherent QED calculation makes a verifiable prediction. The alteration of the force has its best chance of being measured in experiments involving cold atoms bouncing off the evanescent field of a laser beam totally internally reflected in a crystal. In those experiments the laser is blue detuned, which imposes a repulsive potential to counter the attractive potential of the wall and create a barrier for cold atoms moving toward the crystal to bounce against. As the intensity of the evanescent laser field is lowered the height of the barrier is lowered. At some threshold value the barrier height will fall below the classical tunnelling height and no atoms will be reflected. The van der Waals, Casimir-Polder, and our coherent QED (corrected Casimir-Polder) forces all give different predictions for that threshold laser intensity. The calculations done here are for a perfect conductor, not a dielectric boundary, so the modifications predicted here should not be applied directly to the case of a dielectric boundary. However, a general statement can be made that a coherent QED correction will cause a lowered prediction for the threshold laser power, since it will tend to decrease the atom-wall attraction. If one naively applies a dielectric factor to our result for the conducting plate to compensate for the difference, the present prediction for the threshold energy in units of the natural line width ( $14.8 \Gamma$ ) is close to the measured value ( $14.9 \pm 1.5 \Gamma$ ), compared to the previously predicted value of ( $15.3 \Gamma$ ) [6].

### 1.1.2 Qubit in an initially thermal bath

Another situation in which the effects of coherent back-action may be observable is for a 2-level atom (qubit) evolving in an initially low temperature EMF. The atom is in free space. This physical system describes applications where maintaining entanglement of qubits is important. That is especially true in neutral atom and ion proposals for quantum computers, which use internal atomic states as their qubits. Previous analysis has included Markovian thermal vacuum treatments [11] and a non-Markovian zero temperature treatment [12]. The approach of the present work is closely related to the latter. The major distinction between the present and previous thermal bath calculations is that we assume the bath is thermal only initially. In particular, we do not impose that the bath be completely undisturbed by its interaction with the qubit. That allows entanglement between the qubit and bath to be part of the evolution and will give insight into the basic issue of entanglement in quantum mechanics.

The results we find are valid in the low temperature regime (temperature less than the qubit transition temperature). We find thermalization for the diagonal elements of the qubit density matrix (known as the populations) and complete decoherence of the off-diagonals, which is in agreement with Markovian predictions. However, in disagreement with Markovian predictions, we find the decoherence to be non-exponential. Altered decay dynamics is found for the diagonal matrix elements as well. The reason for this difference is back-action of

the quantum correlations that develop between the qubit and EMF modes (i.e. the entangled evolution). That is, via interaction with the qubit the initially thermal EMF becomes entangled with the qubit. Due to the correlations the reduced dynamics is altered from its fixed thermal bath prediction. Particularly interesting, and consistent with the cause, is that initially, when the qubit and bath are assumed to be in a product state, the decoherence and decay rates match the uncorrelated prediction.

This work is relevant to showing how entangled evolution between a qubit and the EMF can lead to qubit dynamics different from the Markovian prediction. Coherent back-action effects like the one found here will not be limited to interaction with a thermal EMF. Altered qubit dynamics due to entangled evolution can be expected when a qubit interacts with the EMF in any initial state [13, 14, 15]. In quantum computing such altered evolution will have special relevance since it is through control fields that single qubit gates are proposed to be realized. For example, laser  $\frac{\pi}{2}$ -pulses are proposed to realize one qubit gates in ion and neutral atom implementations. Although the effect is expected to be small, an understanding of the coherent back-action effects can help tune control pulses to achieve the desired gates.

The method of calculation used to model this system is a path integral for computing transition amplitudes similar to the one used in the previously described computation. Again, Grassmannian and bosonic coherent states are used to represent the qubit and EMF degrees of freedom. By combining the

transition amplitudes and tracing over the final EMF states, we construct the reduced dynamics of the qubit density matrix. The initial state of the qubit-EMF bath combination is taken to be in a factorized state, with the bath in an initial thermal state. During the evolution no assumptions are imposed on the state of the full system. Only after the combined system has been allowed to evolve is the trace over EMF states taken and the reduced qubit density matrix computed. As in the coherent QED calculation of the Casimir-Polder correction 2nd order vertex approximation is used, which allows for coherent evolution valid for all times. In addition, a low temperature approximation is taken which limits the regime of validity to temperatures lower than the qubit transition frequency. Physically that means that EMF modes resonant with the qubit are mostly unoccupied.

### 1.1.3 Qubit with quantized center of mass motion

Another problem of interest which illustrates the effect of coherent back-action is the evolution of a qubit's internal density matrix in the presence of quantized center of mass motion as well as a zero temperature EMF vacuum. The physical system is a qubit in free space coupled to the EMF as in the previous case. In this case the atom's center of mass (COM) motion will be included as an additional quantum degree of freedom with which the qubit interacts. The COM only adds three extra degrees of freedom but they are different from the EMF in

that the coupling between the qubit and COM degree of freedom is non-linear. The significance of adding motional degrees of freedom is that the decoherence and dissipation of the qubit will be altered. For qubits constructed from atoms, center of mass motion will always be present. For that reason understanding its effects are important.

The result for the qubit's density matrix in this case is a small increase in the decoherence and dissipation rates due to the inclusion of the extra degrees of freedom. For infinite mass, the decoherence and dissipation rates asymptote to the stationary atom value. As the mass of the atom is made smaller the decoherence and dissipation rates increase. These results are consistent with the atom's COM motion being more affected by recoil during virtual emission and absorption processes when it has a smaller mass. However, the change in the decoherence and dissipation rates for realistic implementations is well below current AMO experimental measurement limits. For example, for a qubit with an optical transition frequency, the mass of the atom would need to be five orders of magnitude smaller than a typical alkali atomic mass in order for the decoherence and dissipation rates to increase by 1 percent.

The relevance of this work to quantum computing is both in the calculation of motional decoherence and the methodology for entangled qubit-COM dynamics. In the free space decoherence calculation, we set a feasibility requirement on atomic qubit quantum computing by putting a limit on

when motional decoherence can safely be neglected (when  $\log^{10}[\frac{Mc^2}{\hbar\omega_o}] > 1$ ), and find that current atomic qubit implementations are well within that range. More generally, our work is a completely non-Markovian computation of entangled evolution between an atomic qubit and its COM degrees of freedom. It can thus be extended to the computation of motional decoherence in other situations. An important example is the calculation of decoherence when the COM degree of freedom is entangled with the qubit state, as in certain lattice and microarray two qubit gates. In that case the result will also be a feasibility condition relating the separation distance and the extra decoherence.

The evolution of the reduced qubit density matrix is calculated in a modified version of the influence functional formalism. It is modified in that the trace over the unobserved degrees of freedom is postponed to the end of the calculation as a technical simplification for handling the exponential coupling to the COM. As in the two previously discussed computations, Grassmannian and bosonic coherent states represent the qubit and EMF degrees of freedom, respectively, while the COM motion is labelled by the position basis. With the influence functional an initially factorizable qubit-EMF-COM state is allowed to evolve. After fully coherent evolution, the final EMF and center of mass degrees of freedom are traced out to give the reduced qubit density matrix.

## 1.2 Organization of Dissertation

The organization of the dissertation is as follows. In Chapter 2 the approach of this dissertation is placed in perspective with other standard approaches. First, reviews of the Schrödinger-master equation and Heisenberg-Langevin approaches are presented. Special attention is given to the approximations applied in the derivations. In the remaining section of Chapter 2 the path integral approach, as utilized in the main work of this dissertation, is reviewed. In Chapters 3-5, three applications are presented of the use of path integral techniques to derive coherent dynamics. In Chapter 6 the main conclusions of the dissertation are summarized, along with a final comparison of the Schrödinger-master equation, Heisenberg-Langevin, and path integral approaches.

## Chapter 2

### Review of open system dynamics

A closed linearly coupled composite system consisting of two interacting subsystems, the smaller of which is usually denoted as the "system" and the larger as the "bath", is generically described by a Hamiltonian with three terms:

$$H = H_s + H_b + V \tag{2.1}$$

with the last term being the product of a system and bath operator,  $V = SB$ .

The first term in Eq. (2.1) is the free Hamiltonian of the system, the second term is the free Hamiltonian of the bath, and the third term is the interaction between the system and the bath. In principle, the Hamiltonian, the associated Hilbert spaces, and the Schrödinger or Heisenberg equations of motion fully describe the closed composite system. However, predictions of the closed composite system dynamics is often not tractable, nor is it often what is of greatest interest. That is especially true when the bath has infinite degrees of freedom, since in that case tracking all the bath degrees of freedom may not be possible. In those cases in which it is only the few finite number of system degrees of freedom which are

available for experimental measurement and control, maintaining the full complement of bath degrees of freedom can seem unnecessary <sup>1</sup>. Theoretical techniques have thus been developed which can predict the dynamics of the system degrees of freedom without the need to consider the specific evolution of the bath degrees of freedom. Such dynamical techniques are all in some sense "reduced", meaning that the effect of the bath on the system has been incorporated into the effective dynamics of the system. Reduction of the bath degrees of freedom exchanges the closed composite system dynamics for open system only dynamics.

Since they are rooted in quantum mechanics, the techniques applied to calculations in AMO are all based on either Schrödinger or Heisenberg quantum dynamics, the Schrödinger dynamics approach being master equations, and the Heisenberg dynamics approach being Langevin equations. In transforming the full system+bath dynamics into system only reduced dynamics, approximations need to be applied in order to make the solutions tractable. Before continuing with the main topic of the dissertation, which is the application of path integral techniques to two-level systems in order to derive coherent reduced dynamics, it will be interesting to review these two major techniques, and understand better where approximations are applied and why they are applied. Brief summaries are

---

<sup>1</sup>We shall see later that this is not true for certain specific purposes such as keeping the quantum coherence and entanglement of the combined system. That is where the path integral method excels over others.

given in the next few paragraphs followed by more detailed summaries in the next two subsections.

In the derivation of the Markovian master equation [11, 16, 17, 18, 19, 20], approximations applied include the  $2^{nd}$  order Born approximation, the Markov approximation, and the assumption of a bath which is fixed in its initial state. The  $2^{nd}$  order Born approximation is an approximation in the strength of the coupling constant alone, and applying it neglects terms of higher than  $2^{nd}$  order in the coupling. The Markov approximation is an approximation in the backaction correlation time. It is called a Markov approximation because it causes that the backaction of the system onto itself through the bath at time  $t$  to depend only on the state of the combined system+bath at time  $t$ , and not on the past history. The last of the above three approximations is the assumption of a bath state which is fixed for all time. That last assumption specifically excludes any correlation between the system and bath. The usual justification for this assumption is that the bath is so much larger than the system, that interaction with the system will negligibly affect the bath [11, 19]. Although that argument is true to some extent, the order of terms neglected by making such an approximation contains orders of the bath correlation time as well as the coupling constant [16, 18, 21]. It thus neglects any accumulated effect due to finite correlation time, which is a good approximation for short times, but becomes progressively worse as the system+bath continue to interact.

In the derivation of the quantum Langevin equations only the Markov

approximation is in principle necessary to obtain some interesting results (e.g. resonance fluorescence). An important point to emphasize is that, when applied to the quantum Langevin equations, the Markovian approximation still leaves coherent noise in the fluctuation term. It is because of this last point that it is called the 1<sup>st</sup> Markov approximation, and not simply the Markov approximation in Ref. [20]. As is explained in Ref. [20], applying the 1<sup>st</sup> Markov approximation still leaves history dependence through the choice of initial bath state and the bath's subsequent dynamics. As applied in this approach, it is a weak coupling and short correlation time approximation on the reaction term alone. Additional approximations on the fluctuation term are needed to go beyond the vacuum EMF cases, such as making the assumption of a white noise spectrum in a quantum stochastic differential equation or truncation in van Kampen's cumulant expansion. Such additional approximations make the quantum Langevin equations equivalent to the Markovian master equation.

## 2.1 Review of Schrödinger-master equation approach

An approach which has found wide usage in describing system-bath interactions is the master equation technique. The goal of this approach is to find an approximate evolution for the reduced density matrix of the system alone which still satisfies a semigroup property [21]. It is achieved by applying the above mentioned three approximations to the Schrödinger dynamics of the density

operator. The density operator is the outer product of the Hilbert space state of a system,

$$\chi(t) = |\psi(t)\rangle\langle\psi(t)|. \quad (2.2)$$

The master equation is an equation for the evolution of the density matrix operator. It's derivation for a general Hamiltonian,

$$H = H_s + H_b + V, \quad (2.3)$$

begins with the Schrödinger equation for the density operator,

$$\dot{\chi}(t) = \frac{1}{i\hbar}[H_s + H_b + V, \chi(t)]. \quad (2.4)$$

The equation of motion for the density operator is opposite in sign to the Heisenberg equation for a quantum operator since the density operator is actually an outer product of quantum states. Since Eq. (2.4) is in the Schrödinger picture the operators in the Hamiltonian are constant and it is the density operator which evolves in time. By transforming to the interaction picture, the free evolution of the system and bath states can be removed from the dynamics. Operators in the interaction picture will be denoted by a capital "I" subscript, unless specifically defined otherwise. The transformed operators are

$$\dot{\chi}_I(t) = e^{-\frac{i}{\hbar}H_0t}\chi(t)e^{\frac{i}{\hbar}H_0t} \quad (2.5)$$

and

$$V_I(t) = e^{\frac{i}{\hbar}H_0t}V e^{-\frac{i}{\hbar}H_0t}. \quad (2.6)$$

The dynamical equation in the interaction picture is then

$$\dot{\chi}_I(t) = \frac{1}{i\hbar} [V_I(t), \chi_I(t)]. \quad (2.7)$$

Integrating Eq. (2.7) gives an implicit integral equation for the density matrix,

$$\chi_I(t) = \chi_I(t_o) + \frac{1}{i\hbar} \int_{t_o}^t dt' [V_I(t'), \chi_I(t')]. \quad (2.8)$$

The integrated Eq. (2.8) is then substituted back into Eq. (2.7) to give a generalized master equation for the total density operator,

$$\dot{\chi}_I(t) = \frac{1}{i\hbar} [V_I(t), \chi_I(t_o)] - \frac{1}{\hbar^2} \int_{t_o}^t dt' [V_I(t), [V_I(t'), \chi_I(t')]]. \quad (2.9)$$

The reduced dynamics of the system alone is carved from Eq. (2.9) by taking the trace over the bath degrees of freedom. With the reduced density operator defined as the total density operator after the bath state is traced out,

$$\rho_I(t) = tr_B(\chi_I(t)), \quad (2.10)$$

the dynamical equation for the reduced density operator is

$$\dot{\rho}_I(t) = \frac{1}{i\hbar} tr_B [V_I(t), \chi_I(t_o)] - \frac{1}{\hbar^2} \int_{t_o}^t dt' tr_B [V_I(t), [V_I(t'), \chi_I(t')]]. \quad (2.11)$$

From this point the derivation of the Markovian master equation can follow two slightly different lines of reasoning. I shall first describe the line of derivation as detailed by Refs. [11, 19, 20, 22], and then continue with the derivation as detailed by Refs. [16, 18]. The major difference between the two is in how they justify omission of the system+bath correlations which develop during interaction.

### 2.1.1 Fixed bath assumption

In modern treatments of the master equation technique, a simplifying assumption is usually made at this point that the total density matrix,  $\chi_I(t)$ , is *at all times* a direct product of the bath in its initial state and the system state,

$\chi_I(t) = \rho_B \otimes \rho_I(t)$ . The resulting dynamical equation is

$$\dot{\rho}_I(t) = \frac{1}{i\hbar} \text{tr}_B[\mathbf{V}_I(t), \chi_I(t_0)] - \frac{1}{\hbar^2} \int_{t_0}^t dt' \text{tr}_B[\mathbf{V}_I(t), [\mathbf{V}_I(t'), \rho_B \otimes \rho_I(t')]]. \quad (2.12)$$

Rewriting this in the more compact notation of superoperators,

$$L_1(t)\chi = [\mathbf{V}_I(t), \chi], \quad (2.13)$$

and allowing the system to be coupled to each bath mode separately, as it is in QED,

$$L_1(t) = \sum_k l_k(t), \quad (2.14)$$

the master equation of Eq. (2.12) becomes

$$\dot{\rho}_I(t) = \frac{1}{i\hbar} \text{tr}_B \sum_k l_k(t) \chi_I(t_0) - \frac{1}{\hbar^2} \int_{t_0}^t dt' \text{tr}_B \sum_k l_k(t) \sum_p l_p(t') \rho_B \otimes \rho_I(t'). \quad (2.15)$$

Applying the condition

$$\text{tr}_B \sum_k l_k(t) \rho_B = 0 \quad (2.16)$$

gives

$$\dot{\rho}_I(t) = -\frac{1}{\hbar^2} \int_{t_0}^t dt' \text{tr}_B \sum_k l_k(t) l_k(t') \rho_B \otimes \rho_I(t'). \quad (2.17)$$

Simplification beyond this point requires application of the Markovian approximation. In general the correlation function  $\text{tr}_B \sum_k l_k(t) l_k(t') \rho_B$  will die off

on some time scale, which is called the correlation time,  $\tau_c$ . By appealing to the shortness of the correlation time relative to the time scale on which the system density operator,  $\rho_I(t')$ , evolves one can replace  $\rho_I(t') \rightarrow \rho_I(t)$  in the time integral of Eq. (2.17). The result is the Markovian master equation,

$$\dot{\rho}_I(t) = -\frac{1}{\hbar^2} \int_{t_0}^t dt' tr_B \sum_k l_k(t) l_k(t') \rho_B \otimes \rho_I(t). \quad (2.18)$$

In a high temperature thermal bath, the bath correlation time is inverse to the temperature and will be orders of magnitude smaller than the evolution time scale, so the Markovian approximation is very good. As the temperature of the bath is lowered the thermal correlation time becomes infinite and the correlation functions of the bath become inverse quadratic in the time separation [20], due to the remaining vacuum fluctuations. Thus the Markovian master equation of Eq. (2.18) is particularly trustworthy at high temperatures. At low temperature the finite bath correlation time introduces errors in the Markovian approximation [11, 23, 24, 25].

In addition to the Markovian approximation in Eq. (2.18), the shortness of the correlation timescale is critical to the justification of the fixed bath approximation, although it is sometimes attributed to the Born approximation. The reason for the confusion seems to be that the fixed bath assumption, when applied to the second order integro-differential equation, Eq. (2.11), is actually two approximations applied simultaneously, one of them being the Born approximation. In a derivation by Haake [22] he expands Eq. (2.8) before

applying any approximations, in order to more precisely understand the assumptions which are applied to the master equation. Following a line of derivation similar to Haake's <sup>2</sup>, it is possible to split the above assumption into two separate assumptions.

First, iterating Eq. (2.8) to infinite order turns it into an explicit integral equation for the density operator,

$$\begin{aligned} \chi_I(t) = \chi_I(t_o) + \frac{1}{i\hbar} \int_{t_o}^t dt' [V_I(t'), \chi_I(t_o)] \\ - \frac{1}{\hbar^2} \int_{t_o}^t dt' \int_{t_o}^{t'} dt'' [V_I(t'), [V_I(t''), \chi_I(t_o)]] + \dots \end{aligned} \quad (2.19)$$

which, written in the more compact super-operator notation is

$$\begin{aligned} \chi_I(t) = \chi_I(t_o) + \frac{1}{i\hbar} \int_{t_o}^t dt' L_1(t') \chi_I(t_o) - \frac{1}{\hbar^2} \int_{t_o}^t dt' \int_{t_o}^{t'} dt'' L_1(t') L_1(t'') \chi_I(t_o) + \dots \\ = \sum_{n=0}^{\infty} \frac{(-i/\hbar)^n}{n!} \int_{t_o}^t dt_1 \dots \int_{t_o}^{t_n} dt_n T\{L_1(t_1) \dots L_1(t_n)\} \chi_I(t_o). \end{aligned} \quad (2.20)$$

Clearly, Eq. (2.20) is simply the formal Dyson series solution of Eq. (2.7).

Substituting Eq. (2.14), inserting an *initially* uncorrelated state

$\chi_I(t_o) = \rho_B \otimes \rho_I(t_o)$ , and taking the trace over the bath, gives an expression for

the reduced density operator,

$$\rho_I(t) = \sum_{n=0}^{\infty} \frac{(-i/\hbar)^n}{n!} \int_{t_o}^t dt_1 \dots \int_{t_o}^{t_n} dt_n \text{tr}_B T \left[ \sum_{k_1} l_{k_1}(t_1) \dots \sum_{k_n} l_{k_n}(t_n) \right] \rho_B \otimes \rho_I(t_o). \quad (2.21)$$

---

<sup>2</sup>In Haake's derivation there is a small error which hides the distinctness of the second order Born approximation from the unaltered bath assumption. In the derivation detailed in this dissertation that distinction is emphasized.

The time ordering can be removed by rewriting the expression as a sum over imbedded time integrations summed over all orderings, giving

$$\rho_I(t) = \sum_{n=0}^{\infty} (-i/\hbar)^n \int_{t_o}^t dt_1 \int_{t_o}^{t_1} dt_2 \dots \int_{t_o}^{t_{n-1}} dt_n tr_B \sum_{k_1 \dots k_n} l_{k_1}(t_1) \dots l_{k_n}(t_n) \rho_B \otimes \rho_I(t_o). \quad (2.22)$$

This explicit integral equation will now be reorganized to facilitate the application of the second order Born approximation. Imposing first the condition

$$tr_B(l_k)^{2n+1} \rho_B \otimes \rho_I(t_o) = 0, \quad (2.23)$$

which is true for the system-bath interactions in QED if the initial bath state is a diagonal mixed state (e.g. a thermal bath), Eq. (2.21) can be restricted to terms in which each  $k^{th}$  mode super-operator appears an even number of times,

$$\begin{aligned} \rho_I(t) = \sum_{n=0}^{\infty} (-i/\hbar)^{2n} \int_{t_o}^t dt_1 \int_{t_o}^{t_1} dt_2 \dots \int_{t_o}^{t_{2n-1}} dt_{2n} \\ \times tr_B \sum_{k_1 \dots k_n \text{ pairs}} l_{k_1}(t_1) \dots l_{k_n}(t_{2n}) \rho_B \otimes \rho_I(t_o). \end{aligned} \quad (2.24)$$

The interaction with each bath mode is understood to occur an even number of times in the above equation, so the interaction term can be expanded as a sum over all the possible orderings of interactions,

$$\begin{aligned} \sum_{\text{pairs}} l_{k_1}(t_1) \dots l_{k_n}(t_{2n}) = l_{k_1}(t_1) l_{k_1}(t_2) l_{k_2}(t_3) l_{k_2}(t_4) \dots l_{k_n}(t_{2n-1}) l_{k_n}(t_{2n}) \\ + l_{k_1}(t_1) l_{k_2}(t_2) l_{k_1}(t_3) l_{k_2}(t_4) \dots l_{k_n}(t_{2n-1}) l_{k_n}(t_{2n}) \\ + \text{all other permutations.} \end{aligned} \quad (2.25)$$

The first term in the sum over all pairs is the one in which the members of each pair are consecutive. Since the sequence of interactions is time-ordered that

means that each pair of interactions occurs without any overlap from other bath modes. Keeping only this first term is equivalent to making the second order Born approximation. Written in this way a link between the Born approximation applied in the master equation and the same applied in non-perturbative techniques, such as the resolvent and effective action, can be made.

Perturbatively, they are both partial resummations of infinite series, and are both approximations second order in the coupling strength which neglect overlapping diagrams. After restricting to the second order Born approximation, Eq. (2.24) can be rewritten more clearly with a few changes of notation as

$$\rho_I(t) = \sum_{n=0}^{\infty} \left( \frac{-1}{\hbar^2} \right)^n \text{tr}_B \left[ \prod_{m=1}^n \int_{t_0}^{\tau_{m-1}} dt_m \int_{t_0}^{t_m} d\tau_m \sum_{k_m} l_{k_m}(t_m) l_{k_m}(\tau_m) \right] \rho_B \otimes \rho_I(t_0) \quad (2.26)$$

with  $\tau_0 = t$ . Taking the time derivative of Eq. (2.26) yields

$$\begin{aligned} \dot{\rho}_I(t) = & - \int_{t_0}^t d\tau \text{tr}_B \sum_k l_k(t) l_k(\tau) \\ & \times \sum_{n=0}^{\infty} \left( \frac{-1}{\hbar^2} \right)^n \left[ \prod_{m=2}^{n+1} \int_{t_0}^{\tau_{m-1}} dt_m \int_{t_0}^{t_m} d\tau_m \sum_{k_m} l_{k_m}(t_m) l_{k_m}(\tau_m) \right] \rho_B \otimes \rho_I(t_0) \end{aligned} \quad (2.27)$$

with  $\tau_0 = \tau$ . Comparison of Eq. (2.26) and Eq. (2.27) shows that the second line of Eq. (2.27) is the untraced density operator at time  $\tau$  in the Born approximation,

$$\chi_I(\tau) = \sum_{n=0}^{\infty} \left( \frac{-1}{\hbar^2} \right)^n \left[ \prod_{m=2}^{n+1} \int_{t_0}^{\tau_{m-1}} dt_m \int_{t_0}^{t_m} d\tau_m \sum_{k_m} l_{k_m}(t_m) l_{k_m}(\tau_m) \right] \rho_B \otimes \rho_I(t_0), \quad (2.28)$$

so that Eq. (2.27) can be written

$$\dot{\rho}_I(t) = - \int_{t_0}^t d\tau \text{tr}_B \sum_k l_k(t) l_k(\tau) \chi_I(\tau). \quad (2.29)$$

This equation is the dynamical equation for the reduced density operator in the Born approximation, but it still requires the assumption that

$$\chi_I(\tau) = \rho_B \otimes \rho_I(\tau) \quad (2.30)$$

before it will match Eq. (2.17) with the assumption of an unaltered bath state.

Thus although the Born and unaltered bath approximations seem like the same approximation when they are made in a single step in Eq. (2.11), they are actually two separate approximations, and they can be made separately. The significance of this is simply to show that the fixed bath assumption is not just an approximation in orders of the coupling. It is also an order in the bath correlation time approximation.

### 2.1.2 Coarse graining approximation

An alternative derivation which explicitly exploits the separation of time scales between the bath correlation time and the system evolution time scale is pursued by Refs. [16, 18]. Their derivation is based on the recognition that the Markovian master equation gives only a coarse grained dynamics. They begin with a perturbative truncation of the system+bath dynamics, which allows them to circumvent the assumption that the system and bath are in a product state with

the bath fixed in its initial state for all intermediate times. The short time perturbative dynamics is then replaced by a dynamics valid on long time scales via the coarse graining assumption.

The derivation along this line begins with an iterative expansion of Eq. (2.8), as in Eq. (2.19), but this time truncated to second order,

$$\begin{aligned} \chi_I(t) = \chi_I(t_o) + \frac{1}{i\hbar} \int_{t_o}^t dt' [V_I(t'), \chi_I(t_o)] \\ - \frac{1}{\hbar^2} \int_{t_o}^t dt' \int_{t_o}^{t'} dt'' [V_I(t'), [V_I(t''), \chi_I(t_o)]], \end{aligned} \quad (2.31)$$

so that the system+bath density operator in the last term is evaluated at the initial time. This equation is valid only for short time dynamics since it is a truncated series. After the trace over the bath, with the assumptions that the system+bath density operator is a product state at time  $t_o$  and that the trace over the initial state of the interaction is zero,  $tr_B[V_I(t)\chi_I(t_o)] = 0$ , the equation becomes

$$\rho_I(t) = \rho_I(t_o) - \frac{1}{\hbar^2} \int_{t_o}^t dt' \int_{t_o}^{t'} dt'' tr_B[V_I(t'), [V_I(t''), \rho_B \otimes \rho_I(t_o)]]. \quad (2.32)$$

This equation can be used to find the evolution of the reduced density operator over a short period of time,  $\Delta t$ . The short time evolution is

$$\rho_I(t_o + \Delta t) = \rho_I(t_o) - \frac{1}{\hbar^2} \int_{t_o}^{t_o + \Delta t} dt' \int_{t_o}^{t'} dt'' tr_B[V_I(t'), [V_I(t''), \rho_B \otimes \rho_I(t_o)]]. \quad (2.33)$$

The coarse grained rate of variation of the reduced density operator after a change of variables is then

$$\frac{\Delta \rho_I}{\Delta t}(t) = \frac{1}{\Delta t} \frac{-1}{\hbar^2} \int_t^{t+\Delta t} dt' \int_t^{t'} dt'' tr_B[V_I(t'), [V_I(t''), \rho_B \otimes \rho_I(t)]]. \quad (2.34)$$

As before, the fast die off of the correlation function  $tr_B[V_I(t'), [V_I(t''), \rho_B]]$  and the weakness of the interaction are applied, but this time toward extending Eq.(2.34) to long time dynamics. Denoting by  $\tau_r$  the relaxation timescale, the validity of extension is based on the requirement that  $\tau_c \ll \tau_r$ , so that an intermediate timescale can be chosen such that  $\tau_c \ll \Delta t \ll \tau_r$ . Following Ref. [18], the order of magnitude of the RHS of Eq.(2.34) is

$$\frac{1}{\tau_r} \approx \frac{V^2 \tau_c}{\hbar^2} \quad (2.35)$$

so that the the separation of time scales,  $\tau_c \ll \tau_r$ , requires

$$\frac{V^2 \tau_c}{\hbar} \ll 1. \quad (2.36)$$

The shortness of the coarse graining time versus the system dynamical timescale,  $\Delta t \ll \tau_r$ , then justifies extending the perturbative treatment of Eq. (2.8) to long time predictions. However, by doing so the fixed bath assumption is implicitly introduced. The shortness of the bath correlation time scale versus the coarse graining time,  $\tau_c \ll \Delta t$ , then justifies the neglect of system+bath correlations [16].

## 2.2 Review of Heisenberg-Langevin approach

In the Heisenberg-Langevin approach, quantum Langevin equations are derived by evolving the Heisenberg picture system and bath operators, rather than evolving the density matrix of the system. In that sense it is the Heisenberg

dynamics complement to the master equation. As for the master equation, the quantum Langevin equation can also be traced over bath degrees of freedom to leave reduced quantum Langevin equations for the system operators alone. The Schrödinger and Heisenberg pictures are equivalent, however, the approximations applied to the master equation and quantum Langevin approaches make them inequivalent. It is interesting to examine how the approximations which are made in their respective derivations compare. After a short review of the quantum Langevin equations a linkage between the two methods shall be drawn.

Derivations of quantum Langevin equations are given by many different authors [16, 18, 19, 20]. They all follow a standard sequence of steps. I will follow most closely the derivations of Refs. [18, 20]. First, being more specific about the Hamiltonian, for a two-level system interacting with a harmonic oscillator bath in the RWA the Hamiltonian is

$$H_s = \frac{1}{2}\hbar\omega_o S_z \quad (2.37)$$

$$H_b = \hbar \sum_n \omega_n b_n^\dagger b_n \quad (2.38)$$

$$V = \hbar \sum_n \kappa_n (S_+ b_n + b_n^\dagger S_-), \quad (2.39)$$

where  $S$  and  $b_n$  are the qubit and bath operators satisfying the usual commutation relations. Since the Hamiltonian commutes with itself, it is constant and its form at time  $t$  requires simply the replacement of the operators within it by their evolved versions. Let  $M(t)$  denote any arbitrary system

operator. Then the Heisenberg equation for it is

$$\begin{aligned}\dot{M}(t) &= \frac{i}{\hbar} [H(t), M(t)] \\ &= \frac{i\omega_o}{2} [S_z(t), M(t)] + i \sum_n \kappa_n ([S_+(t), M(t)] b_n(t) + b_n^\dagger(t) [S_-(t), M(t)]) .\end{aligned}\tag{2.40}$$

System and bath operators at equal time commute, but they do not generally commute at unequal times. The ordering in Eq. (2.40) is chosen to maintain normal ordering in proceeding expressions. The Heisenberg equation for the bath operators is

$$\begin{aligned}\dot{b}_n(t) &= \frac{i}{\hbar} [H(t), b_n(t)] \\ &= -i\omega_n b_n(t) - i\kappa_n S_-(t)\end{aligned}\tag{2.41}$$

and its conjugate, with the solutions

$$b_n(t) = b_n(0)e^{-i\omega_n t} - i\kappa_n \int_0^t e^{i\omega_n(t-t')} S_-(t') dt' \tag{2.42}$$

and its conjugate. Substituting Eq. (2.42) into Eq. (2.40) gives a dynamical equation for the system operators,

$$\begin{aligned}\dot{M}(t) &= \frac{i\omega_o}{2} [S_z(t), M(t)] + \int_0^t \sum_n \kappa_n^2 e^{-i\omega_n(t-t')} [S_+(t), M(t)] S_-(t') dt' \\ &\quad - \int_0^t \sum_n \kappa_n^2 e^{i\omega_n(t-t')} S_+(t') [S_-(t), M(t)] dt' + F(t),\end{aligned}\tag{2.43}$$

with the quantum Langevin force given by

$$F(t) = i \sum_n \kappa_n ([S_+(t), M(t)] b_n(0) e^{-i\omega_n t} + b_n^\dagger(0) [S_-(t), M(t)] e^{i\omega_n t}). \tag{2.44}$$

In this form the quantum Langevin equation, Eq. (2.43), has no approximations and is therefore exact within the chosen Hamiltonian.

The function  $\kappa_n$  is related to the density of modes. As  $\omega^2\kappa(\omega)$  tends to a flat distribution, the sum over modes tends to  $\delta(t - t')$  [20]. Assuming then a short correlation for the sum over modes, replacements  $S_{\pm}(t') \rightarrow S_{\pm}(t)e^{\mp i\omega_o(t-t')}$  are applied [18], which assumes that the evolution of  $S_{\pm}$  due to the interaction is small over the bath correlation time. The time integration, in the condition that  $t > \tau_c$  then gives  $\delta(\omega - \omega_o)$ . Subsequently evaluating the integration over bath modes gives the quantum Langevin equation under the 1<sup>st</sup> Markov approximation,

$$\dot{M}(t) = \frac{i\omega_o}{2} [S_z(t), M(t)] + \frac{\gamma}{2} [S_+(t), M(t)] S_-(t) - \frac{\gamma}{2} S_+(t) [S_-(t), M(t)] + F(t). \quad (2.45)$$

The damping rate,  $\gamma$ , comes from the density of modes evaluated at  $\omega_o$ . It includes a frequency shift (Lamb shift) which can be renormalized into the atomic frequency. The approximation applied here is a weak coupling and short correlation time approximation. If  $M$  denotes the qubit operators  $S_+$ ,  $S_-$ , and  $S_z$ ,

the quantum Langevin equations are

$$\dot{S}_+(t) = -\left(-i\omega_o + \frac{\gamma}{2}\right) S_+(t) - 2i \sum_n \kappa_n b_n^\dagger(0) e^{i\omega_n t} S_z(t) \quad (2.46)$$

$$\dot{S}_-(t) = -\left(i\omega_o + \frac{\gamma}{2}\right) S_-(t) + 2i S_z(t) \sum_n \kappa_n b_n(0) e^{-i\omega_n t} \quad (2.47)$$

$$\dot{S}_z(t) = -\gamma(S_z(t) + 1) - 2i S_+(t) \sum_n \kappa_n b_n(0) e^{-i\omega_n t} + 2i \sum_n \kappa_n b_n^\dagger(0) e^{i\omega_n t} S_-(t). \quad (2.48)$$

The Langevin forces (the last terms in Eqs. (2.46-2.48)) couple the spin operators with each other. As a result of the coupling the above equations are a non-linear set which can not be solved. The effects of the Langevin force on a two-level system (and thus the nonlinearity) can be removed if the bath is assumed to be in vacuum. In that case the creation and annihilation operators,  $b_n^\dagger$  and  $b_n$ , annihilate the vacuum state on the left and right, respectively, and the Langevin force will not be a part of the bath averaged dynamical equations. That will not generally be the case for bath averages of products of system operators.

It is important to remark that the quantum Langevin equations are not equivalent to the Markovian master equation. As mentioned before, even though the 1<sup>st</sup> Markov approximation has been applied to the quantum Langevin equations, they still retain non-Markovian dependence in the quantum noise source [20]. An easy way to see that is to integrate Eqs. (2.46-2.48), and substitute them into each other. The result will be integro-differential equations with non-local kernels. It is clear that the approximations applied to the Markovian master equation are more restrictive than those applied to the

quantum Langevin equations. An interesting distinction between the quantum Langevin and Markovian master equation approaches is that, since the quantum Langevin equations come from an evolution of the operators rather than the state, the assumption that the system+bath are in a product state with the bath state fixed at all intermediate times is not relevant. The state of the system+bath does not evolve in the Heisenberg picture, so imposing an initial system+bath state is all that is necessary.

The quantum Langevin equations can be made equivalent to the Markovian master equation by applying approximations of short correlation time and weak coupling to the quantum noise source, as well as the reaction terms. A conceptually clear method of doing so, which will be sketched below, is described in Ref. [20] using van Kampen's cumulant expansion [21]. By first constructing an adjoint object,  $\mu(t)$ , with the definition

$$tr_s [M(t)\rho(0)] = tr_s [M(0)\mu(t)] \quad (2.49)$$

enforced to be true for any system operator,  $M(t)$ , the quantum Langevin equations are transformed into an equivalent equation for the adjoint,  $\mu(t)$ . The trace over the bath on the adjoint then reconstructs the reduced density operator,

$$\rho(t) = tr_B [\rho_B \mu(t)], \quad (2.50)$$

and leads to a master equation generated from the quantum Langevin equation.

After transforming to the interaction picture this master equation is of the form

$$\dot{\rho}_I(t) = \int_0^t tr_B [V_I(t)V_I(t')\mu_I(t')] dt'. \quad (2.51)$$

Compare this and Eq. (2.29) with the parallel identification  $\mu_I \leftrightarrow \chi_I$ . The assumption needed to put this into the form of the Markovian master equation is

$$\mu_I(t) = \rho_B \otimes tr_B \mu_I(t) = \rho_B \otimes \rho_I(t), \quad (2.52)$$

which is exactly Eq. (2.30). The natural interpretation of this derivation is that the quantum Langevin equation is more exact than the Markovian master equation in that it includes more of the system+bath correlations, by avoiding the fixed bath assumption. In the same reference as the above cumulant technique, the authors of Ref. [20] show that the quantum Langevin equations can be transformed to a form equivalent to the Markovian master equation by transforming it into a quantum stochastic differential equation, and imposing a white noise spectrum for the Langevin force. Assumption of such a spectrum apparently also discards system+bath correlations and is equivalent to the above assumption.

### 2.3 Review of influence functional approach

In contrast to Schrödinger-master equation and Heisenberg-Langevin approaches, in path integral approaches to reduced system dynamics it is not necessary to neglect system+bath correlations during the evolution. The maintenance of the

system+bath correlations is implicit in the path integrals because they are constructed from integration over complete sets of states at all intermediate times. Such approximation is avoided by simply allowing the combined system+bath to evolve coherently throughout the interaction period. Then, only at the end of all coherent evolution, the bath variables are traced out to leave the reduced system evolution. The major difficulty of path integral techniques, besides the identification of a suitable representation, is the evaluation of the path integrals themselves. That step requires the weak coupling approximation, but not the short correlation time approximation. In the work of this dissertation that approximation is applied as a  $2^{nd}$  order pole approximation equivalent to the  $2^{nd}$  order Born approximation, and a neglect of branch cut contributions.

### 2.3.1 General overview

The general idea behind the application of path integral techniques to quantum mechanics is to break the evolution operator,  $U(t, 0) = T e^{-\frac{i}{\hbar} \int_0^t H(s) ds}$ , into a series of infinitesimal steps,

$$U(t, 0) = \prod_{n=1}^N U(\epsilon n, \epsilon(n-1)), \quad (2.53)$$

with  $t = N\epsilon$ . After inserting a complete set of states between each evolution operator the transition amplitude  $\langle x_f | U(t, 0) | x_i \rangle$  becomes

$$\begin{aligned} K(x_f, t | x_i, 0) = \int \left[ \prod_{n=1}^{N-1} d\mu(x_n) \right] & \langle x_N | U(\epsilon N, \epsilon(N-1)) | x_{N-1} \rangle \\ & \times \left[ \prod_{n=1}^{N-1} \langle x_n | U(\epsilon n, \epsilon(n-1)) | x_{n-1} \rangle \right], \end{aligned} \quad (2.54)$$

with  $x_N = x_f$ ,  $x_0 = x_i$ , and  $d\mu(x)$  the measure in the resolution of unity for the complete set of states,

$$1 = \int d\mu(x) |x\rangle \langle x|. \quad (2.55)$$

The evolution operator for an infinitesimal step can be expanded to  $O(\epsilon^2)$ ,

$$\begin{aligned} U(\epsilon n, \epsilon(n-1)) &= e^{-\frac{i}{\hbar} \int_0^{\epsilon n} H(s) ds} \\ &= 1 - \frac{i}{\hbar} H_n \epsilon + O(\epsilon^2), \end{aligned} \quad (2.56)$$

so that the infinitesimal transition amplitude is

$$\begin{aligned} K(x_n, n | x_{n-1}, n-1) &= \langle x_n | x_{n-1} \rangle - \frac{i}{\hbar} \langle x_n | H_n | x_{n-1} \rangle \epsilon + O(\epsilon^2) \\ &= \langle x_n | x_{n-1} \rangle e^{-\frac{i}{\hbar} H(x_n, x_{n-1}) \epsilon + O(\epsilon^2)}. \end{aligned} \quad (2.57)$$

The matrix element of the Hamiltonian in Eq. (2.57) may be called the "x-rep"

Hamiltonian and is denoted  $H(x_n, x_{n-1}) = \langle x_n | H_n | x_{n-1} \rangle / \langle x_n | x_{n-1} \rangle$ . The states

$|x\rangle$  are not assumed to be orthogonal in this derivation. This expression

substituted into Eq.(2.54) gives

$$\begin{aligned} K(x_f, t | x_i, 0) &= \int \left[ \prod_{n=1}^{N-1} d\mu(x_n) \langle x_N | x_{N-1} \rangle \langle x_n | x_{n-1} \rangle \right] \\ & e^{-\frac{i}{\hbar} H(x_N, x_{N-1}) \epsilon + O(\epsilon^2) - \frac{i}{\hbar} \sum_{n=1}^{N-1} [H(x_n, x_{n-1}) \epsilon + O(\epsilon^2)]}. \end{aligned} \quad (2.58)$$

In the limit that  $\epsilon \rightarrow 0$  and  $N \rightarrow \infty$  such that  $t = N\epsilon$ , the product in square brackets becomes the path integral measure and Eq. (2.58) becomes a continuous path integral,

$$K(x_f, t|x_i, 0) = \int_{x(0)=x_i}^{x(t)=x_f} D\mu[x(s)] e^{-\frac{i}{\hbar} \int_0^t H[x(s)] ds}. \quad (2.59)$$

In the continuous limit the  $O(\epsilon^2)$  terms no longer contribute to the transition amplitude, so Eq. (2.59) as written is exact. It is interesting to note that although the path integral is defined by a discrete sequence, it is equal to the transition amplitude is only in the continuous limit. Any operator ambiguities that arise in the continuous version can be resolved by appealing to the discrete version.

Although Eq. (2.59) is an exact expression for the transition amplitude, it is obviously not a final result in any sense. Evaluation of the path integral constitutes the major difficulty in this approach. The best method with which to evaluate Eq. (2.59) will depend on the details of the Hamiltonian and the representation chosen. Some popular methods are diagonalization of the Hamiltonian, Gelfand-Yaglom, stationary phase, and recursive evaluation of the action. Diagonalization of the Hamiltonian involves finding the basis in which the Hamiltonian is diagonal so that the path integral can be evaluated as a determinant [26, 27]. The Gelfand-Yaglom method is similar to the diagonalization method. In it a discrete equation is found for the determinant of the discrete version of Eq. (2.59) with  $(n+1)$ -steps in terms of the determinant with  $n$ -steps. In the continuous limit an equation of motion for the determinant

is acquired, which is used to solve for the transition amplitude [28]. In the stationary phase method the destructive interference of paths which deviate from the "classical path" is exploited. By applying a variation over the path  $x(s)$  in the action of Eq. (2.59), Euler-Lagrange type equations can be found for the stationary path. Evaluation of the action along the stationary path then leads to an approximate result for the transition amplitude. In the case of a quadratic action the stationary path evaluation is exact since in that case the action is Gaussian [26, 27]. Finally, recursive evaluation of the action is a type of Gelfand-Yaglom method in that discrete equations are derived for the action of the path integral. This last method is used in much of the original work of this dissertation. It is described in more depth in subsequent sections.

The transition amplitude can be used to derive the reduced dynamics of a system interacting with a bath by constructing from it the reduced propagator, which is forward and backward versions of the transition amplitude integrated over the final state. Working with the density operator of Eq. (2.2), the evolved density operator can be written in terms of the evolution operators,

$$\chi(t) = U(t, 0)\chi(0)U^\dagger(t, 0). \quad (2.60)$$

A matrix element of the density operator is then  $\langle z_f, x_f | \chi(t) | z'_f, x'_f \rangle$ , with  $|x\rangle$  and  $|z\rangle$  denoting system and bath states, respectively. A trace over the bath of Eq. (2.60) gives the reduced density matrix,

$$\langle x_f | \rho(t) | x'_f \rangle = \int d\mu(z_f) \langle z_f, x_f | U(t, 0)\chi(0)U^\dagger(t, 0) | z_f, x'_f \rangle. \quad (2.61)$$

Inserting complete sets of states at the initial times puts the reduced density matrix in terms of the transition matrix elements. With the definition from Eq. (2.59) expanded to include an interacting system and bath, the transition amplitude is

$$\begin{aligned} K(z_f, x_f, t | z_i, x_i, 0) &= \langle z_f, x_f | U(t, 0) | z_i, x_i \rangle \\ &= \int D\mu[z] D\mu[x] e^{-\frac{i}{\hbar} \int_0^t (\mathbb{H}_s[x, z] + \mathbb{H}_b[x, z] + V[x, z]) ds}, \end{aligned} \quad (2.62)$$

and the reduced density operator becomes:

$$\begin{aligned} \langle x_f | \rho(t) | x'_f \rangle &= \int d\mu(z_f) d\mu(z_i) d\mu(x_i) d\mu(z'_i) d\mu(x'_i) \\ &\quad \times K(z_f, x_f, t | z_i, x_i, 0) \chi(0) K^*(z_f, x'_f, t | z'_i, x'_i). \end{aligned} \quad (2.63)$$

If the initial state of the system is assumed to be a product state,  $\rho_B(0) \otimes \rho(0)$ , the integrations over the bath and system states can be separated to define the reduced propagator,

$$J(x_f, x'_f, t | x_i, x'_i, 0) = \int D\mu[x] D\mu[x'] e^{-\frac{i}{\hbar} \int_0^t (\mathbb{H}_s[x] - \mathbb{H}_s[x']) ds} F[x, x'], \quad (2.64)$$

and the influence functional,

$$\begin{aligned} F[x, x'] &= \int d\mu(z_f) d\mu(z_i) d\mu(z'_i) \int D\mu[z] D\mu[z'] \\ &\quad \times e^{-\frac{i}{\hbar} \int_0^t (\mathbb{H}_b[z] + V[x, z] - \mathbb{H}_b[z'] - V[x', z']) ds} \langle z_i | \rho_B(0) | z'_i \rangle. \end{aligned} \quad (2.65)$$

In terms of the above expressions the matrix elements of the reduced density operator are

$$\langle x_f | \rho(t) | x'_f \rangle = \int d\mu(x_i) d\mu(x'_i) J(x_f, x'_f, t | x_i, x'_i, 0) \langle x_i | \rho(0) | x'_i \rangle. \quad (2.66)$$

The most important point to take away from this derivation is that in this technique the system and bath evolve coherently throughout their period of interaction. Except initially, no assumptions are made about the system+bath state, and the reduced dynamics is obtained only after all coherent interaction. This characteristic of the path integral approach allows circumvention of the assumption of free evolution over a short bath correlation time, which is critical to both the master equation and quantum Langevin approaches.

## 2.3.2 Coherent state path integrals

### 2.3.2.1 coherent state representation

Grassmannian coherent states were first formulated for use in a path integral by Ohnuki and Kashiwa [29]. An excellent review of their properties is available from Cahill and Glauber [30]. Those of the bosonic coherent states are detailed in Refs. [31, 32]. Coherent states are defined as any set of states generated by the exponentiated operation of a creation operator and a suitable label on a chosen fiducial state [29, 31],

$$|z_{\mathbf{k}}\rangle = \exp(z_{\mathbf{k}}b_{\mathbf{k}}^{\dagger})|0_{\mathbf{k}}\rangle \quad (2.67)$$

$$|\eta\rangle = \exp(\eta S_+)|0\rangle. \quad (2.68)$$

In the case of the bosonic coherent states, defined in Eq. (2.67), the label  $z_{\mathbf{k}}$  is a complex number, and in the case of the Grassmann coherent states, defined in Eq. (2.68), the label  $\eta$  is an anti-commuting number. The chosen fiducial states

are the harmonic oscillator ground state and the lower two-level state, respectively. A state of the combined atom-field system can be expanded in a direct product coherent state basis,

$$|\{z_{\mathbf{k}}\}, \eta\rangle = |\{z_{\mathbf{k}}\}\rangle \otimes |\eta\rangle. \quad (2.69)$$

A bosonic coherent state basis,  $|z_{\mathbf{k}}\rangle$ , is used to represent the EM field. A Grassmann coherent state basis,  $|\eta\rangle$ , is used to represent the atomic internal two-level degree of freedom.

In order for any set of states to be useful for an equivalent decomposition they must have a resolution of unity. The EM field and Grassmannian coherent states have the following decompositions of unity:

$$1 = \int d\mu(z_{\mathbf{k}}) |z_{\mathbf{k}}\rangle \langle \bar{z}_{\mathbf{k}}| = \int d\mu(\eta) |\eta\rangle \langle \bar{\eta}|, \quad (2.70)$$

with the measures

$$d\mu(z_{\mathbf{k}}) = \exp(-\bar{z}_{\mathbf{k}} z_{\mathbf{k}}) \quad (2.71)$$

$$d\mu(\eta) = \exp(-\bar{\eta} \eta). \quad (2.72)$$

The fact that these measures are exponential functions is what makes the coherent states a particularly suitable representation for transition amplitudes written as path integrals. The time discretization involved in the construction of the path integral necessarily involves the product of infinitesimal exponentials. The exponential form for the measure facilitates rewriting the products of exponentials as the exponential of a sum. Grassmann coherent states also share

other well known properties of bosonic coherent states, such as being non-orthogonal and eigenstates of the annihilator,

$$\langle \bar{z}_{\mathbf{k}} | z'_{\mathbf{k}} \rangle = \exp(\bar{z}_{\mathbf{k}} z'_{\mathbf{k}}) \quad \langle \bar{\eta} | \eta' \rangle = \exp(\bar{\eta} \eta') \quad (2.73)$$

$$b_{\mathbf{k}} | z_{\mathbf{k}} \rangle = z_{\mathbf{k}} | z_{\mathbf{k}} \rangle \quad S_- | \eta \rangle = \eta | \eta \rangle. \quad (2.74)$$

The non-orthogonality property is a minor complication, but since the inner products are exponential in form they can be absorbed into the measure. A great simplification is created by the annihilator eigenstate property, that gives any operator which can be written in terms of creation and annihilation operators, such as the Hamiltonian, a label space Q-representation,

$$H(\{z_{\mathbf{k}}\}, \eta, \{z'_{\mathbf{k}}\}, \eta') = \frac{\langle \{z_{\mathbf{k}}\}, \eta | H | \{z'_{\mathbf{k}}\}, \eta' \rangle}{\langle \eta | \eta' \rangle \langle \{z_{\mathbf{k}}\} | \{z'_{\mathbf{k}}\} \rangle}. \quad (2.75)$$

Using the coherent states as a representation the transition amplitude can be written as a path integral over the coherent state label spaces.

For the bosonic coherent states, the evaluation of the path integrals can be done using any of the methods previously mentioned, however with the Grassmann coherent states extra care must be taken. A particular point of concern is that these Grassmann coherent states are not single fermion coherent states that are generated by the fermionic creation operator. As a result, Hamiltonians which contain single spin up/down operator terms will contain odd terms in this representation and the recombination of infinitesimal transition amplitudes becomes problematic due to the anticommutivity of the terms. The

correct expressions can be found with the introduction of time-indexed anticommuting partners to the Grassmann variables. These anticommuting partners make the formulation more consistent by carrying the effect of the nilpotency and anticommutation of the Grassmann variables in the infinitesimal propagators into the full propagator. As a result, when the Grassmann variables at intermediate times are integrated over all values, the effect of their anticommutivity will be carried along. The resulting path integrals look similar to a boson coherent state path integral. The difference is that the anticommutivity of the Grassmann partners must be remembered during further evaluation with the amplitude. A recursive evaluation of the path integrals maintains the effects the anticommutivity. Details are given in the next section

### 2.3.2.2 Evaluation of Grassmann path integrals

In the use of coherent state path integrals to describe spin systems three representations have been prevalent. Two of them have been to describe the spin degrees of freedom via coherent states of  $SU(2)$  [33, 34] and to use a stereographic projection of the  $SU(2)$  sphere onto the complex plane (i.e. boson mapping) [35]. These two representations do not mesh well with the path integral approach because they have non-exponential measures. The third choice, which is the one taken here, is to use Grassmannian coherent states to represent the spin [12, 36]. One drawback of this approach is that it is restricted to representations of spin- $\frac{1}{2}$  or two-level systems. Within the Grassmannian representation there are also two

variations. One variation to generate Grassmannian coherent states by an exponentiation of the single fermion creation operators. The other variation is to generate them by exponentiation of spin increasing operators. The advantage of the first is that the Hamiltonian so defined always has definite even parity since the fermion operators always appear in pairs, thereby avoiding mixed Grassmann parity in the Hamiltonian. This fact has caused the first variation to be predominant [37]. However an advantage to the second variation is that the interaction terms in many Hamiltonians of interest remain bilinear, thereby allowing more straightforward evaluation of the path integrals. The advantages of these two variations are combined in the treatment here. The framework is sketched below. In the appendices two simple examples are developed and shown to match known exact results.

The construction of a Grassmann path integral begins to diverge from the bosonic case at Eq. (2.54). At that point the product of infinitesimal transition amplitudes can not be naturally combined into a single exponential, as is desirable in a path integral formulation. The reason is that there can be odd terms which anticommute in the infinitesimal amplitudes. With bosonic path integrals that is not a problem since c-numbers commute. In order to avoid this problem a time-indexed anticommuting partner is introduced to all Grassmann coherent state variables. Then the transition amplitude can be written as a

discrete time path integral of a single exponential, e.g.

$$K(t, 0) = \int \prod_{j=1}^N d\mu(\eta_j) \exp\{\bar{\eta}_f \eta_N - \frac{i\epsilon}{\hbar} \sum_{i=1}^N H_{i,i-1}\}. \quad (2.76)$$

Although the introduction of the Grassmann factors allows the amplitudes to be written as above in Eq. (2.76) (since they make each infinitesimal amplitude even), that does not justify their introduction or elucidate their use. The justification for introducing the anticommuting partners is that they are a counting tool that helps to preserve the truncations and signs of formal expressions. That can be most clearly illustrated by a sample evaluation of the amplitude. For example, the transition amplitude for a single infinitesimal interval can generically be written

$$K(\epsilon, 0) = \exp\{\bar{\eta}_1 \eta_0 - \frac{i\epsilon}{\hbar} H_{1,0}\} = e^{\bar{\eta}_1 \psi_1 + \phi_1}, \quad (2.77)$$

with  $\psi$  and  $\phi$  being Hamiltonian dependent and containing a mixture of even and odd terms. For two infinitesimal intervals the amplitude is

$$\begin{aligned} K(2\epsilon, 0) &= \int d\mu(\eta_1) \exp\{\bar{\eta}_2 \eta_1 - \frac{i\epsilon}{\hbar} H_{2,1}\} K(\epsilon, 0) \\ &= \int d\mu(\eta_1) e^{\bar{\psi}_2 \eta_1 + \bar{\phi}_2} e^{\bar{\eta}_1 \psi_1 + \phi_1} \neq \int d\mu(\eta_1) e^{\bar{\psi}_2 \eta_1 + \bar{\eta}_1 \psi_1 + \bar{\phi}_2 + \phi_1}. \end{aligned} \quad (2.78)$$

If any of the terms in the exponent are odd then simply adding the exponents in the integrand, as would be done for c-numbers, does not give the correct expression, which is the source of the inequality of the integrands. However, if one introduces anticommuting factors multiplying each Grassmann coherent state variables, then the inequality becomes an equality and the integral can be done

with standard Grassmann integration techniques. The distinction may seem small, but at later points effects due to Grassmann anticommutivity are retained in the anticommuting factors. It should be emphasized that the anticommuting factors do not impose the equality, but make the RHS simplify to the correct expression for the LHS.

A recursive evaluation which continues the above single step to successive infinitesimal unitary evolutions can now be performed. After each evolution anticommuting partners are introduced at that time index and the amplitude is rewritten in a standard form to facilitate the next evolution,

$$K(\epsilon, 0) = \exp\left\{\bar{\eta}_1\eta_0 - \frac{i\epsilon}{\hbar}H_{1,0}\right\} = e^{\bar{\eta}_1\psi_1+\phi_1} \quad (2.79)$$

$$K(2\epsilon, 0) = \int d\mu(\eta_1) \exp\left\{\bar{\eta}_2\eta_1 - \frac{i\epsilon}{\hbar}H_{2,1}\right\}K(\epsilon, 0) = e^{\bar{\eta}_2\psi_2+\phi_2} \quad (2.80)$$

.

.

$$K(N\epsilon, 0) = \int d\mu(\eta_{N-1}) \exp\left\{\bar{\eta}_N\eta_{N-1} - \frac{i\epsilon}{\hbar}H_{N,N-1}\right\}K((N-1)\epsilon, 0) = e^{\bar{\eta}_N\psi_N+\phi_N}. \quad (2.81)$$

At each step the terms in the action for a  $j$  step transition amplitude are computed from those for a  $j-1$  action,

$$\psi_j \equiv F(\psi_{j-1}, \phi_{j-1}) \quad (2.82)$$

$$\phi_j \equiv G(\psi_{j-1}, \phi_{j-1}), \quad (2.83)$$

with  $F$  and  $G$  being the equations governing the forward steps.

Although the continuous limit of Eq. (2.82) can give first order differential equations from which the transition amplitude can be computed, that is not the correct procedure. The amplitude in this form is only formally valid because the introduction of the time-indexed anticommuting parts to the couplings cause complicated truncations in the polynomial expansion of Eq. (2.81). The next step is to instead expand the propagator into a polynomial series,

$$K(t, 0) = e^{\bar{\eta}_f \psi_N + \phi_N} = \sum_{m=0}^{\infty} \frac{1}{m!} (\bar{\eta}_f \psi_N + \phi_N)^m, \quad (2.84)$$

and use the finite difference equations for the exponents and the anticommutation properties to find finite difference equations for the terms in the polynomial series,

$$[\psi_j]^m = [F(\psi_{j-1}, \phi_{j-1})]^m \quad (2.85)$$

$$[\phi_j]^m = [G(\psi_{j-1}, \phi_{j-1})]^m \quad (2.86)$$

$$[\psi_j]^m [\phi_j]^n = [F(\psi_{j-1}, \phi_{j-1})]^m [G(\psi_{j-1}, \phi_{j-1})]^n. \quad (2.87)$$

Each of the left hand sides (e.g.  $[\psi_j]^m [\phi_j]^n$ ) should be thought of as a new function. Differential equations for these new functions can be found by taking Eqs. (2.85-2.87) to the continuous limit. Substituting the solutions back into the expansion of the amplitude and resumming gives the final expression for the transition amplitude. Only in the form of Eq. (2.84) with the solutions from Eqs. (2.85-2.87) does the amplitude cease to be a formal expression. Two examples of this applied to exactly solvable situations are given in Appendix A to illustrate the technique and to demonstrate its efficacy.

## Chapter 3

### Casimir-Polder Retardation Force

The physical system studied in this chapter is an atom in a polarizable ground state near a conducting wall. The interaction of the atom with the quantum electromagnetic field (EMF) vacuum, whose spatial modes are restricted by the wall with imposed boundary conditions, generates a force that pulls it toward the conducting wall (for general discussion see Ref. [38]). The details of such a force is important in any experiments and applications in which an atom is held near a surface by a trapping scheme using evanescent waves or magnetic fields. The atom-wall force is divisible into two parts. First, there is the electrostatic attraction that the atom feels toward its image on the other side of the wall, called the van der Waals (vdW) force. Second is a quantum mechanical modification of the vdW force first calculated by Casimir and Polder [4]. They dubbed the quantum modification "retardation" of the vdW force, because its source is the non-instantaneous transverse EMF. Extensions of Casimir and Polder's results for a polarizable atom were later derived for an atom in a cavity [39] and near a dielectric wall [40, 41]. Closest in philosophy to what is

done in this chapter is the work of Milonni in Ref. [42]. There, the author computes the second order alteration of the EMF mode functions due to the presence of the atom, from which the ground state energy shift is the expectation value of the interaction Hamiltonian in the altered vacuum <sup>1</sup>. However, the author neglects time dependence in the mode functions and thus neglects effects due to Doppler shifts of the EMF modes. Retardation correction of the vdW force has been demonstrated experimentally [5, 6]. Verification of the Casimir-Polder force can be viewed as a demonstration of the entangled quantum behavior of the entire system, since it involves the dressing of the atom by the EMF vacuum.

Although Casimir and Polder and others' calculations do treat the quantum entanglement in the system, analysis up to now has been restricted to stationary atoms. It has been assumed (wrongly, as we shall show) that such a method can also treat the adiabatic motion of the atom. Adiabatic motion means in this context that as the atom moves, it continuously shifts into the position dependent stationary dressed ground state on a timescale much shorter than the timescale of motion. Treatments assuming that the atom is stationary or is instantaneously static exclude correlations that are developed in the system during the motion. The key point is that the adiabatic and stationary dressed

---

<sup>1</sup>The author of Ref. [42] refers to this method as radiation reaction. We would advise against using this terminology because it is different from the usual meaning referring radiation reaction to the force exerted on a charged object due to its emitted radiation, which manifests as a classical effect.

vacuum states are not the same. An example where this situation is encountered generically and dealt with in depth is in cosmology, specifically, quantum field processes in an expanding universe [43]. For stationary systems a vacuum state is well defined at all times (due to the existence of a Killing vector), but not for arbitrary dynamics, especially fast motion. However, for slow dynamics, adiabatic vacuum states can be defined and renormalization procedures constructed [44, 45, 46]. The adiabatic method we use here is similar in spirit (though not in substance, as our purpose is somewhat different from that in cosmology). To predict motional effects, entanglement in the evolution needs to be accounted for theoretically. We use the influence functional (IF) method here, which keeps track of full coherence in the evolution to derive the force between the atom and the wall while allowing the atom to move adiabatically. In the case of a stationary atom, our result is in exact agreement with the Casimir-Polder force. In the case of an adiabatically moving atom, we find a coherent retardation correction up to twice the stationary value, thus our coherent QED calculation will make verifiable predictions. This chapter shows the derivation and explains the cause due to coherent back-action. Section 3.1 outlines the model and details of the calculation. The results for stationary and adiabatic motion are then given in Section 3.2, and discussed in Section 3.3.

### 3.1 Model and Approach

In contrast to obtaining the force via the gradient of the ground state energy shift, we obtain it through the expectation value of an atom's center of mass (COM) momentum. Our system consists of an atom placed near a conducting wall. We assume an initially factorized state of the atom in its ground state and the EMF in its vacuum. A path integral technique is used to derive the ground state-EMF vacuum transition amplitude of the evolving system. Inclusion of coherent back-action allows the system to self-dress [47, 48, 49] and preserves maximal entanglement in the non-Markovian evolution of an atom-EMF quantum system. The expectation value of the momentum operator is then computed. In the path integral, Grassmannian and bosonic coherent states are used to label the atomic and EMF degrees of freedom, respectively. The position and momentum basis are used for the atom's center of mass degree of freedom. The major approximation applied here is a second order vertex approximation. With the second order vertex, the propagator is partially resummed to all orders of the coupling constant. The result is a non-perturbative propagator which yields coherent long time dynamics [18, 50]. The mass of the atom and the size of its external wavepacket are kept finite throughout the calculation. Only at the end of the calculation do we allow the mass of the atom to go to infinity and its extension shrunk to a point, while retaining finite terms due to their effect on the dynamics.

Highlights of the calculation are given in this section and details are given in the Appendices B and C. In Section 3.1.1 the Hamiltonian and spatial mode functions that describe the system are introduced. In Section 3.1.2 the transition amplitude of the EMF vacuum with the atom in its ground state is calculated in a coherent state path integral, with an effective action expanded to second order in the coupling (equivalent to a second order vertex resummation), and semiclassically in the COM motion. The momentum expectation value and the retardation correction force is then calculated from the transition amplitude in Section 3.1.3.

### 3.1.1 Hamiltonian

The spinless non-relativistic QED Hamiltonian is given by <sup>2</sup>

$$H = \frac{\mathbf{P}^2}{2M} + \frac{1}{2m}(\mathbf{p} + e\mathbf{A})^2 + eV(\mathbf{X}) + H_b. \quad (3.1)$$

The first term is the COM kinetic energy of an atom with mass  $M$ . The second term is the kinetic energy of the electron sitting in the transverse EMF. The third term is the potential energy of the electron around the atomic nucleus. The last term is the energy of the free EMF. After taking the dipole approximation,

---

<sup>2</sup>The Hamiltonian takes the form of Eq. (3.1) and Eq. (3.2), with separated internal and external degrees of freedom because, for an atom, the mass of the nucleus is much greater than the mass of the electrons. For an arbitrary system of charges and masses forming a bound state, a valid separation of the internal from the external degrees of freedom would require going to the multipolar form of the Hamiltonian [51, 52, 53].

and restricting to two internal levels of the atom, the Hamiltonian in minimal coupling form becomes (see Appendix A of Ref. [12] without the rotating wave approximation)

$$H = \frac{\mathbf{P}^2}{2M} + \hbar\omega_0 S_+ S_- + \hbar \sum_{\mathbf{k}} \omega_{\mathbf{k}} b_{\mathbf{k}}^\dagger b_{\mathbf{k}} + H_{I1} + H_{I2} = H_0 + H_I. \quad (3.2)$$

The operators  $S_{\pm}$  are the up and down operators of the atomic qubit and  $\omega_0$  is the atomic transition frequency. The operators  $b_{\mathbf{k}}$  and  $b_{\mathbf{k}}^\dagger$  are the EMF mode annihilation and creation operators, and  $\omega_{\mathbf{k}}$  are the frequencies of the EMF modes. The two parts of the interaction Hamiltonian are

$$H_{I1} = \hbar \sum_{\mathbf{k}e} \frac{g}{\sqrt{\omega_{\mathbf{k}}}} [\mathbf{p}_{eg} S_+ + \mathbf{p}_{ge} S_-] \cdot [\mathbf{u}_{\mathbf{k}} b_{\mathbf{k}} + \mathbf{u}_{\mathbf{k}}^\dagger b_{\mathbf{k}}^\dagger] \quad (3.3)$$

$$H_{I2} = \hbar \sum_{\mathbf{k}l} \frac{\lambda^2}{\sqrt{\omega_{\mathbf{k}}\omega_l}} [\mathbf{u}_{\mathbf{k}} \cdot \mathbf{u}_l b_{\mathbf{k}} b_l + \mathbf{u}_{\mathbf{k}}^\dagger \cdot \mathbf{u}_l (\delta_{\mathbf{k}l} + 2b_{\mathbf{k}}^\dagger b_l) + \mathbf{u}_{\mathbf{k}}^\dagger \cdot \mathbf{u}_l^\dagger b_{\mathbf{k}}^\dagger b_l^\dagger]. \quad (3.4)$$

The vector  $\mathbf{p}_{eg}$  is the dipole transition matrix element, which is defined as  $\mathbf{p}_{eg} = \langle e | \mathbf{p} | g \rangle = -im\omega_0 \langle e | \mathbf{r} | g \rangle$ . The vectors  $\mathbf{u}_{\mathbf{k}}$  contain the photon polarization vectors  $\hat{\mathbf{e}}_{\mathbf{k}}$  and the spatial mode functions  $f_{\mathbf{k}}(\mathbf{X})$ , i.e.,  $\mathbf{u}_{\mathbf{k}}(\mathbf{X}) = \hat{\mathbf{e}}_{\mathbf{k}} f_{\mathbf{k}}(\mathbf{X})$ . The coupling constants are  $g = -\sqrt{\frac{8\pi^2\alpha c}{m^2}}$  and  $\lambda = \sqrt{\frac{4\pi^2\hbar\alpha c}{m}}$ , with  $\alpha$  being the fine structure constant.

In the presence of a conducting plane the spatial mode functions of the EMF which satisfy the imposed boundary conditions are the TE and TM polarization modes [42],

$$\mathbf{u}_{\mathbf{k}1}(\mathbf{X}) = \sqrt{\frac{2}{L^3}} \hat{\mathbf{k}}_{\parallel} \times \hat{\mathbf{Z}} \sin(k_Z Z) e^{i\mathbf{k}_{\parallel} \cdot \mathbf{X}} \quad (3.5)$$

$$\mathbf{u}_{\mathbf{k}2}(\mathbf{X}) = \sqrt{\frac{2}{L^3}} \frac{1}{k} [k_{\parallel} \hat{\mathbf{Z}} \cos(k_Z Z) - ik_Z \hat{\mathbf{k}}_{\parallel} \sin(k_Z Z)] e^{i\mathbf{k}_{\parallel} \cdot \mathbf{X}}, \quad (3.6)$$

and their complex conjugates.

### 3.1.2 Transition amplitude

The transition amplitude between the initial and final coherent states with initial and final positions is given by

$$\langle \mathbf{X}_f, \{\bar{z}_{\mathbf{k}f}\}, \bar{\psi}_f; t + \tau | \exp[-\frac{i}{\hbar} \int_t^{t+\tau} H(s) ds] | \mathbf{X}_i, \{z_{\mathbf{k}i}\}, \psi_i; t \rangle. \quad (3.7)$$

The transition amplitude relevant to the atom-wall force is the amplitude that the atom moves from  $\mathbf{X}_i$  to  $\mathbf{X}_f$  without the emission of any physical photons.

This is a very good assumption, since the probability for *physical* photon emission is extremely small [49]. The initial and final states are thus characterized by the atom being in its ground state and the EMF in vacuum, with arbitrary COM position states. The initial and final coherent state labels can be set to zero to reflect those states, although during the evolution the system evolves freely, and the motion of the COM is affected by recoil from emission and re-absorption of virtual photons,

$$K[\mathbf{X}_f; t + \tau, \mathbf{X}_i; t] = \langle \mathbf{X}_f; t + \tau | \exp[-\frac{i}{\hbar} \int_t^{t+\tau} H(s) ds] | \mathbf{X}_i; t \rangle. \quad (3.8)$$

Normally, a variational approach would be a sensible way to compute the functional integrals that make up the transition amplitude. However, since in this case both the anti-resonant as well as resonant rotating wave terms are included in the Hamiltonian (i.e., no RWA), the variational equations for the

Grassmann variables will have bosonic sources even when the EMF is taken to be in the vacuum. We know from earlier work that when a Grassmann field variable has a bosonic source, the variational technique cannot unambiguously define the evolution of the Grassmann variable. A better way is to leave the transition amplitude as a discrete product of infinitesimal propagators. The necessary functional integrals can then be computed recursively. Details are in Appendix B. After the EMF and Grassmann path integrals are evaluated, the transition amplitude from the initial motional state  $\mathbf{X}_i$  to the final motional state  $\mathbf{X}_f$  (while keeping the same initial and final atomic ground state and EMF vacuum) is given to  $O(e^2)$  vertex by

$$\begin{aligned}
K[\mathbf{X}_f; t + \tau, \mathbf{X}_i; t] = & \\
& \int D\mathbf{X} \exp \left\{ i \int_t^{t+\tau} \left[ \frac{M\dot{\mathbf{X}}^2}{2\hbar} - \sum_{\mathbf{k}} \frac{\lambda^2}{\omega_{\mathbf{k}}} \mathbf{u}_{\mathbf{k}}^*(\mathbf{X}(s)) \cdot \mathbf{u}_{\mathbf{k}}(\mathbf{X}(s)) + O(e^4) \right. \right. \\
& \left. \left. + i\mathbf{p}_z^2 \int_t^s dr \sum_{\mathbf{k}} \frac{g^2}{\omega_{\mathbf{k}}} e^{-i(\omega_{\mathbf{k}} + \omega_0)(s-r)} \mathbf{u}_{\mathbf{k}}(\mathbf{X}(s)) \cdot \mathbf{u}_{\mathbf{k}}^*(\mathbf{X}(r)) \right] ds \right\}
\end{aligned} \tag{3.9}$$

where  $\mathbf{p}_z^2 = \langle g | \mathbf{p}_z^2 | g \rangle$  is the ground state expectation value of  $\mathbf{p}_z^2$ .

A semi-classical approximation to the transition amplitude Eq. (3.9) is obtained by evaluating the action along its classical path. This will neglect the fluctuation terms of order  $O(\frac{1}{M})$ . The classical path is the straight line path plus terms of order  $O(\frac{e^2}{M})$ ,

$$\mathbf{X}_c(s) = \mathbf{X}_i + \frac{\mathbf{X}_f - \mathbf{X}_i}{\tau}(s - t) + O\left(\frac{e^2}{M}\right) = \mathbf{X}_c^0(s) + O\left(\frac{e^2}{M}\right). \tag{3.10}$$

Evaluating the transition amplitude along that path gives

$$\begin{aligned}
K[\mathbf{X}_f; t + \tau, \mathbf{X}_i; t] &= \left( \frac{M}{2\pi i \hbar \tau} \right)^{3/2} \\
&\times \exp \left\{ i \int_t^{t+\tau} \left[ \frac{M \dot{\mathbf{X}}_c^2}{2\hbar} - \sum_{\mathbf{k}} \frac{\lambda^2}{\omega_{\mathbf{k}}} \mathbf{u}_{\mathbf{k}}^*(\mathbf{X}_c^0(s)) \cdot \mathbf{u}_{\mathbf{k}}(\mathbf{X}_c^0(s)) + O(e^4/M) \right. \right. \\
&\quad \left. \left. + i \mathbf{p}_z^2 \int_t^s d\mathbf{r} \sum_{\mathbf{k}} \frac{g^2}{\omega_{\mathbf{k}}} e^{-i(\omega_{\mathbf{k}} + \omega_0)(s-r)} \mathbf{u}_{\mathbf{k}}(\mathbf{X}_c^0(s)) \cdot \mathbf{u}_{\mathbf{k}}^*(\mathbf{X}_c^0(r)) \right] ds \right\}.
\end{aligned} \tag{3.11}$$

Using the spatial mode functions of Eqs. (3.5-3.6) in the above gives the semi-classical transition amplitude in the presence of a conducting wall (see Eq. (C.1)).

### 3.1.3 Momentum expectation and force

Given the above expression for the transition amplitude and an initial center of mass wavefunction for the atom,  $\Psi(\mathbf{P})$ , the momentum expectation and the force on the atom (the time derivative of the expectation momentum) can be computed. The momentum expectation is

$$\begin{aligned}
\langle \hat{\mathbf{P}} \rangle(t + \tau) &= \frac{\hbar}{N} \int \frac{d\mathbf{P}_f}{(2\pi)^3} \mathbf{P}_f \int d\mathbf{X}_i d\mathbf{X}'_i K[\mathbf{P}_f; t + \tau | \mathbf{X}_i; t] \Psi(\mathbf{X}_i) \\
&\quad \times \Psi^*(\mathbf{X}'_i) K^*[\mathbf{P}_f; t + \tau | \mathbf{X}'_i; t],
\end{aligned} \tag{3.12}$$

with the normalization factor

$$N = \int \frac{d\mathbf{P}_f}{(2\pi)^3} \int d\mathbf{X}_i d\mathbf{X}'_i K[\mathbf{P}_f; t + \tau | \mathbf{X}_i; t] \Psi(\mathbf{X}_i) \Psi^*(\mathbf{X}'_i) K^*[\mathbf{P}_f; t + \tau | \mathbf{X}'_i; t]. \tag{3.13}$$

The initial wavefunction can be taken to be a Gaussian centered at  $(\mathbf{R}, \mathbf{P}_0)$  with the standard deviations  $(\sigma, 1/\sigma)$ . Such a choice will allow for the possibility that

the atom and the wall are moving toward or away from one another. Following the line of calculation detailed in Appendix C, a momentum moment generating function is computed in the limits  $M \rightarrow \infty$  and  $\sigma \rightarrow 0$  such that  $\frac{\mathbf{P}_0}{M} \rightarrow \mathbf{V}$  and  $\sigma^2 M \rightarrow \infty$  (see Eq. (C.12)). From the generating function the momentum expectation value can be computed,

$$\mathbf{P}(t + \tau) = \frac{\hbar}{iZ(0)} \left. \frac{\partial Z(\mathbf{J})}{\partial \mathbf{J}} \right|_{\mathbf{J}=0}. \quad (3.14)$$

In the above limits

$$\begin{aligned} \mathbf{P}(t + \tau) = \mathbf{P}_0 - \frac{2i\lambda^2\hbar}{L^3} \sum_{\mathbf{k}} \frac{\mathbf{k}_z \cos^2 \theta}{\omega_{\mathbf{k}}} \int_t^{t+\tau} ds e^{-2i\mathbf{k}_z \cdot (\mathbf{R} + \mathbf{V}(s-t))} \\ + \frac{g^2 \mathbf{P}_z^2 \hbar}{L^3} \sum_{\mathbf{k}} \frac{\mathbf{k}_z \cos^2 \theta}{\omega_{\mathbf{k}}} \int_t^{t+\tau} ds \int_t^s dr e^{-i\mathbf{k}_z \cdot (2\mathbf{R} + \mathbf{V}(s+r-2t))} \\ \times \left[ e^{-i(\omega_{\mathbf{k}} + \omega_0)(s-r)} - e^{i(\omega_{\mathbf{k}} + \omega_0)(s-r)} \right]. \end{aligned} \quad (3.15)$$

The momentum depends on the position and velocity only through the distance from the wall and the velocity toward or away from the wall, so motions parallel to the wall have no effects. Define  $R = \hat{\mathbf{e}}_z \cdot \mathbf{R}$  and  $v = \hat{\mathbf{e}}_z \cdot \mathbf{V}$ , with  $\hat{\mathbf{e}}_z$  defined as positive away from the wall. Taking the time derivative of the momentum expectation value will give the force that is exerted on the atom by the transverse EMF in the presence of the wall. Doing so, as well as applying the Thomas-Reiche-Kuhn sum rule,

$$\lambda^2 = \frac{g^2 \mathbf{P}_z^2}{\omega_0}, \quad (3.16)$$

and rewriting in terms of the static ground state polarizability,  $\alpha_0$ , the force is

$$\begin{aligned} \mathbf{F}_c(\mathbf{R}, \mathbf{v}, t + \tau) = & -\frac{2\pi i \alpha_0 \hbar \omega_0^2}{L^3} \sum_{\mathbf{k}} \frac{\mathbf{k}_z \cos^2 \theta}{\omega_{\mathbf{k}}} e^{-2i\mathbf{k}_z \cdot (\mathbf{R} + \mathbf{V}\tau)} \\ & + \frac{\pi \alpha_0 \hbar \omega_0^3}{L^3} \sum_{\mathbf{k}} \frac{\mathbf{k}_z \cos^2 \theta}{\omega_{\mathbf{k}}} \int_t^{t+\tau} ds e^{-i\mathbf{k}_z \cdot (2\mathbf{R} + \mathbf{V}(\tau+s-t))} \\ & \times \left[ e^{-i(\omega_{\mathbf{k}} + \omega_0)(t+\tau-s)} - e^{i(\omega_{\mathbf{k}} + \omega_0)(t+\tau-s)} \right]. \end{aligned} \quad (3.17)$$

The subscript "c" is a reminder that the force calculated from the transverse field is the retardation correction to the electrostatic force. Inspection of the force reveals that it is a sum over recoil momenta weighted by amplitudes which depend on the distance of the atom from the wall and the velocity of the atom. As will be discussed in Section IV, the recoil momenta come from virtual photon emission and re-absorption. In that sense the net force reflects an interference phenomenon, since it is the net sum of many different possible virtual processes.

## 3.2 Results

### 3.2.1 Stationary atom

If the atom is stationary, then setting  $\mathbf{v} = 0$  gives the retardation force to be

$$\begin{aligned} \mathbf{F}_c^{(0)}(\mathbf{R}, \mathbf{v} = 0, t + \tau) = & -\frac{2\pi i \alpha_0 \hbar \omega_0^2}{L^3} \sum_{\mathbf{k}} \frac{\mathbf{k}_z \cos^2 \theta}{\omega_{\mathbf{k}}} e^{-2i\mathbf{k}_z \cdot \mathbf{R}} \\ & + \frac{\pi \alpha_0 \hbar \omega_0^3}{L^3} \sum_{\mathbf{k}} \frac{\mathbf{k}_z \cos^2 \theta}{\omega_{\mathbf{k}}} \int_t^{t+\tau} ds e^{-2i\mathbf{k}_z \cdot \mathbf{R}} \\ & \times \left[ e^{-i(\omega_{\mathbf{k}} + \omega_0)(t+\tau-s)} - e^{i(\omega_{\mathbf{k}} + \omega_0)(t+\tau-s)} \right]. \end{aligned} \quad (3.18)$$

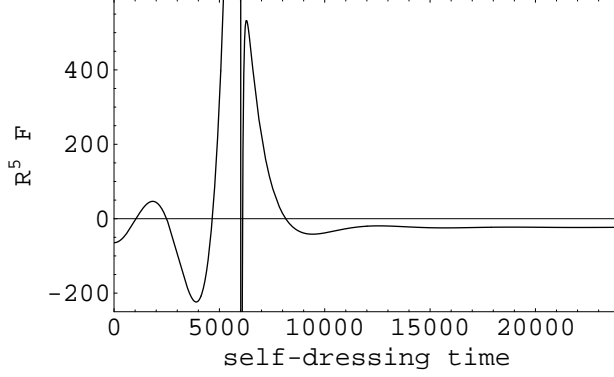


Figure 3.1: This plot shows the transient behavior in the atom-wall force as it rings down to steady state. The value of the atom-wall force at  $R = 3000$  vs time in atomic units is plotted. The spike at  $\tau = 6000$  is the time at which a photon emitted at  $\tau = 0$  will have just returned. Before  $\tau = 6000$  the force is experiencing transient behavior, and afterward it rings down to the stationary atom value.

Combining the correction force with the electrostatic force gives the total force on a stationary atom,

$$\mathbf{F}_{sa}(\mathbf{R}, t + \tau) = -\hat{\mathbf{e}}_z \frac{3\alpha_0 \hbar \omega_0}{8R^4} + \mathbf{F}_c^{(0)}(\mathbf{R}, \mathbf{v} = 0, t + \tau). \quad (3.19)$$

The stationary atom force exhibits a transient behavior when the atom first "sees" itself in the wall. Then, on a timescale of several atom-wall round trip light travel times it asymptotes to a constant steady state value. The transient behavior is plotted in Fig. (3.1) and Fig. (3.2) for an optical transition frequency in an alkali atom.

The steady state value of the stationary atom-wall force can also be

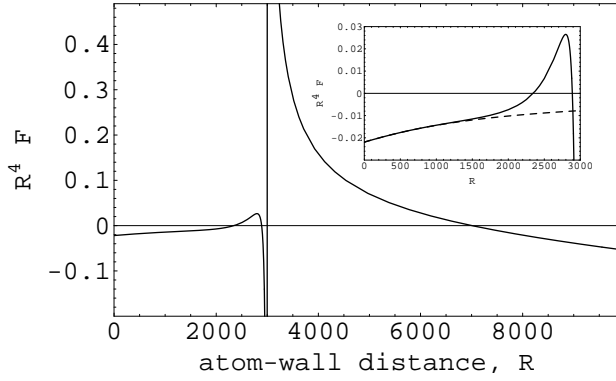


Figure 3.2: This plot shows a snapshot of the coefficient of the  $\frac{1}{R^4}$  behavior of the atom-wall force at a time  $\tau = 6000$  in atomic units. The location of the spike at  $R = 3000$  corresponds to the location at which a photon emitted at  $\tau = 0$  will have just returned to  $R = 3000$ . At locations  $R < 3000$  the force has begun to asymptote to its steady state behavior, and those at  $R > 3000$  are still experiencing transient behavior. The inset image is a magnification near the wall. The dotted line is the coefficient of the  $\frac{1}{R^4}$  dependence of a stationary atom.

determined analytically to be

$$\mathbf{F}_{sa}(\mathbf{R}, \tau \gg 2\mathbf{R}/c) = -\hat{\mathbf{e}}_z \frac{3\alpha_o \hbar \omega_0}{8\mathbf{R}^4} - \hat{\mathbf{e}}_z \frac{\alpha_o \hbar \omega_0^2}{4\pi} \left( \frac{d}{d\mathbf{R}} \right)^3 \int_0^\infty \frac{dk}{kc + \omega_0} \frac{\sin(2k\mathbf{R})}{2k\mathbf{R}}, \quad (3.20)$$

which can be simplified to

$$\mathbf{F}_{sa}(\mathbf{R}, \tau \gg 2\mathbf{R}/c) = \hat{\mathbf{e}}_z \frac{\alpha_o \hbar \omega_0^2}{8\pi} \left( \frac{d}{d\mathbf{R}} \right)^3 \frac{1}{\mathbf{R}} \int_0^\infty \frac{dx}{x^2 + \omega_0^2} e^{-2\mathbf{R}x/c}. \quad (3.21)$$

From Eq. (3.21) the potential which a stationary atom feels is easily found to be

$$U_{sa}(\mathbf{R}) = -\frac{\alpha_o \hbar \omega_0^2}{8\pi} \left( \frac{d}{d\mathbf{R}} \right)^2 \frac{1}{\mathbf{R}} \int_0^\infty \frac{dx}{x^2 + \omega_0^2} e^{-2\mathbf{R}x/c}, \quad (3.22)$$

with asymptotic limits

$$\begin{aligned} U_{sa}(\mathbf{R}) &\rightarrow -\frac{\alpha_o \hbar \omega_0}{8} \frac{1}{\mathbf{R}^3} && \text{for } \mathbf{R} \ll \frac{c}{\omega_0}, \\ U_{sa}(\mathbf{R}) &\rightarrow -\frac{3\alpha_o \hbar c}{8\pi} \frac{1}{\mathbf{R}^4} && \text{for } \mathbf{R} \gg \frac{c}{\omega_0} \end{aligned}, \quad (3.23)$$

which exactly reproduces the results of energy gradient approaches. Although the results are the same as those previously derived, the interpretation behind how the results are obtained is different. The energy gradient approach can be described as a kinematic approach since the atom-EMF system is assumed to be held static in its entangled dressed ground state. The self-dressing approach used here, on the other hand, allows the atom-EMF entanglement to evolve dynamically. That is, the atom and EMF system, beginning in a factorized state, evolves into a stationary dressed state (i.e. it self-dresses). When the atom is stationary the two forces match because after some time to 'get acquainted', the self-dressing atom does indeed evolve into the stationary dressed state. It should

be stressed that the agreement between the results of the two methods demonstrates the coherence of the self-dressing method as applied here.

### 3.2.2 Adiabatic motion

The self-dressing method prediction of the retardation correction force for a slowly moving atom will now be shown to differ from the energy gradient prediction<sup>3</sup>. The key difference will be that as a moving atom and EMF get acquainted, they evolve into an entangled dressed state which is different from the stationary atom dressed state. The reason for the difference is the Doppler shift of the EMF modes in combination with the presence of the wall, as will be discussed in more detail in Section 3.3.

#### 3.2.2.1 Adiabatic evaluation

The retardation force for a moving atom can be determined from Eq. (3.17) by applying a separation of short time scale dynamics from long time scale dynamics and determining how they affect each other. The adiabaticity will be applied here in the same way that it is applied in standard methods for determining the dipole force on an atom in a laser beam [10]. There, assuming that the atom's position is constant on short time-scales, the optical Bloch equations are solved

---

<sup>3</sup>Strictly speaking, such a comparison can not be made since energy gradient approaches implicitly assume the atom to be stationary, although they are often assumed to be applicable to moving atoms often with no justification.

for the steady state values of the internal state density matrix elements. On long time-scales the matrix elements are replaced by their steady state values and put into the Heisenberg equation of motion for the atomic COM momentum. Such a procedure is justified when the internal and external dynamics evolve on vastly different timescales. The analogous separation here will be of the short timescale describing the self-dressing of the atom-EMF system and the long timescale describing the motion of the atom.

In order to be explicit about the timescale separation it will be elucidating to first rewrite Eq. (3.17) with the definition  $x = s - t$ , and remember that  $t$  is the time at which the atom-EMF system begins to evolve from a factorized state,

$$\begin{aligned} \mathbf{F}_c(\mathbf{R}_t, \mathbf{v}_t, \tau) = & -\frac{2\pi i \alpha_0 \hbar \omega_0^2}{L^3} \sum_{\mathbf{k}} \frac{\mathbf{k}_z \cos^2 \theta}{\omega_{\mathbf{k}}} e^{-2i\mathbf{k}_z \cdot (\mathbf{R}_t + \mathbf{V}_t \tau)} \\ & + \frac{\pi \alpha_0 \hbar \omega_0^3}{L^3} \sum_{\mathbf{k}} \frac{\mathbf{k}_z \cos^2 \theta}{\omega_{\mathbf{k}}} \int_0^\tau dx e^{-i\mathbf{k}_z \cdot (2\mathbf{R}_t + \mathbf{V}_t(\tau+x))} \\ & \times \left[ e^{-i(\omega_{\mathbf{k}} + \omega_0)(\tau-x)} - e^{i(\omega_{\mathbf{k}} + \omega_0)(\tau-x)} \right], \end{aligned} \quad (3.24)$$

so that the short timescale dynamics (parameterized by  $\tau$  and  $x$ ) is explicitly separated from the long timescale dynamics (parameterized by  $t$ ) on which  $\mathbf{R}_t$  and  $\mathbf{V}_t$  evolve. An adiabatic evaluation of the retardation correction for a moving atom can be extracted from a Taylor series expansion of Eq. (3.24),

$$\mathbf{F}_c(\mathbf{R}_t, \mathbf{v}_t, \tau) = \sum_{n=0}^{\infty} \frac{\mathbf{v}_t^n}{n!} \mathbf{F}^{(n)}(\mathbf{R}_t, \mathbf{v}_t = 0, \tau) \quad (3.25)$$

where  $n$  denotes the  $n$ th derivative with respect to velocity. The Taylor series expansion is an equivalent representation of the LHS as long as the RHS

converges. Each function  $\mathbf{F}^{(n)}(\mathbf{R}_t, \mathbf{v}_t = 0, \tau)$  exhibits a transient behavior while the atom first "sees" itself in the wall (during times  $\tau \sim \frac{2R}{c}$ ) and asymptotes to steady state behavior on a timescale of several round trip light travel times. The adiabatic approximation is applied at this point by replacing each function  $\mathbf{F}^{(n)}(\mathbf{R}_t, \mathbf{v}_t = 0, \tau)$  by its asymptotic behavior

$$\mathbf{F}^{(n)}(\mathbf{R}_t, \mathbf{v}_t = 0, \tau) \rightarrow \mathbf{F}_{ss}^{(n)}(\mathbf{R}_t, \tau) = -\hat{\mathbf{e}}_z \frac{\tau^n}{2^n} \frac{\alpha_0 \hbar \omega_0^2}{4\pi} \left( \frac{d}{d\mathbf{R}_t} \right)^{n+3} \int_0^\infty \frac{dk}{kc + \omega_0} \frac{\sin(2kR_t)}{2kR_t}, \quad (3.26)$$

which means replacing the Taylor expansion, Eq. (3.25), by its steady state form,

$$\mathbf{F}_c(\mathbf{R}_t, \mathbf{v}_t, \tau) \rightarrow \mathbf{F}_c^{ss}(\mathbf{R}_t, \mathbf{v}_t, \tau) = \sum_{n=0}^{\infty} \frac{v_t^n}{n!} \mathbf{F}_{ss}^{(n)}(\mathbf{R}_t, \tau) \quad (3.27)$$

This is the step that is analogous to replacing the internal state density matrix by its steady state value in adiabatic computations of the dipole force on an atom in a laser beam. Replacing the Taylor expansion by its steady state behavior is adiabatic because it assumes that the expansion terms asymptote to their dressed state form on a timescale much shorter than the timescale on which either the position or velocity of the atom changes. More specifically, for the change in position, the adiabatic condition means that during a round trip light travel time the the atom-wall distance has very little relative change,  $v \frac{2R}{c} \ll R$ , which is equivalent to the condition that the atomic velocity be non-relativistic,

$$\frac{v}{c} \ll \frac{1}{2}. \quad (3.28)$$

Similarly, the adiabatic condition for the change in velocity is that it has very little relative change during a round trip light travel time,  $\frac{\mathbf{F}_{net}}{M} \frac{2R}{c} \ll \mathbf{V}$ , which

can be restated as the net force not changing the kinetic energy of the atom much during a light travel time,

$$(F_{net} v) \frac{R}{c} \ll \frac{1}{2} M v^2, \quad (3.29)$$

since  $F_{net} v$  is the power that the net force puts into the atoms mechanical motion. Both these conditions are satisfied in typical experimental setups.

Note that rather than tending to a constant steady state value the terms in the Taylor expansion, Eq. (3.26), asymptote to steady state polynomial time dependence, the source of the polynomial time dependence being the  $\mathbf{k}_z \cdot \mathbf{V}$  Doppler shift term in the exponents of Eq. (3.24). In distinction to the stationary atom case those polynomial time dependencies will lead to non-zero *partial* time derivatives as well as the convective changes due simply to motion of the atom

$$\frac{d}{ds} \mathbf{F}_c = \left( \frac{dR}{ds} \frac{\partial}{\partial R} + \frac{dv}{ds} \frac{\partial}{\partial v} + \frac{\partial}{\partial s} \right) \mathbf{F}_c. \quad (3.30)$$

The differential change in  $\mathbf{F}_c$  can then be split into two parts, one coming from the convective change and the other from the partial time derivative,

$$d\mathbf{F}_c = d\mathbf{F}_c|_{convective} + ds \frac{\partial \mathbf{F}_c}{\partial s}. \quad (3.31)$$

The convective differential change is the differential change in the force not including any short timescale time dependence, in other words, the steady state expression at  $\tau = 0$ ,

$$d\mathbf{F}_c = d\mathbf{F}_c^{ss} \Big|_{\tau=0} + ds \frac{\partial \mathbf{F}_c}{\partial s}, \quad (3.32)$$

with, from Eq. (3.27),  $d\mathbf{F}_c^{ss}|_{\tau=0} = d\mathbf{F}_c^{(0)}$ . The behavior of the force on long time-scales is computed by integrating the differential change from an initial time at which  $v = 0$  up to the final time,

$$\mathbf{F}_c(t) = \mathbf{F}_c^{(0)}(t) + \int_{t_0}^t ds_1 \frac{\partial \mathbf{F}_c}{\partial s}(s_1), \quad (3.33)$$

where it has been substituted that  $\mathbf{F}_c(t_0) = \mathbf{F}_c^{(0)}(t_0)$  (since  $v = 0$  at  $t_0$ ). A similar analysis for the differential of the first partial time derivative gives,

$$d\left(\frac{\partial \mathbf{F}_c}{\partial s}\right) = d\left(\frac{\partial \mathbf{F}_c^{ss}}{\partial s}\right)_{\tau=0} + ds \frac{\partial}{\partial s} \left(\frac{\partial \mathbf{F}_c}{\partial s}\right) \quad (3.34)$$

from which,

$$\frac{\partial \mathbf{F}_c}{\partial s}(s_1) = \frac{v_{s_1}}{2} \frac{d}{dR} \mathbf{F}_c^{(0)}(s_1) + \int_{t_0}^{s_1} ds_2 \frac{\partial^2 \mathbf{F}_c}{\partial s^2}(s_2). \quad (3.35)$$

Carrying on similar analysis (and rewriting in terms of the zeroth order expansion term) leads to the general expression

$$\frac{\partial^n \mathbf{F}_c}{\partial s^n}(s_n) = \frac{v_{s_1} v_{s_2} \dots v_{s_n}}{2^n} \frac{d^n}{dR^n} \mathbf{F}_c^{(0)}(s_n) + \int_{t_0}^{s_n} ds_{n+1} \frac{\partial^{n+1} \mathbf{F}_c}{\partial s^{n+1}}(s_{n+1}). \quad (3.36)$$

Concatenating Eq. (3.33) with Eqs. (3.36) leads to an expression for the retardation correction force which is the sum of a series of imbedded integrals,

$$\begin{aligned} \mathbf{F}_c(t) = & \mathbf{F}_c^{(0)}(t) + \int_{t_0}^t ds_1 \frac{v_{s_1}}{2} \frac{d}{dR} \mathbf{F}_c^{(0)}(s_1) \\ & + \int_{t_0}^t ds_1 \int_{t_0}^{s_1} ds_2 \frac{v_{s_1} v_{s_2}}{2^2} \frac{d^2}{dR^2} \mathbf{F}_c^{(0)}(s_2) + \dots \end{aligned} \quad (3.37)$$

This result could have been written down directly since it has a straightforward interpretation of being the sum of the integrated effects of each of the partial time derivatives. Each term in Eq. (3.37) can be evaluated by making a change of

variables from time to position with the identity  $v = dR/dt$ . For example, the first term gives,

$$\int_{t_o}^t ds_1 \frac{v}{2} \frac{d}{dR} \mathbf{F}_c^{(0)}(s_1) = \int_{R(t_o)}^{R(t)} dR_1 \frac{1}{2} \frac{d}{dR} \mathbf{F}_c^{(0)}(R_1) = \frac{1}{2} \left[ \mathbf{F}_c^{(0)}(R_t) - \mathbf{F}_c^{(0)}(R_0) \right], \quad (3.38)$$

and further terms give,

$$\int_{t_o}^t ds_1 \int_{t_o}^{s_1} ds_2 \dots \int_{t_o}^{s_{n-1}} ds_n \frac{v_{s_1} v_{s_2} \dots v_{s_n}}{2^n} \frac{d^n}{dR^n} \mathbf{F}_c^{(0)}(s_n) = \frac{1}{2^n} \left[ \mathbf{F}_c^{(0)}(R_t) - \mathbf{F}_c^{(0)}(R_0) \right]. \quad (3.39)$$

Substituting these into Eq. (3.37) gives a geometric series with the result

$$\begin{aligned} \mathbf{F}_c(R) &= \mathbf{F}^{(0)}(R) + \sum_{n=1}^{\infty} \left( \frac{1}{2} \right)^n \left( \mathbf{F}^{(0)}(R) - \mathbf{F}^{(0)}(R_0) \right) \\ &= 2\mathbf{F}^{(0)}(R) - \mathbf{F}^{(0)}(R_0), \end{aligned} \quad (3.40)$$

where  $R_o = R(t_o)$  is the distance from the conducting wall at which the atom was originally at rest. The force  $\mathbf{F}^{(0)}(R)$  is the stationary atom retardation correction to the vdW force.

### 3.2.2.2 Force and potential

Inspection of Eq. (3.40) shows that if the atom is released but remains stationary, then the retardation force will be the stationary atom value. On the other hand if the atom is released infinitely far from the conducting wall and moves in toward the wall, then the retardation force near the wall will be twice the stationary value. At a finite initial distance the retardation force will vary between these values. The force in all cases will depend only on the position.

Thus the atom still moves as if it were in a conservative potential and the potential it feels depends on where it started.

Combining the retardation correction force with the electrostatic force and simplifying as in Eq. (3.21) gives the atom-wall force to be

$$\begin{aligned} \mathbf{F}_{am}(\mathbf{R}) = \hat{\mathbf{e}}_z \frac{\alpha_o \hbar \omega_0^2}{8\pi} \left( \frac{d}{dR} \right)^3 \frac{1}{R} \int_0^\infty \frac{dx}{x^2 + \omega_0^2} e^{-2Rx/c} \\ - \hat{\mathbf{e}}_z \frac{\alpha_o \hbar \omega_0^2}{4\pi} \left( \frac{d}{dr} \right)^3 \int_0^\infty \frac{dk}{kc + \omega_0} \frac{\sin(2kr)}{2kr} \Bigg|_{R_0}^R. \end{aligned} \quad (3.41)$$

The first term is the stationary atom-wall force and the second term is a residual force which pulls the atom back to its original point of release. The force can easily be turned into the potential which the atom feels:

$$\begin{aligned} U_{am}(\mathbf{R}) = -\frac{\alpha_o \hbar \omega_0^2}{8\pi} \left( \frac{d}{dR} \right)^2 \frac{1}{R} \int_0^\infty \frac{dx}{x^2 + \omega_0^2} e^{-2Rx/c} \\ + \frac{\alpha_o \hbar \omega_0^2}{4\pi} \left( \frac{d}{dr} \right)^2 \int_0^\infty \frac{dk}{kc + \omega_0} \frac{\sin(2kr)}{2kr} \Bigg|_{R_0}^R. \end{aligned} \quad (3.42)$$

Since the first term in the potential is the stationary atom-wall potential, in the regions near and far from the wall it will have the expected inverse powers of distance dependence, as shown in Eq. (3.23). The second term is the residual potential due to the motion.

## 3.3 Discussion

### 3.3.1 Physical interpretation

In the energy gradient approach, one interprets the force between a polarizable atom and a wall as arising from the Lamb shift in the atomic ground state

energy. Spatial variation of the ground state energy is expected to generate a force which pushes the atom to lower energy positions, but the mechanism for such a force is not given explicitly. In the final analysis, since the only players in the full system are the atom and the EMF field, such a force must come from the emission and reabsorption of photons. Our approach provides an interpretation of how a net force arises from the emission-reabsorption processes in the presence of a boundary.

The connection between the Lamb shift calculation and our calculation is the dressed ground state of the atom, which is the true ground state of the full Hamiltonian. Expanded in the free (or bare) Hamiltonian basis, the dressed ground state is a quantum superposition of bare atom-EMF states, and is often described as an atom surrounded by a cloud of virtual photons which it continually emits and reabsorbs. In the energy gradient approach, the atom-EMF is assumed to always be in the stationary dressed ground state. By contrast, in our approach a bare state is allowed to evolve quantum mechanically into the dressed ground state. The difference between these two is crucial to understanding how the coherent QED correction comes about. By allowing the atom-EMF to evolve into a dressed ground state we leave open the possibility that the motion of the atom can affect how closely to the stationary dressed ground state the system evolves. Or in the language of the virtual photon cloud, the distribution of virtually occupied modes is allowed to differ from the stationary atom case.

### 3.3.1.1 Stationary atom

Even without motion, the atom's virtual photon cloud is altered by the presence of the wall. For a perfectly conducting wall, the TE and TM spatial mode functions of the EMF are given by Eqs. (3.5- 3.6). Those mode functions are determined by solving the wave equations with the given boundary conditions on the wall, and are constructed by linear combinations of plane wave modes. The creation and annihilation operators of the TE and TM EMF modes ( $b^\dagger, b$ ) are thus combinations of the creation and annihilation operators of plane wave modes ( $a^\dagger, a$ ) moving toward and away from the wall. Inspection of the Hamiltonian and the propagator shows that it is emission followed by absorption, which is the source of the force. In the interest of finding a physical interpretation, one can think of virtual processes in the presence of the wall in terms of plane waves.

Then the emission-reabsorption of a wall-constrained mode is:

$$b_{\mathbf{k}} b_{\mathbf{k}}^\dagger u_{\mathbf{k}}(\mathbf{X}) \sim (a_{\mathbf{k}} e^{i\mathbf{k}\cdot\mathbf{X}} - a_{-\mathbf{k}} e^{-i\mathbf{k}\cdot\mathbf{X}})(a_{\mathbf{k}}^\dagger e^{-i\mathbf{k}\cdot\mathbf{X}} - a_{-\mathbf{k}}^\dagger e^{i\mathbf{k}\cdot\mathbf{X}}) \quad (3.43)$$

$$\sim a_{\mathbf{k}} a_{\mathbf{k}}^\dagger + a_{-\mathbf{k}} a_{-\mathbf{k}}^\dagger - a_{-\mathbf{k}} a_{\mathbf{k}}^\dagger e^{-2i\mathbf{k}\cdot\mathbf{X}} - a_{\mathbf{k}} a_{-\mathbf{k}}^\dagger e^{2i\mathbf{k}\cdot\mathbf{X}} \quad (3.44)$$

The first two terms are emission-reabsorption of the same photon and contribute no net momenta to the atom. The second two terms are emission of one photon and reabsorption of the reflected photon. Each of those contributes a  $2\mathbf{k}_z$  momentum to the atom. The effect of those processes on the force can be seen explicitly in Eq. (3.24). The first term in Eq. (3.24) originates from the  $H_{I2}$  interaction and the second terms from the  $H_{I1}$  interaction. In both terms, the

sum over wavevectors is a sum over emission followed by reflected absorption processes, with each contributing a  $2\mathbf{k}_z$  momentum. Thus, the presence of the wall alters the atoms virtual photon cloud by reflecting some of the modes. The process of emission and reabsorption puts the photon cloud into a steady state distribution with the net effect on the atom of a retardation force.

### 3.3.1.2 Moving atom

Once the stationary retardation force is understood in terms of the wall effect on the virtual photon cloud, the modification of it for an adiabatically moving atom can be interpreted as part of the Doppler effect. The effect is easiest to explain in the reference frame of the atom, in which it is the wall which will be moving toward or away from the atom. Then, as in the stationary case, the virtual photon cloud will be altered by reflection off the wall. However, in the case of the moving wall, the reflected photons will be Doppler shifted due to the walls motion. In the language of the virtual photon cloud, the distribution of photons around a moving atom will be Doppler shifted. This shift builds up in the photon cloud much like charge in a capacitor connected to a loop of wire in a changing magnetic field, and it can only be discharged through absorption into the atom. The net effect, over the retardation force, will be to push the atom against such built up Doppler shift, back to its original point of release.

## 3.3.2 Prospects for experimental observation

### 3.3.2.1 Reflection from an evanescent laser

A situation in which the motional modification of the retardation correction will be important is for the reflection of cold atoms off the evanescent field of an otherwise totally internally reflected laser beam. For example, in an experiment by Landragin et. al. [6], cold alkali atoms are dropped onto a crystal with an evanescent wave running along the surface. The atom-wall interaction pulls the atoms towards the wall. The dipole potential of the evanescent wave, on the other hand, causes a repulsion of the atoms from the crystal. The combination of those two creates a barrier through which some fraction of the atoms tunnel and the rest reflect back out. The authors measure the fraction of reflected atoms versus the barrier height. As the barrier height is lowered it will at some point drop below the energy of the incoming atoms. At that point, all the atoms will be able to classically roll over the barrier, and no atoms will be reflected. The evanescent laser power required to reach that barrier height depends sensitively on the the atom-wall attraction. By comparison of measurement with theory, the authors show that the electrostatic attraction alone does not accurately predict the threshold laser power. They show that the prediction of a retardation corrected force is closer to the measured value. When we combine the motional modification to the retardation correction we are able to make a further modified prediction for the threshold. The calculations done in this chapter are for a

perfect conductor, not a dielectric boundary, so the modifications predicted here should not be applied directly to the case of a dielectric boundary. However, a general statement can be made that a coherent QED correction will cause a lowered prediction for the threshold laser power, since it will tend to decrease the atom-wall attraction. If one naively applies a dielectric factor to our result for the conducting plate to compensate for the difference, the present prediction for the threshold energy in units of the natural line width ( $14.8 \Gamma$ ) is closer to the measured value ( $14.9 \pm 1.5 \Gamma$ ), compared to the previously predicted value ( $15.3 \Gamma$ ) [6], but both are still within the error bounds. Extension of the present work to a dielectric wall is ongoing.

### 3.3.2.2 Transmission between parallel plates

Another experiment which has been able to observe the retardation of the van der Waals force involves a stream of ground state atoms passing between two plates [5]. Due to the attraction of the atoms toward the plates, some of the atoms fall onto and stick to the plates. The fraction of atoms that pass through the gap depends on the atom-wall potential. By measuring the opacity (fraction of atoms that do not pass through) for different gap widths, the authors probe the attractive atom-wall potential. This experiment holds less promise of observing a coherent QED correction to the retardation, than the previous example. The reason being that in this experiment the atoms first come into interaction with the walls at a distance of only a few resonant atomic

wavelengths. The atom and EMF thus do not have as much motion over which to develop a coherent effect. Within that caveat, a general prediction can be made that the coherent correction will tend to decrease the opacity.

### 3.3.3 Conclusion

Our result exactly reproduces the Lamb shift result for a stationary atom. For an adiabatically slowly moving atom, a correction due to the Doppler shift is found. Agreement with the energy gradient result in the stationary atom case shows that our non-perturbative approach captures the effects of entanglement which we sought. The physical interpretation is that the atom-EMF system evolves from an initially factorizable bare state into the interacting Hamiltonian ground state, which is an entangled state in the free Hamiltonian basis. This process is known as self-dressing. The correction for a slowly moving atom shows how our approach can go beyond Lamb shift calculations. The correction is due to the Doppler shift in that the virtual photon cloud which dresses the atom is shifted.

## Chapter 4

### Thermal Bath

The situation we analyze is that of a qubit interacting with a thermal EMF bath in the Jaynes-Cummings Hamiltonian. This model is a very well studied one and is a frequent subject of textbook discussions. Treatments include, for example Refs. [36, 54], and references therein. However, the most well known analysis remains the Schrödinger-master equation approach, which is a coarse grained dynamical equation that is valid at high temperature, as explained in Chapter 1. In particular, by making the assumption that the bath is fixed in its initial state, that analysis a priori excludes effects due to correlation between the qubit and the bath. A thorough Markovian analysis can be found in Ref. [11]. In this chapter we extend our pursuit of the third option of path integral approaches to the coherent reduced dynamics of qubit in a thermal bath. As previously discussed, the path integral approach offers advantages over the master equation approach in that it does not require the imposition of an unaltered bath assumption. Path integral approaches to reduced system dynamics avoid that approximation by allowing the combined system+bath to evolve coherently throughout the

interaction period. Then, only at the end of all coherent evolution, the bath variables are traced out to leave the reduced system evolution. In that way the effects of system+bath correlations are incorporated into the reduced dynamics.

The approach we take to computing the reduced qubit density matrix is straightforward, although the actual implementation includes some non-standard techniques involving Grassmann path integrals. First, we compute the transition matrix elements of the evolution operator constructed from the multi-mode Jaynes-Cummings Hamiltonian. We utilize the coherent state representation for the bosonic degrees of freedom and Grassmann states for the qubit degrees of freedom. Doing so will involve a recursive computation which exploits the semigroup property of the transition matrix. The reason for this type of evaluation, rather than a stationary phase evaluation, is that a stationary phase evaluation has ambiguities in the Grassmann evolution whenever the Grassmann variables have both bosonic and Grassmann sources. In the special case of an initial EM field vacuum, the Grassmann variables have only Grassmann sources, and a stationary phase evaluation is sufficient. After evaluating the transition amplitudes in an intermediate form, we combine the forward and backward versions and trace over the final bosonic coherent states to construct the reduced propagator. The final step is to insert an initial state, which in this case is a thermal EMF, and compute the qubit reduced density matrix elements.

## 4.1 Model and Approach

### 4.1.1 Hamiltonian

The model of atom-field interaction used is the standard Jaynes-Cummings Hamiltonian of a two-level system interacting with a harmonic oscillator bath. Under the dipole, rotating wave (RWA) and two-level approximations the Hamiltonian is given by

$$H = \hbar\omega_o \left( S_z + \frac{1}{2} \right) + \hbar \sum_{\mathbf{k}} \left[ \omega_{\mathbf{k}} b_{\mathbf{k}}^\dagger b_{\mathbf{k}} + \left( \lambda_{\mathbf{k}} S_+ b_{\mathbf{k}} + \bar{\lambda}_{\mathbf{k}} S_- b_{\mathbf{k}}^\dagger \right) \right] \quad (4.1)$$

where  $\hat{b}_{\mathbf{k}}^\dagger, \hat{b}_{\mathbf{k}}$  are the creation and annihilation operators for the  $\mathbf{k}^{th}$  bath mode with frequency  $\omega_{\mathbf{k}}$  of the electromagnetic field, and  $\hbar\omega_o$  is the energy separation between the two levels. Here

$$\hat{S}_z = \frac{1}{2} \hat{\sigma}_z \quad (4.2)$$

$$\hat{S}_\pm = \hat{\sigma}_\pm \equiv \frac{1}{2} (\hat{\sigma}_x \pm i \hat{\sigma}_y) \quad (4.3)$$

where  $\sigma_{x,y,z}$  are the standard 2x2 Pauli matrices with  $\sigma_z = \text{diag}(1, -1)$ , etc. The coupling constant  $\lambda_{\mathbf{k}} = d_{21\mathbf{k}} f_{\mathbf{k}}(\mathbf{X})$  where

$$d_{ij\mathbf{k}} \equiv -\frac{i\omega_{ij}}{\sqrt{2\hbar\omega_{\mathbf{k}}\epsilon_0 V}} \mathbf{d}_{ij} \cdot \hat{\mathbf{e}}_{\mathbf{k}\sigma} \quad (4.4)$$

and  $\mathbf{d}_{ij} \equiv \mathbf{e} \int \bar{\phi}_i \mathbf{x} \phi_j d^3\mathbf{x}$  is the dipole matrix element between the eigenfunctions  $\phi_i$  of the electron-field system,  $\hat{\mathbf{e}}_{\mathbf{k}\sigma}$  is the unit polarization vector ( $\sigma = 1, 2$  are the two polarizations), and  $f_{\mathbf{k}}(\mathbf{x})$  is the spatial mode functions of the vector potential of the electromagnetic field (in free space,  $f_{\mathbf{k}}(\mathbf{x}) = e^{-i\mathbf{k}\cdot\mathbf{x}}$ ,  $V$  is the

volume of space.). Under the dipole approximation  $f_{\mathbf{k}}$  is evaluated at the position of the atom  $\mathbf{X}$ . Since  $\mathbf{d}_{ij} = \bar{\mathbf{d}}_{ji}$ ,  $\bar{d}_{ij\mathbf{k}} = d_{ji\mathbf{k}}$ , we will choose a mode function representation such that  $g_{\mathbf{k}}$  is real.

The model Hamiltonian of Eq. (4.1) is not complete due to the use of the rotating wave approximation [55, 56]. However, we use this model to provide a comparison between the non-Markovian dynamics, which we derive below, and the Markovian dynamics of previous analysis [11]. The neglect of the  $\mathbf{A}^2$  terms is justified since they do not couple the two-level activity with the EMF modes. In the case of a stationary qubit, for which the center-of-mass degrees of freedom are irrelevant, the contribution of the  $\mathbf{A}^2$  term can be absorbed into the free EMF hamiltonian [50]. That is not generally true for a moving qubit, and if one wanted to know something about the motion of the atom, the  $\mathbf{A}^2$  terms would need to be included [52, 53].

The coherent state and Grassmann representation which is used throughout this dissertation is described in Chapter 1. As previously mentioned, any functions containing Grassmann variables are only formal expressions. Since a Grassmann variables have no actual "values", as c-numbers do, they are always to be thought of as labels in a general sense. One may ask: what is the exponential of a Grassmann number? The answer is that the exponential of a Grassmann variable is defined by the polynomial expansion of an exponential function. That fact needs to always be remembered when working with Grassmann variables, although often it seems to be hidden during the

calculations since the result of Grassmann manipulations in which the functions are expanded, manipulated, and reconstituted, is usually the same as the result of working with the functions directly as if the Grassmann variables were c-numbers. The application of the stationary phase method in the case for which the Grassmann variables are combinations of Grassmann and c-number sources is one case in which there is a distinction. Physical results in terms of Grassmann variables also require further simplification. Only when all the Grassmann variables are eliminated, which always requires polynomial expansion, can the results of the Grassmann manipulations be obtained. The process of expanding the Grassmann functions and finding physical results will be the main focus of one of the below sections.

#### 4.1.2 Transition amplitude

Here we construct and evaluate the transition amplitude in the Grassmann and coherent state representation. In a shorthand notation of writing  $K(t_2, t_1)$  to mean the transition amplitude from coherent states at time  $t_1$  to coherent states at time  $t_2$ ,

$$K(t, 0) = \langle \bar{\eta}_f \bar{z}_f | U(t, 0) | \eta_i z_i \rangle. \quad (4.5)$$

with  $U(t, 0)$  being the time evolution operator,

$$U(t, 0) = e^{-\frac{i}{\hbar} \int_0^t H ds}, \quad (4.6)$$

In the usual methodology the path integral is a product of infinitesimal steps. That is, the interval  $[0, t]$  is partitioned into a large number ( $N$ ) of time steps, such that  $t = N\epsilon$ . The  $n$ -step transition amplitude ( $n < N$ ) can then be written as the exponential of a set of general action terms,

$$K(n\epsilon, 0) = \exp \left\{ \bar{\eta}_n \psi_n + \sum_k \bar{z}_{nk} f_{nk} + \sum_k \bar{\eta}_n g_{nk} + \sum_k \bar{z}_{nk} \phi_{nk} \right\}. \quad (4.7)$$

By applying the semigroup property of the transition amplitude,

$$K((n+1)\epsilon, 0) = \int d\mu(\eta_n) \int d\mu(\{z_{\mathbf{k}}\}) K((n+1)\epsilon, n\epsilon) K(n\epsilon, 0), \quad (4.8)$$

finite difference relations can be found for the coefficients in the action,

$$\begin{aligned} \psi_n &= (1 - i\omega_o\epsilon)\psi_{n-1} + \sum_{\mathbf{k}} (i\lambda_{n,\mathbf{k}}\epsilon)\phi_{n-1,\mathbf{k}} & \psi_0 &= \eta_i \\ \phi_{n,\mathbf{k}} &= (i\bar{\lambda}_{n,k}\epsilon)\psi_{n-1} + (1 - i\omega_{\mathbf{k}}\epsilon)\phi_{n-1,\mathbf{k}} & \phi_{0,\mathbf{k}} &= 0 \end{aligned} \quad (4.9)$$

$$\begin{aligned} g_{n,\mathbf{k}} &= (1 - i\omega_o\epsilon)g_{n-1,\mathbf{k}} + (i\lambda_{n,\mathbf{k}}\epsilon)f_{n-1,\mathbf{k}} & g_{0,\mathbf{k}} &= 0 \\ f_{n,\mathbf{k}} &= (i\bar{\lambda}_{n,\mathbf{k}}\epsilon)\sum_{\mathbf{l}} g_{n-1,\mathbf{l}} + (1 - i\omega_{\mathbf{k}}\epsilon)f_{n-1,\mathbf{k}} & f_{0,\mathbf{k}} &= z_{i,\mathbf{k}} \end{aligned} \quad (4.10)$$

The coupling constants in the above relations have time indices because they are in fact an indexed set of Grassmann pairs. The necessity for their introduction is to make manipulations with functions of Grassmann variables match their expanded and manipulated form. As explained previously we use this evaluation technique rather than a stationary phase evaluation because the Grassmann variables in this case have both bosonic and Grassmann sources. It is the necessity of introducing these time-indexed Grassman variables, and their ordering when they are introduced, that is lost in the stationary phase method,

since taking the continuous limit without accounting for the nilpotency of the Grassmann sources would lead to an erroneous result.

Using the recursive method the transition amplitude can be written

$$K(t, 0) = \exp\{\bar{\eta}_f \psi_N + \sum_k \bar{z}_{fk} f_{Nk} + \sum_k \bar{\eta}_f g_{Nk} + \sum_k \bar{z}_{fk} \phi_{Nk}\}. \quad (4.11)$$

Since this equation is a function of Grassmann variables it is to be treated as a formal expression that has meaning only in its polynomial expansion. In that polynomial expansion many terms will be truncated due to the nilpotency of the Grassmann variables. Expanding out Eq. (4.11) and defining the functionals

$$\begin{aligned} F[m_k] &= \prod_k (f_{Nk})^{m_k} & G_l[m_k] &= g_{Nl} \prod_k (f_{Nk})^{m_k} \\ \Psi^f[m_k] &= \psi_N \prod_k (f_{Nk})^{m_k} & \Phi_p^f[m_k] &= \phi_{Np} \prod_k (f_{Nk})^{m_k} \\ \Phi_{lp}^g[m_k] &= g_{Np} \phi_{Nl} \prod_k (f_{Nk})^{m_k} \end{aligned} \quad (4.12)$$

gives the following expanded expression for the transition amplitude:

$$\begin{aligned} K(t, 0) = \sum_{\{m_k\}=0}^{\infty} \left[ \prod_{\mathbf{k}} \frac{(\bar{z}_{f\mathbf{k}})^{m_{\mathbf{k}}}}{m_{\mathbf{k}}!} \right] & \left( F[m_k] + \bar{\eta}_f \Psi^f[m_k] + \sum_l \bar{\eta}_f G_l[m_k] \right. \\ & \left. + \sum_p \bar{z}_{fp} \Phi_p^f[m_k] + \sum_{lp} \bar{\eta}_f \bar{z}_{fl} \Phi_{lp}^g[m_k] \right). \end{aligned} \quad (4.13)$$

The variable  $m_{\mathbf{k}}$  is the number of photons in the  $\mathbf{k}^{th}$  mode. The transition amplitude as written above is a functional sum over all distributions  $\{m_{\mathbf{k}}\}$ .

Differential equations for the functionals that appear in the transition

amplitude can be found from the finite difference equations of Eqs. (4.9-4.10).

$$\dot{F}[m_k] = -i \sum_q m_q \omega_q F[m_k] + i \sum_{lp} m_l \bar{\lambda}_l G_p[m_k - \delta_{kl}] \quad (4.14)$$

$$\dot{G}_p[m_k] = -i(\omega_o + \sum m\omega) G_p[m_k] + i \lambda_p F[m_k + \delta_{kp}] \quad (4.15)$$

$$\begin{aligned} \dot{\Psi}^f[m_k] = & -i(\omega_o + \sum m\omega) \Psi^f[m_k] + i \sum_p \lambda_p \Phi_p^f[m_k] \\ & + i \sum_{lp} m_l \lambda_l \Psi_p^g[m_k - \delta_{kl}] \end{aligned} \quad (4.16)$$

$$\begin{aligned} \dot{\Psi}_p^g[m_k] = & -i(2\omega_o + \sum m\omega) \Psi_p^g[m_k] - i \sum_l \lambda_l \Phi_{lp}^g[m_k] \\ & + i \lambda_p \Psi^f[m_k + \delta_{kp}] \end{aligned} \quad (4.17)$$

$$\begin{aligned} \dot{\Phi}_q^f[m_k] = & -i(\omega_q + \sum m\omega) \Phi_q^f[m_k] + i \lambda_q \Psi^f[m_k] \\ & + i \sum_{lp} m_l \lambda_l \Phi_{qp}^g[m_k - \delta_{kl}] \end{aligned} \quad (4.18)$$

$$\begin{aligned} \dot{\Phi}_{qp}^g[m_k] = & -i(\omega_o + \omega_q + \sum m\omega) \Phi_{qp}^g[m_k] - i \lambda_q \Psi_p^g[m_k] \\ & + i \lambda_p \Phi_q^f[m_k + \delta_{kp}] \end{aligned} \quad (4.19)$$

The transition amplitude of Eq. (4.13) and the differential equations of Eqs. (4.14-4.19) can be used from this point onward, but it is simpler instead to work with Eq. (4.11) during the trace over final EMF states. The differential equations, Eqs. (4.14-4.19), will still be needed in the expansion of the reduced propagator.

### 4.1.3 Reduced propagator

Now that the form of the transition amplitude is known, the reduced density matrix can be computed. The reduced evolution of an initial atomic state is

$$\rho(t) = \int d\mu(\eta_i) d\mu(\eta'_i) \prod_k [d\mu(\{z_{ik}\}) d\mu(\{z'_{ik}\})] J_R(t, 0) \rho(0) \quad (4.20)$$

from which  $J_R(t, 0)$  is the reduced propagator,

$$J_R(t, 0) = \int d\mu(\{z_f\}) K(t, 0) \bar{K}'(t, 0). \quad (4.21)$$

Carrying out the integration with Eq. (4.11) and its barred conjugate, the reduced propagator is found to be

$$J_R(t, 0) = \exp \left\{ \bar{\eta}_f \psi_N + \psi'_N \eta'_f + \sum_{\mathbf{k}} \bar{\eta}_f g_{N\mathbf{k}} + \sum_{\mathbf{k}} \bar{g}'_{N\mathbf{k}} \eta'_f + \sum_k (\bar{f}'_{Nk} + \phi'_{Nk}) (f_{Nk} + \phi_{Nk}) \right\}. \quad (4.22)$$

## 4.2 Results

For thermal vacuum the initial state is,

$$\rho(0) = \left[ \prod_k \exp\{e^{-\beta\omega_k} \bar{z}_{ik} z'_{ik}\} \right] \times [\rho_{00} + \bar{\eta}_i \rho_{10} + \eta'_i \rho_{01} + \bar{\eta}_i \eta'_i \rho_{11}] \quad (4.23)$$

Evaluating Eq. (4.20) with substitutions from Eq. (4.22) and Eq. (4.23) one may obtain the evolved reduced density operator. After expanding completely, the

reduced density matrix elements become

$$\begin{aligned} \rho_{11}(t) = & \rho_{00} \sum_{\{m_k\}} \sum_l m_l G_l[m_k - \delta_{kl}] \bar{G}'_l[m_k - \delta_{kl}] e^{-\beta \sum m \omega} \\ & + \rho_{11} \sum_{\{m_k\}} \left( \Psi^f[m_k] + \sum_l m_l \Phi_{ll}^g[m_k - \delta_{kl}] \right) \\ & \times \left( \bar{\Psi}'^f[m_k] + \sum_l m_l \bar{\Phi}'_{ll}^g[m_k - \delta_{kl}] \right) e^{-\beta \sum m \omega} \end{aligned} \quad (4.24)$$

$$\begin{aligned} \rho_{00}(t) = & \rho_{11} \sum_{\{m_k\}} \sum_l (m_l + 1) \Phi_l^f[m_k] \bar{\Phi}'_l^f[m_k] e^{-\beta \sum m \omega} \\ & + \rho_{00} \sum_{\{m_k\}} F[m_k] \bar{F}'[m_k] e^{-\beta \sum m \omega} \end{aligned} \quad (4.25)$$

$$\rho_{10}(t) = \rho_{10} \sum_{\{m_k\}} \left( \Psi^f[m_k] + \sum_l m_l \Phi_{ll}^g[m_k - \delta_{kl}] \right) \bar{F}'[m_k] e^{-\beta \sum m \omega} \quad (4.26)$$

$$\rho_{01}(t) = \rho_{10} \sum_{\{m_k\}} F[m_k] \left( \bar{\Psi}'^f[m_k] + \sum_l m_l \bar{\Phi}'_{ll}^g[m_k - \delta_{kl}] \right) e^{-\beta \sum m \omega} \quad (4.27)$$

in terms of the definitions of Eq. (4.12).

### 4.2.1 Low temperature

The computation of the reduced density matrix elements involves the calculation of the the functionals of Eq.(4.12) and the evaluation of the functional summations in Eqs. (4.24-4.27). In order to calculate the functionals a low temperature and a weak coupling approximation are applied to Eqs.(4.14-4.19).

The solutions are given in Appendix D, as is the evaluation of the functional summations of Eqs. (4.24-4.27). The resulting expressions for the reduced density

matrix elements, valid at low temperature and weak coupling, are

$$\rho_{11}(t) = \left[1 - \Upsilon(t)\right] \rho_{00} + \left[1 - \left(\frac{1 - e^{-\Gamma_o t}}{1 - e^{-\beta\omega_o - \Gamma_o t}}\right) \Upsilon(t)\right] \rho_{11} \quad (4.28)$$

$$\rho_{00}(t) = \left(\frac{1 - e^{-\beta\omega_o}}{1 - e^{-\beta\omega_o - \Gamma_o t}}\right) \rho_{00} + \left(\frac{1 - e^{-\Gamma_o t}}{1 - e^{-\beta\omega_o - \Gamma_o t}}\right) \Upsilon(t) \rho_{11} \quad (4.29)$$

$$\rho_{10}(t) = e^{-\Gamma_o t/2 - i\omega_o t} \Upsilon(t) \rho_{10} \quad (4.30)$$

with the definition

$$\Upsilon(t) = \frac{1 - e^{-\beta\omega_o}}{1 - e^{-\beta\omega_o - \Gamma_o t}} \quad (4.31)$$

and  $\Gamma_o = \frac{2\lambda^2\omega_o}{\pi}$  being the zero temperature spontaneous emission rate. In the long time limit the populations tend to their low temperature thermal values

$$\rho_{11}(t \rightarrow \infty) = e^{-\beta\omega_o} \quad (4.32)$$

$$\rho_{00}(t \rightarrow \infty) = 1 - e^{-\beta\omega_o} \quad (4.33)$$

and the off-diagonal coherence decays completely

$$\rho_{10}(t \rightarrow \infty) = 0. \quad (4.34)$$

## 4.2.2 Zero temperature limit

At zero temperature  $\beta = \infty$  and Eqs. (4.28-4.30) become,

$$\rho_{11}(t) = \rho_{11} e^{-\Gamma_o t} \quad (4.35)$$

$$\rho_{00}(t) = \rho_{00} + \rho_{11} \left(1 - e^{-\Gamma_o t}\right) \quad (4.36)$$

$$\rho_{10}(t) = \rho_{10} e^{-\Gamma_o t/2 - i\omega_o t} \quad (4.37)$$

which is the expected result from Ref [12].

## 4.3 Discussion

We have studied the two level atom coupled to a photon bath at finite temperature in the multimode Jaynes-Cummings model. We have computed the reduced evolution of the two level degree of freedom and focused on the two issues of decoherence and relaxation. Our approach is that of a modified influence functional technique. Within that approach it is possible to compute the reduced system dynamics while including the evolution of the bath degrees of freedom as well as those of the qubit. Standard master equation approaches make the assumption of a fixed bath, which by definition excludes any dynamics in the bath. The method we use relies on low temperature and weak coupling approximations in a Grassmann coherent state path integral for the atom degrees of freedom and bosonic coherent state path integral for the electromagnetic field. The results we have found are as follows.

### 4.3.1 Decoherence

The decoherence rate is found by computation of the off-diagonal elements of the reduced density matrix  $\rho_{10}(t)$ . The inclusion of bath as well as system dynamics causes the fall off of the off-diagonal matrix elements to become slightly non-exponential. From previous work [12] we know that at zero temperature the decoherence rate is  $\Gamma_0/2 = \lambda^2\omega_o/\pi$ , and master equation approach predicts a decoherence rate at non-zero temperatures of  $\frac{\Gamma_0}{2} \coth(\beta\omega_o/2)$  [11]. To contrast

with that, the predictions of the present calculation can be interpreted as a decoherence rate that changes as the total system evolves. In Fig. (4.1) the decoherence rate is plotted as a function of time. The decoherence rate at  $t = 0$ , when the bath is by assumption in a thermal state uncorrelated with the qubit, agrees with the prediction of master equation approaches. As the system and bath evolve together the decoherence rate falls back down to the zero temperature value. Our interpretation of this is that initially the system truly is (by assumption) in the state assumed in master equation approaches (i.e. a product state of qubit and thermal bath), which is why the two predictions for the decoherence rate match. As the combined system-bath interact, its state evolves away from that initial state, and the correlations that arise cause changes in the reduced system dynamics.

### 4.3.2 Relaxation

The relaxation time scale is measured by the value of  $\rho_{11}(t)$ , assuming that  $\rho_{11}(0) = 1$ . Fig. (4.2) shows a comparison of the prediction here and the Markovian prediction. As for the decoherence, our method yields a prediction which matches that of master equation approaches at  $t = 0$ , at which time the states of the combined system-bath match by assumption. Then as the system and bath interact, dynamics in the bath as well as in the qubit cause a deviation in the reduced system dynamics from the master equation prediction. However,

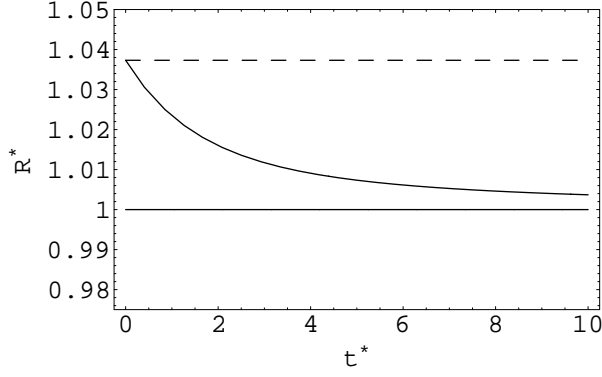


Figure 4.1: This plot shows the ratio of the decoherence rate predicted here over the zero temperature decoherence rate,  $R^* = \frac{\Gamma(t)/2}{\Gamma_o/2}$ , versus a non-dimensionalized time,  $t^* = \Gamma_o t$ , for  $e^{\beta\omega_o} = 0.02$ . The dotted line is the value of the Markovian thermal prediction,  $R_T^* = \frac{\cosh(\beta\omega_o/2)\Gamma/2}{\Gamma_o/2}$ . Note that initially the prediction here matches the Markovian finite temperature result. As the qubit and EMF become correlated the reduced dynamics deviates from the Markovian prediction and asymptotes back to the zero temperature decoherence rate.

the long time behavior of our prediction matches the thermalization prediction of the master equation prediction. It is only evolution at intermediate times which varies.

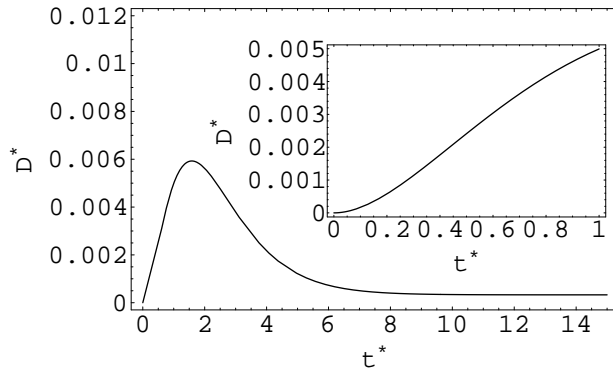


Figure 4.2: This plot shows the difference between the prediction here and the Markovian prediction for the diagonal matrix element,  $D^* = \rho_{11} - \rho_{11}^{\text{markov}}$ , versus the non-dimensionalized time,  $t^* = \Gamma_o t$ , for  $e^{\beta\omega_o} = 0.02$ . The inset image is a magnification near  $t^* = 0$  and shows that the two predictions match initially, then deviate away from each other as the qubit and EMF become correlated.

## Chapter 5

### Motional Decoherence

Atomic motion is an unavoidable element in the consideration of any AMO system and an integral part of experimental designs in atom trapping devices. At issue here is the interaction between the internal degrees of freedom of an atom, assumed to contain an effective two-level system (qubit), and the electromagnetic field (EMF), modified by the atom's quantal motional degree of freedom. This problem has two aspects: 1) How does the two level activity affect the atomic motion? and 2) How does atomic motion affect the two level activity? The first aspect is the basis for laser cooling and atom trapping, which have been studied in great detail and successfully implemented by well-known experiments (for reviews see [10, 57, 58, 59]). This chapter is aimed at the second aspect, specifically, how quantized motion affects the qubit-EMF system dynamics, which is of interest in the design of quantum computers based on atomic qubits (in the form of a neutral atom [60, 61, 62, 63, 64, 65] or ion [66]) in a QED cavity or optical potential. Effects on internal dynamics due to quantized center of mass (COM) motion have previously been studied in the situations of an atom in free

space [67], in a cavity [68, 69, 70], and when the atom’s qubit and COM degrees of freedom are entangled [71]. However, all have focused on spontaneous emission rather than decoherence. The present work probes the non-Markovian regime of atom-EMF interaction, under the modest aim of explicitly computing how entanglement with quantized motion through recoil affects the decoherence and relaxation rates of an atomic qubit in free space. In order to achieve that end, we first discuss two issues of importance in computations of *coherent* reduced dynamics, using path integral methods.

The importance of including back-action

It is well-known that the interaction between a two-level system (2LS, or qubit) and the EMF is the primary source of its relaxation and decoherence, while effects associated with the atom’s motional degrees of freedom are usually relegated to the background. Assuming that the atom moves adiabatically limits one’s consideration to those circumstances wherein the external degrees of freedom act merely as a passive parameter in the environment (here comprised of the EMF and atomic motion) of our system (the qubit), with no dynamical interplay. In technical terms, this amounts to a ‘test-field’ approximation – that the qubit lives in a fixed environment defined by a set of parameters, amongst them the adiabatic motion <sup>1</sup>. The test field approximation leaves out effects of

---

<sup>1</sup>A familiar example is a thermal bath: When characterized only by its temperature one ignores its dynamical response to the system in question.

changes in the environment on the system. To include the effects of the environmental variables *dynamically* it is essential to perform a self-consistent back-action calculation. This was done for the effect of a cavity EMF on the 2LA in Ref. [12, 72].

Full coherence requires self-consistent treatment

In tackling problems where many factors enter, it is useful to isolate one factor after another so that the remaining factors of interest to us can be simplified enough to yield some solution. For quantum coherence and entanglement such simplifications can lead to erroneous results, since phase information is lost if one artificially isolates the linking components of the complete quantum system. This brings up the necessity of self-consistency in any treatment of quantum coherence and entanglement issues. In the present case of a qubit in an EMF this requires that the fully entangled system of atomic 2LS (internal), the EMF, and the center of mass (external) degrees of freedom be treated coherently as a whole and each factor involved be allowed to evolve under the influence of the others in a self-consistent manner. This self-consistency requirement leads to non-Markovian dynamics since memory effects arise naturally and are necessary to preserve maximal coherence during the evolution <sup>2</sup>.

---

<sup>2</sup>A familiar example is given by Zwanzig in his discussion of the projection operator approach: one can write down two differential equations for two interacting subsystems which make up the total system, but if one decides to focus only on one of these subsystems, its dynamics is governed

## Grassmannian and coherent state representation of influence functional

A theoretical scheme we found satisfactory in meeting these requirements is the influence functional (IF) formalism of Feynman and Vernon [73] or the related closed-time-path (CTP) effective action of Schwinger and Keldysh [74]. The influence of the environmental variables on the system of interest is incorporated in the IF (or effective action) in such a way that the equations of motion obtained for the system will already have included the back-action of the environmental variables on the system in a dynamically self-consistent manner. This scheme has been applied to a two-level atom (2LA) interacting with an electromagnetic field (EMF) in reference [12]. There, a first-principles derivation of the general master equations is given and applied to the study of the decoherence of a 2LA in an EMF, for the cases of a free quantum field and a cavity field in the vacuum at zero temperature. The authors found that for the standard resonant type of coupling characteristic of such systems the decoherence time is close to the relaxation time.

---

by an integro-differential equation with nonlocal kernels, signifying memory effects. Note that the Markov approximation underlies many common treatments of quantum systems, such as the Fermi Golden rule, the Wigner-Weisskopf form, the Pauli master equation, to name a few. It clamps down on the dynamical interactions which may result in the violation of the consistency requirement described above, and hence could yield inadequate or erroneous results pertaining to issues of quantum coherence and entanglement in certain circumstances, such as under strong interaction, at low temperature or for a supra-ohmic environment.

Here we use the influence functional method for the treatment of the back-action of the quantum field and the quantal motion of the atom on the qubit. In Section 5.1 we compute the transition amplitude between an initial and final state using a coherent state label for the (bosonic) states of the EMF and a Grassmannian for the (fermionic) 2LS. The coherent state basis allows us to identify the Hilbert space of states with a space of coherent states. The sum over all quantum evolutions is then a sum over all paths in this space. Once the transition amplitude is computed in some sufficiently simplified form, forward and backward versions can be combined and reduced to form the reduced density matrix evolutionary operator. In Section 5.2 we calculate the evolutionary operator for the reduced density matrix when the EMF and motional degrees of freedom are integrated over. We derive an equation describing the evolution of the on and off-diagonal elements, the latter is the coherence function we seek. We end in Section 5.3 with a discussion of our results and comments on possible further developments on this subject.

## 5.1 Transition amplitude

Our system is a 2-level atom interacting with its own center of mass (COM) motion and the EMF. We begin with a modified multi-mode Jaynes-Cummings

type Hamiltonian (see Appendix A of Ref. [12]),

$$H = \frac{\mathbf{P}^2}{2M} + \hbar\omega_o S_z + \hbar \sum_{\mathbf{k}} [\omega_{\mathbf{k}} b_{\mathbf{k}}^\dagger b_{\mathbf{k}} + g_{\mathbf{k}}(\mathbf{X}) S_+ b_{\mathbf{k}} + \bar{g}_{\mathbf{k}}(\mathbf{X}) S_- b_{\mathbf{k}}^\dagger]. \quad (5.1)$$

The first term in the Hamiltonian is the COM kinetic energy. The next two terms are the qubit and EMF energies, respectively. The last two terms are the interaction between the qubit, EMF, and the atom's COM degree of freedom.

Note that  $\mathbf{P}$  and  $\mathbf{X}$  are both operators. Coupling of the qubit to its COM motion is through the spatial mode functions of the EMF. We shall restrict our consideration to an initial vacuum EMF at zero temperature. The result of this calculation will thus be the modification of the vacuum decoherence and relaxation rates of a qubit when the effects of quantized atomic motion are included.

The first step towards obtaining the reduced system dynamics while retaining the full system's coherence is to compute the transition amplitudes between the initial and final states which are the matrix elements of the evolution operator of the full system. We do this with coherent state path integrals. For the EMF we use a bosonic coherent state representation and for the 2-level system (qubit) degree of freedom we use the Grassmannian coherent states [29, 31, 32]. Coherent states are by definition generated by the exponentiated operation of the creation operator and a suitable label on a chosen fiducial state:

$$|z_{\mathbf{k}}\rangle = \exp(z_{\mathbf{k}} b_{\mathbf{k}}^\dagger) |0_{\mathbf{k}}\rangle \quad (5.2)$$

$$|\eta\rangle = \exp(\eta S_+) |0\rangle \quad (5.3)$$

In the case of bosonic coherent states defined in Eq. (5.2) the label,  $z_{\mathbf{k}}$ , is a complex number, and in the case of the Grassmann coherent states defined in Eq. (5.3) the label,  $\eta$ , is an anti-commuting number. The chosen fiducial states are the EMF vacuum and the lower 2-level state, respectively.

In order for any set of states to be useful for the decomposition of the transition matrix they must have a resolution of unity. The EMF and Grassmannian coherent states have the following decompositions of unity

$$1 = \int d\mu(z_{\mathbf{k}}) |z_{\mathbf{k}}\rangle \langle \bar{z}_{\mathbf{k}}| = \int d\mu(\eta) |\eta\rangle \langle \bar{\eta}| \quad (5.4)$$

with the measures

$$\begin{aligned} d\mu(z_{\mathbf{k}}) &= \exp(-\bar{z}_{\mathbf{k}} z_{\mathbf{k}}) \\ d\mu(\eta) &= \exp(-\bar{\eta} \eta) \end{aligned}$$

Grassmann coherent states also share other well known properties of coherent states such as being non-orthogonal and eigenstates of the annihilator:

$$\begin{aligned} \langle \bar{z}_{\mathbf{k}} | z'_{\mathbf{k}} \rangle &= \exp(\bar{z}_{\mathbf{k}} z'_{\mathbf{k}}) & \langle \bar{\eta} | \eta' \rangle &= \exp(\bar{\eta} \eta') \\ b_{\mathbf{k}} | z_{\mathbf{k}} \rangle &= z_{\mathbf{k}} | z_{\mathbf{k}} \rangle & S_- | \eta \rangle &= \eta | \eta \rangle \end{aligned}$$

The center of mass or external degree of freedom can be represented in either the position or momentum basis. In the coherent state basis the Hamiltonian Eq. (5.1) can be written in its Q-representation [75, 17, 19, 50] as [cf Eq. (2.8)

of [12]]

$$H(\{\bar{z}_{\mathbf{k}}\}, \{z_{\mathbf{k}}\}, \bar{\eta}, \eta, \mathbf{X}) = \frac{M\dot{\mathbf{X}}^2}{2} + \hbar\omega_o\bar{\eta}\eta + \hbar \sum_{\mathbf{k}} [\omega_{\mathbf{k}}\bar{z}_{\mathbf{k}}z_{\mathbf{k}} + \bar{\eta}g_{\mathbf{k}}(\mathbf{X})z_{\mathbf{k}} + \bar{z}_{\mathbf{k}}\bar{g}_{\mathbf{k}}(\mathbf{X})\eta]. \quad (5.5)$$

The transition matrix elements between the initial and final coherent states are then

$$K(t, 0) = \langle \{\bar{z}_{f\mathbf{k}}\} \bar{\eta}_f \mathbf{X}_f, t | \exp(-\frac{i}{\hbar}Ht) | \{z_{i\mathbf{k}}\} \eta_i \mathbf{X}_i, 0 \rangle. \quad (5.6)$$

Using the completeness<sup>1</sup> property of the (EMF and Grassmann) coherent state basis to facilitate time-discretization of the transition matrix [73] puts the transition matrix elements in a coherent state path integral representation. After inserting the Q-representation, the transition elements transform into a sum over paths in the coherent state labels. Having done the above the transition matrix becomes a triple functional integral:

$$\begin{aligned} K(t, 0) = & \int D\mathbf{X} \int D\bar{\eta} D\eta \prod_{\mathbf{k}} D\bar{z}_{\mathbf{k}} D z_{\mathbf{k}} \exp \left[ \bar{\eta}_f \eta(t) + \sum_{\mathbf{k}} \bar{z}_{f\mathbf{k}} z_{\mathbf{k}}(t) - \frac{iM}{2} \int_0^t \dot{\mathbf{X}} ds \right] e^{i\omega_o t/2} \\ & \times \exp \left[ - \int_0^t (\bar{\eta}\dot{\eta} + i\omega_o\bar{\eta}\eta + \sum_{\mathbf{k}} \bar{z}_{\mathbf{k}}\dot{z}_{\mathbf{k}} \right. \\ & \left. + i \sum_{\mathbf{k}} \omega_{\mathbf{k}}\bar{z}_{\mathbf{k}}z_{\mathbf{k}} + i \sum_{\mathbf{k}} \bar{\eta}g_{\mathbf{k}}(\mathbf{X})z_{\mathbf{k}} + i \sum_{\mathbf{k}} \bar{z}_{\mathbf{k}}\bar{g}_{\mathbf{k}}(\mathbf{X})\eta) ds \right] \end{aligned} \quad (5.7)$$

In this form the transition matrix elements can be evaluated exactly by a combination of stationary phase and correlation function methods which exploit the truncating properties of Grassmann variables. The order of evaluation will be

the EMF, COM, and then Grassmann functional integrals. The details follow.

### 5.1.1 EMF path integral

First, the EMF coherent state part of the triple path integral can be evaluated by the stationary phase method [73]. The variational equations of motion for the electromagnetic field variables in Eq. (5.7) are

$$\dot{z}_{\mathbf{k}} = -i\omega_{\mathbf{k}}z_{\mathbf{k}} - i\bar{g}_{\mathbf{k}}(\mathbf{X})\eta \quad (5.8)$$

which have integral solutions [cf Eq. (2.14) of [12]]

$$z_{\mathbf{k}}(s) = z_{i\mathbf{k}}e^{-i\omega_{\mathbf{k}}s} - i \int_0^s dr \bar{g}_{\mathbf{k}}(\mathbf{X}(r))e^{-i\omega_{\mathbf{k}}(s-r)}\eta(r). \quad (5.9)$$

The transition amplitude from an initial EMF vacuum ( $\{z_{i\mathbf{k}}\} = 0$ ) to an arbitrary final state becomes

$$\begin{aligned} K(t, 0) = & \int D\mathbf{X} \int D\bar{\eta}D\eta \exp \left[ \bar{\eta}_f\eta(t) - \int_0^t (\bar{\eta}\dot{\eta} + i\omega_o\bar{\eta}\eta + \frac{iM}{2}\dot{\mathbf{X}})ds \right] e^{i\omega_o t/2} \\ & \times \prod_{\mathbf{k}} \exp \left[ -i \int_0^t ds \bar{g}_{\mathbf{k}}(\mathbf{X}(s))e^{-i\omega_{\mathbf{k}}(t-s)}\bar{z}_{f\mathbf{k}} \eta(s) \right. \\ & \left. - \int_0^t ds \int_0^s dr g_{\mathbf{k}}(\mathbf{X}(s))\bar{g}_{\mathbf{k}}(\mathbf{X}(r))e^{-i\omega_{\mathbf{k}}(s-r)}\bar{\eta}(s)\eta(r) \right]. \end{aligned} \quad (5.10)$$

The path integral for the EMF degrees of freedom is now complete.

### 5.1.2 COM path integral

Second, the position path integral can be evaluated as a set of 0, 1 and 2 point functions. Note in the transition amplitude of Eq. (5.10) that since the EMF is

taken to be in an initial vacuum, any source term for  $\eta(s)$  will be proportional to  $\eta_i$ . The variational equation of motion derived from Eq. (5.10) for  $\eta(s)$  yields

$$\dot{\eta}(s) = -i\omega_o\eta(s) - i \int_0^s dr \sum_{\mathbf{k}} g_{\mathbf{k}}(\mathbf{X}(s))\bar{g}_{\mathbf{k}}(\mathbf{X}(r))e^{-i\omega_{\mathbf{k}}(s-r)}\eta(r) \quad (5.11)$$

with the boundary condition  $\eta(0) = \eta_i$ . Therefore  $\eta(s) = u(s)\eta_i$ . We use this to expand the exponent in the transition amplitude of Eq. (5.10). Due to the nilpotency of the Grassmann variables (i.e.  $\eta_i^2 = 0$ ) it will truncate after the first term in the expansion.

After expanding and truncating the integrand, the position path integral is

$$\begin{aligned} & \int D\mathbf{X} \exp \left[ -\frac{iM}{2} \int_0^t ds \dot{\mathbf{X}} \right] \\ & \times \left[ 1 - i \int_0^t ds \sum_{\mathbf{k}} \bar{g}_{\mathbf{k}}(\mathbf{X}(s))e^{-i\omega_{\mathbf{k}}(t-s)}\bar{z}_{f\mathbf{k}} \eta(s) \right. \\ & \quad \left. - \int_0^t ds \int_0^s dr \sum_{\mathbf{k}} g_{\mathbf{k}}(\mathbf{X}(s))\bar{g}_{\mathbf{k}}(\mathbf{X}(r))e^{-i\omega_{\mathbf{k}}(s-r)}\bar{\eta}(s)\eta(r) \right]. \end{aligned} \quad (5.12)$$

There are thus three correlation functions which need to be computed.

First the spatial mode functions must be chosen in order to specify the targeted correlation functions. For an electromagnetic field in free space (no cavity or boundaries)

$$g_{\mathbf{k}}(\mathbf{X}) = \frac{\lambda}{\sqrt{\omega_k}} \exp(i\mathbf{k} \cdot \mathbf{X}), \quad (5.13)$$

the correlations functions are computed in Appendix E. Substituting these

expressions back into the Eq. (5.10) gives for the transition amplitude

$$\begin{aligned}
K(t, 0) &= \left( \frac{M}{2\pi i t} \right)^{3/2} e^{i\omega_o t/2} e^{-i\omega_{\mathbf{k}}(s-r)} \\
&\times \int D\bar{\eta} D\eta \exp \left[ \frac{iM}{2t} (\mathbf{X}_f - \mathbf{X}_i)^2 + \bar{\eta}_f \eta(t) - \int_0^t (\bar{\eta} \dot{\eta} + i\omega_o \bar{\eta} \eta) ds \right] \\
&\times \left\{ 1 - i \int_0^t ds \sum_{\mathbf{k}} \frac{\lambda}{\sqrt{\omega_{\mathbf{k}}}} \exp \left[ i \frac{s}{t} \mathbf{k} \cdot (\mathbf{X}_f - \mathbf{X}_i) - \frac{i}{2M} \frac{s(t-s)}{t} \mathbf{k}^2 \right] e^{-i\omega_{\mathbf{k}}(t-s)} \bar{z}_{f\mathbf{k}} \eta(s) \right. \\
&\quad - \int_0^t ds \int_0^s dr \sum_{\mathbf{k}} \frac{\lambda^2}{\omega_{\mathbf{k}}} \exp \left[ -i \frac{s-r}{t} \mathbf{k} \cdot (\mathbf{X}_f - \mathbf{X}_i) \right. \\
&\quad \quad \left. \left. - \frac{i}{2M} \frac{(t-(s-r))(s-r)}{t} \mathbf{k}^2 \right] \bar{\eta}(s) \eta(r) \right\}.
\end{aligned} \tag{5.14}$$

The path integral for the external degrees of freedom is now complete.

### 5.1.3 Qubit path integral

Finally, the Grassmann variable path integral can be evaluated along its stationary path. The variational equation of motion for the Grassmann field variable in Eq. (5.14) is

$$\dot{\eta}_t(s) = -i\omega_o \eta_t(s) - \int_0^s dr \sum_{\mathbf{k}} \frac{\lambda^2}{\omega_{\mathbf{k}}} \mu_t(s-r) \eta_t(r) \tag{5.15}$$

with the definition:

$$\mu_t(s) = \exp \left[ -i\omega_{\mathbf{k}} s - i \frac{s}{t} \mathbf{k} \cdot (\mathbf{X}_f - \mathbf{X}_i) - \frac{i}{2M} \frac{s(t-s)}{t} \mathbf{k}^2 \right]. \tag{5.16}$$

Note that the final time  $t$  enters as a parameter in the variational equation of motion just as the mass or position do. The reason for this is that the above

variational equation of motion is for the evolution of the atom from an initial time to a final time, so the time is an explicit parameter.

Rewriting the above variational equation in Laplace space allows the non-local integral part to be transformed with the convolution theorem. The solution is in terms of an inverse Laplace transform,

$$\eta_t(s) = \eta_i u_t(s) = \frac{\eta_i}{2\pi i} \int_{\gamma-i\infty}^{\gamma+i\infty} \frac{e^{sz} dz}{z + i\omega_o + \tilde{\mu}(z)} \quad (5.17)$$

with the definition:

$$\tilde{\mu}_t(z) = \frac{\lambda^2}{\omega_{\mathbf{k}}} \int_0^\infty e^{-sz} \exp \left[ -i\omega_{\mathbf{k}} s - i \frac{s}{t} \mathbf{k} \cdot (\mathbf{X}_f - \mathbf{X}_i) - \frac{i}{2M} \frac{s(t-s)}{t} \mathbf{k}^2 \right] dz. \quad (5.18)$$

The solution thus becomes a contour integral. The pole of the denominator in Eq. (5.17) can be found to  $O(\lambda^2)$

$$z_o = -i\omega_o - \tilde{\mu}(-i\omega_o) + O(\lambda^4). \quad (5.19)$$

Finding the pole to order  $O(\lambda^2)$  gives a solution to the same order:

$$u_t(s) = e^{-i\omega_o t} \exp \left\{ -\lambda^2 t \sum_{\mathbf{k}} \frac{1}{\omega_{\mathbf{k}}} \int_0^\infty ds \right. \\ \left. \times \exp \left[ -i \left( \omega_{\mathbf{k}} - \omega_o + \frac{\mathbf{k} \cdot (\mathbf{X}_f - \mathbf{X}_i)}{t} - \frac{\mathbf{k}^2}{2M} \right) s - \frac{i\mathbf{k}^2}{2Mt} s^2 \right] \right\}. \quad (5.20)$$

Evaluating the transition amplitude along its stationary path with the second order pole approximation yields an expression for the transition matrix

that is second order in its action:

$$\begin{aligned}
K(t, 0) = & \left( \frac{M}{2\pi i t} \right)^{3/2} \exp \left[ i\omega_o t/2 + \frac{iM}{2t} (\mathbf{X}_f - \mathbf{X}_i)^2 + O(\lambda^4) \right] \\
& \times \exp \left[ \bar{\eta}_f \eta_t(t) - i \int_0^t ds \sum_{\mathbf{k}} \frac{\lambda}{\sqrt{\omega_{\mathbf{k}}}} \right. \\
& \left. \times \exp \left[ -i\omega_{\mathbf{k}}(t-s) + i\frac{s}{t} \mathbf{k} \cdot (\mathbf{X}_f - \mathbf{X}_i) - \frac{is(t-s)}{2Mt} \mathbf{k}^2 \right] \bar{z}_{f\mathbf{k}} \eta_t(s) \right].
\end{aligned} \tag{5.21}$$

All three functional integrals are now evaluated. In the next section we proceed to derive the evolutionary operator for the density matrix by combining the transition amplitudes into a closed loop.

## 5.2 Evolutionary operator

At this point the expression of Eq. (5.21) for the transition amplitude can be combined with its counterpart propagating backwards in time and traced over all final EMF states. The result gives the evolutionary operator for the reduced density matrix (we may call it the reduced propagator, for short),

$$J_R = \int d\mathbf{X}_f \prod_{\mathbf{k}} d\mu(z_{f\mathbf{k}}) K(t, 0) K^*(t, 0), \tag{5.22}$$

and is formed by integrating out the environmental variables which in our case are the EMF and the atom's motional degrees of freedom.

The evolution of the qubit density matrix elements with back-action from the EMF and the atomic motion can be calculated from the reduced propagator

$$\rho_R(t) = \int d\mu(\eta_i) d\mu(\eta'_i) d\mu(\mathbf{X}_i) J_R \rho_A(0) \otimes \rho_{\mathbf{X}}(0). \tag{5.23}$$

The functions  $\rho_A(0)$  and  $\rho_{\mathbf{X}}(0)$  are initial states for the 2-level atomic and external degrees of freedom, respectively:

$$\rho_A(t) = \rho_{00}(0) + \bar{\eta}_i \rho_{10}(0) + \eta'_i \rho_{01}(0) + \bar{\eta}_i \eta'_i \rho_{11}(0) \quad (5.24)$$

$$\rho_{\mathbf{X}}(t) = \Phi(\mathbf{X}_i) \Phi^*(\mathbf{X}_i) \quad (5.25)$$

The function  $\Phi(\mathbf{X})$  is the initial (external) center of mass wavefunction of the atom. From Eq. (5.23) the on and off-diagonal components of the reduced density matrix elements evolved to time  $t$  are given by

$$\begin{aligned} \rho_{11}(t) = \rho_{11}(0) \left( \frac{M}{2\pi i t} \right)^3 \int d\mathbf{X}_f \int d\mathbf{X}'_i \int d\mathbf{X}_i \Phi(\mathbf{X}_i) \Phi^*(\mathbf{X}'_i) \bar{u}_t(t) u_t(t) \\ \times \exp \left\{ \frac{iM}{2t} (\mathbf{X}_f - \mathbf{X}_i)^2 - \frac{iM}{2t} (\mathbf{X}_f - \mathbf{X}'_i)^2 \right\} \end{aligned} \quad (5.26)$$

$$\begin{aligned} \rho_{10}(t) = \rho_{10}(0) \left( \frac{M}{2\pi i t} \right)^3 \int d\mathbf{X}_f \int d\mathbf{X}'_i \int d\mathbf{X}_i \Phi(\mathbf{X}_i) \Phi^*(\mathbf{X}'_i) u_t(t) \\ \times \exp \left\{ \frac{iM}{2t} (\mathbf{X}_f - \mathbf{X}_i)^2 - \frac{iM}{2t} (\mathbf{X}_f - \mathbf{X}'_i)^2 \right\}. \end{aligned} \quad (5.27)$$

The EMF, as previously stated, is in a vacuum state, but the choice of an initial center of mass wavefunction has not yet been made. To closely model an atom with fixed position and momentum, we use a minimum uncertainty Gaussian wavefunction centered at  $(\mathbf{X}_o = 0, \mathbf{P}_o = 0)$ .

$$\Phi(\mathbf{X}) = \pi^{-3/4} \sigma^{-3/2} \exp \left[ -\frac{\mathbf{X}^2}{2\sigma^2} \right] \quad (5.28)$$

Such an initial wavefunction simplifies the expressions for the diagonal and off-diagonal matrix elements of the qubit.

The result for the off-diagonal components which measures the coherence of the qubit under such conditions is shown here:

$$\rho_{10}(t) = \rho_{10}(0) \frac{4}{\sqrt{\pi}} \left( \frac{M^2 \sigma^2}{t^2 - 2iM\sigma^2 t} \right)^{3/2} \int_0^\infty dx x^2 u(x, t) \exp \left[ - \frac{M^2 \sigma^2}{t^2 - 2iM\sigma^2 t} x^2 \right] \quad (5.29)$$

The function  $u(x, t)$  is given by Eq. (5.20) with  $x = |\mathbf{X}_f - \mathbf{X}_i|$ .

The evolution of the coherence function is found to follow an exponential decay with a decay rate slightly faster than in the infinite mass case. The percentage change in the decoherence rate of the off-diagonal versus the stationary qubit case is plotted in Fig. (5.1). The decay rate increases with decreasing mass and matches the stationary qubit result given by [12] in the limit of infinite mass. We expect that a qubit in a smaller mass object is more affected by recoil than a qubit in heavy mass. The variation in the decoherence rate with changes in the external wavefunction size is relatively flat and cannot reliably be resolved with the available computing power and machine accuracy. We find that so long as the resonant frequency is small enough or the mass large enough that the atomic recoil velocity is non-relativistic, which is where this theory is valid, then the motional decoherence will contribute negligibly to the decay of the qubit.

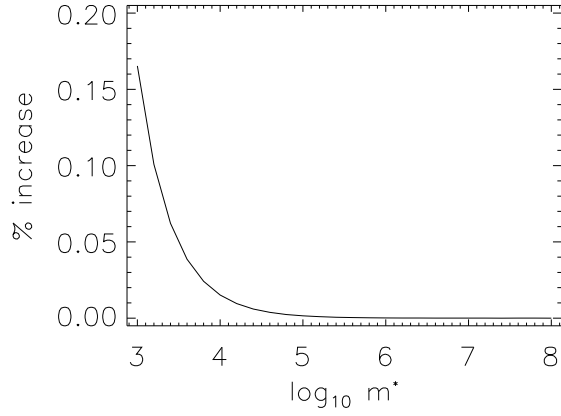


Figure 5.1: A plot of the percentage increase in the decoherence of the off-diagonal matrix elements of the reduced density matrix versus the non-dimensionalized mass ( $m^* = \frac{Mc^2}{\hbar\omega_o}$ ). The decoherence rate increases as the mass of the atom containing the qubit is decreased. As the mass is increased the decoherence rate asymptotes to the value of a stationary atom obtained by Anastopoulos and Hu [12]. This is consistent with a smaller mass qubit being more affected by its recoil than a heavy mass qubit. Typical experimental parameters fall to the right end of the shown plot.

### 5.3 Discussion

Often, one may separate the dynamics of an atom's motion from those of its internal degrees of freedom by arguing that the time scales associated with the motion of the atom are much longer than those of the two level activity. This is the rationale behind the adiabatic approximation adopted for most considerations of the atomic dynamics. However, coherence requirements in quantum computing implementations may prompt one to question this assumption. One aim of our investigation is to test for non-adiabatic effects in atomic quantum computing schemes. Another is to describe the effect of recoil from the emission and re-absorption of virtual particles in the atom-EMF interaction upon the center of mass motion. These two problems correspond to the two aspects described in the Introduction. Here we consider the second aspect mentioned above, aiming at the effect of quantum motional decoherence of the qubit, i.e., the back-action of atomic motion on a two level system in free space as mediated by the EMF.

We find that the inclusion of the external degrees of freedom only slightly alters the decoherence and relaxation rates as compared to a stationary atom. Typical experimental parameters fall to the right end in the plot of Fig. (5.1). A Rubidium atom used as a qubit would have a non-dimensionalized mass of approximately  $\log_{10}(\frac{Mc^2}{\hbar\omega_o}) = 8$ , which places it in a regime in which the effect of motion-induced decoherence is negligible. For optical qubit transition frequencies in general, motion-induced decoherence will not be a factor unless the mass of

the qubit is four to five orders of magnitude smaller than the mass of a typical alkali atom. One can conclude tentatively that in general AMO implementations, motion-induced decoherence of a free qubit is negligibly small. Since the calculation done here is coherent and non-Markovian, one can view our result as confirming the validity of the adiabatic approximation in alkali atom qubits.

Although the result of the calculation is the expected one, the technique described here is the first able to compute the decoherence of a qubit coupled to its own quantized COM without any form of Markovian approximation, while allowing the qubit-EMF coupling to be the non-linear form derived from the EMF spatial mode functions. Useful applications of this method will include any situations in which the COM motion of an atom back-acts onto its internal qubit dynamics and the full multi-mode structure of the EMF is relevant. Two such examples, as drawn from the references cited in the Introduction, are an atomic qubit in a cavity and an atom with entangled qubit and EMF degrees of freedom. In the former, the presence of the cavity walls increases the cavity mode recoils on the atom [76]. The latter is at the center of certain two qubit gate implementations [64, 65], with the question there being how well coherence is maintained when a qubit is entangled both internally and externally. Calculation in that case can provide an important feasibility test of quantum computing applications which utilize such entanglement.

# Chapter 6

## Discussion

Approaches to quantum dynamics can be categorized into three major subheadings. There are those based on the Schrödinger picture, those based on the Heisenberg picture, and path integral approaches. The work of this dissertation has focused on the last of the three, path integral approaches. Reviews of the first two as they are applied to AMO systems have been given. In the reviews, particular emphasis was placed on the approximations made during transformation from closed system+bath to open system only dynamics. In all cases the approximations can be boiled down to combinations of the small coupling and short correlation time approximations. By small coupling is meant the weakness of the interaction term relative to the free Hamiltonian terms. By short correlation time is meant the time scale over which backaction of the system state onto itself dephases. It is given by the timescale  $\tau_c$ , above which the bath correlation function  $tr_B \sum_k l_k(t)l_k(t - \tau)\rho_B$  dies off.

The derivation of open system dynamics in the Schrödinger picture leads to a Markovian master equation for the system density operator. Two equivalent

derivations of the Markovian master equation exist. Both apply the weak coupling and short correlation time approximations, but do so in different ways. The derivation of the Markovian master equation as described in [11] makes two assumptions. The first is the assumption that the total system+bath density operator is a product state with a fixed bath at all times, and the second is the Markov approximation. The assumption of a product state with fixed bath specifically neglects any correlations between the system and bath. The reason that this is a weak coupling plus short correlation time approximation is that the order of the terms neglected are  $O(V^2\tau_c)$  [18, 21]. The Markov approximation, as applied in the derivation of Ref. [11], is the standard one. It was pointed out that the Markov approximation is also an approximation in both the coupling strength and correlation time. That is, since the density operator is in the interaction picture, the substitution of  $\rho_I(t') \rightarrow \rho_I(t)$  in the expression

$$\dot{\rho}_I(t) = -\frac{1}{\hbar^2} \int_{t_0}^t dt' tr_B \sum_k l_k(t) l_k(t') \rho_B \otimes \rho_I(t') \quad (6.1)$$

implicitly assumes that the evolution of  $\rho_I(t)$  during a correlation time can be approximated by its free evolution during that period [20, 21].

The second equivalent derivation of the Markovian master equation is described in, for example, Ref. [18]. There, the master equation is derived from a perturbative truncation that is valid only for short time dynamics.

Approximations are then applied which extend it to a coarse grained dynamical equation that is valid for long times under the given assumptions. The validity of

extension of the perturbative result to long time dynamics is based on a separation of time scales between the bath correlation time,  $\tau_c$ , and the system evolution time scale,  $\tau_r$ , such that  $\tau_c \ll \tau_r$ . If there is wide separation between those time scales, then a coarse graining time scale can be chosen between them such that  $\tau_c \ll \Delta\tau \ll \tau_r$ . The relation  $\Delta\tau \ll \tau_r$  is required for the coarse graining time to be short enough that the perturbative result is valid. The relation  $\tau_c \ll \Delta\tau$  is required so that the system+bath correlations can be ignored, as in the previous derivation. The condition for large separation of time scales is found to be the same as for the approximations in the previous derivation,

$$V^2\tau_c \ll 1. \tag{6.2}$$

The major difference between this and the previous derivation is that the Markovian master equation is shown to be a coarse grained equation.

In the Heisenberg picture it is the quantum operators which are evolved, while the states are static. This leads to quantum Langevin equations for interacting systems. Application of this technique to AMO systems is described in Refs. [18, 20], among others. The major approximation applied in the derivation of the quantum Langevin equations is the 1<sup>st</sup> Markov approximation [20], which is the usual Markov approximation, but applied to the reaction term only and not to the noise operator. It is an approximation of weak coupling and short correlation time, since as mentioned previously, it assumes

that the system evolution due to the interaction term is small during a correlation time, so it neglects terms of order  $O(V^2\tau_c)$ . Since the Markov approximation is applied only to the reaction term, the quantum Langevin approach is more exact than the Markovian master equation approach. By applying weak coupling and short time approximations to the noise operator, via an adjoint equation or quantum stochastic differential equation, the two approaches can be made equivalent [20].

In path integral approaches, rather than evolving either the states or operators of a system, it is directly the transition amplitudes which are the focus. After the choice of a suitable representation, they can be used to compute objects, such as the reduced propagator, which lead to reduced system dynamics. Unlike the Markovian master equation and quantum Langevin approaches, in path integral approaches interesting results can be found with the weak coupling approximation alone via a  $2^{nd}$  order vertex approximation. That leads to an order  $O(V^2)$  approximation, compared to  $O(V^2\tau_c)$  for the other methods. The source of their advantage that they allow coherent evolution of the full system+bath. Then, after the full evolution of the closed system, unobserved bath degrees of freedom can be traced out, leaving reduced system dynamics. In this way the effects due to correlations that develop between the system and bath are retained. That is the approach taken in the three applications described in the previous three chapters.

The results of analysis in these three problems involving the qubit-EMF

system are briefly summarized as follows. First, in our coherent computation of the Casimir-Polder retardation of the van der Waals force, a result is obtained which is up to twice the stationary atom correction. The modification is due to correlations that develop between the atom and its virtual photon cloud during adiabatic motion. Second, in the entangled evolution of a qubit with an *initially* thermal low temperature bath, quantum correlations that evolve between the qubit and bath alter the reduced dynamics. The diagonal matrix elements thermalize and the off-diagonal decohere as expected, however they do so non-exponentially. The result can be interpreted as a time dependent decoherence rate. Third, in the calculation of qubit dynamics in the presence of quantized atomic motion the decoherence rates increase slightly due to the additional degree of freedom.

The message of the first two results is that when the entanglement between a system and an environment is maintained in their evolution, the dynamics of the system can exhibit novel behavior different from Markovian predictions. The message of the third is that including extra degrees of freedom in an environment interacting with a qubit will increase the decay of the qubit. The novel behavior in the first two problems can be interpreted as the accumulated back-action of each individual mode of the EMF. The influence on the system of the individual field modes do not cancel each other out because it is through the interaction with the system itself that the EMF modes become correlated. The inclusion of coherent back-action leads to new effects in

circumstances like this when no mechanism exists for the environmental degrees of freedom to randomize their quantum correlations independent of the system.

Future work can follow three main lines, but all involve computation of entangled evolution effects. The first, involving the coherent QED modification of the Casimir-Polder force is to change either the reflective characteristics or geometry of the walls. An extension which is important for comparison with experimental results is allowing the wall to be a dielectric. When the wall is a dielectric rather than a perfect conductor the boundary conditions on the wall become somewhat more complicated, but in principle the decomposition of modes that satisfy the boundary conditions can be found in terms of evanescent and travelling modes [41]. Changing the geometry of the wall will also change the mode decomposition of the EMF. Two interesting geometries, which may have quantum computing relevance are a curved surface (trapping over a curved surface) [77], and a cavity (pair of parallel walls) [78].

The second extends the finding of altered reduced qubit dynamics due to entangled evolution with a thermal EMF to entangled evolution with EMF control fields. Normally the laser fields that mediate and control the atomic qubits are treated as classical fields. Such treatments are generally good approximations to the true nature of the control fields, although in reality the control fields are quantum. The major distinction between the two from an applications point of view is that classical fields are unaffected by interaction with quantum systems, while a quantum field will become entangled with any

quantum system with which it interacts. For rough usage in applications where quantum coherence is not important, the distinction between quantum and classical control fields can be neglected. However, for applications such as quantum processing, for which the entangled evolution of the system is of paramount importance, the entanglement between the system and control fields should be considered. The modifications of the evolution of a neutral atom qubit due to entanglement with the control fields will include additional decoherence of the qubits and changes in the evolution during gates [14].

The third line of future work extends the computation of decoherence due to COM motional degrees of freedom. It can be extended to the computation of motional decoherence when the COM position is entangled with the qubit state, as in some two qubit gate proposals [64, 65]. The result will be an important feasibility condition relating the separation distance and the extra decoherence.

# Appendix A

## Simple examples of Grassmann path integrals

### A.1 Spin- $\frac{1}{2}$ in a general time-dependent classical magnetic field

To illustrate the use of time-indexed anticommuting couplings the following is a calculation of the evolution of a spin- $\frac{1}{2}$  in a classical magnetic field. The simplest non-trivial case is that of a spin in a  $B_z$  field with the addition of a possibly time-dependent  $B_x$  and  $B_y$  field. The Hamiltonian for this system is

$$H = \gamma \mathbf{S} \cdot \mathbf{B} \equiv \frac{1}{2} \hbar \omega S_z + \hbar B_x S_x + \hbar B_y S_y = \hbar \omega S_+ S_- - \frac{1}{2} \hbar \omega + \hbar [S_+ B + B^* S_-]. \quad (\text{A.1})$$

Here it is written in a “hermitian” form in anticipation of the addition of a Grassmann part to the classical field. The propagator between initial and final Grassmann coherent states is

$$K(t, 0) = \langle \bar{\eta}_t | e^{-\frac{i}{\hbar} \int_0^t H(s) ds} | \eta_0 \rangle. \quad (\text{A.2})$$

In the usual way ( $t = N\epsilon$ ) the propagator can be time sliced into a discrete time formulation. The propagator for one infinitesimal time step is (up to  $O(\epsilon)$ )

$$K(j, j-1) = \langle \bar{\eta}_j | e^{-\frac{i}{\hbar} H \epsilon} | \eta_{j-1} \rangle = \exp\{(1 - i\omega\epsilon)\bar{\eta}_j \eta_{j-1} - \bar{\eta}_j (iB_j \epsilon) - (iB_j^* \epsilon) \eta_{j-1}\}. \quad (\text{A.3})$$

With Eq. (A.3) the propagator for a single infinitesimal step can be written down,

$$K(\epsilon, 0) = e^{(1 - i\omega\epsilon)\bar{\eta}_1 \eta_0 - \bar{\eta}_1 (iB_1 \epsilon) - (iB_1^* \epsilon) \eta_0} = e^{\bar{\eta}_1 \eta_1 - \phi_1} \quad (\text{A.4})$$

and the propagator for two infinitesimal time steps is

$$\begin{aligned} K(2\epsilon, 0) &= \int d\mu(\eta_1) \langle \bar{\eta}_2 | e^{-\frac{i}{\hbar} H_2 \epsilon} | \eta_1 \rangle \langle \bar{\eta}_1 | e^{-\frac{i}{\hbar} H_1 \epsilon} | \eta_0 \rangle \\ &= e^{(1 - i\omega\epsilon)^2 \bar{\eta}_2 \eta_0} [1 - \eta_2 (iB_2 \epsilon) - (iB_1^* \epsilon) \eta_0 - B_2 B_1^* \epsilon^2 \bar{\eta}_2 \eta_0 - \bar{\eta}_2 (iB_1 \epsilon) (1 - i\omega\epsilon) \\ &\quad - (1 - i\omega\epsilon) (iB_2^* \epsilon) \eta_0 - B_2^* B_1 \epsilon^2 + B_2 B_1^* \epsilon^2 (1 - i\omega\epsilon)^2 \bar{\eta}_2 \eta_0]. \end{aligned} \quad (\text{A.5})$$

These two propagators have very different forms. However if at this point a time-indexed anticommuting part is given to the classical field such that  $\{B_n, B_m\} = 0$  and  $\{B_n, \eta\} = \{B_n, \bar{\eta}\} = 0$  then the  $2\epsilon$  propagator can be rewritten as a single exponential,

$$\begin{aligned} K(2\epsilon, 0) &= e^{\bar{\eta}_2 [-iB_2 \epsilon + (1 - i\omega\epsilon)(-iB_1 \epsilon + (1 - i\omega\epsilon)\eta_0)] + [-iB_1^* \epsilon \eta_0 - (iB_2^* \epsilon)(-iB_1 \epsilon + (1 - i\omega\epsilon)\eta_0)]} \\ &\equiv e^{\bar{\eta}_2 \eta_2 + \phi_2} \end{aligned} \quad (\text{A.6})$$

with the definitions

$$\eta_2 = (1 - i\omega\epsilon)\eta_1 - iB_2 \epsilon \quad (\text{A.7})$$

$$\phi_2 = \phi_1 - iB_2^* \epsilon \eta_1. \quad (\text{A.8})$$

Now the  $2\epsilon$  propagator is in the same form as the  $\epsilon$  propagator. This facilitates a recursive evaluation, so that process can be continued to find the propagator for any number of steps,

$$K(j\epsilon, 0) = e^{\bar{\eta}_j \eta_j + \phi_j} \quad (\text{A.9})$$

with the recursive definitions

$$\begin{aligned} \eta_j &= (1 - i\omega\epsilon)\eta_{j-1} - iB_j\epsilon & \eta_0 &= \eta_i \\ \phi_j &= \phi_{j-1} - iB_j^*\epsilon\eta_{j-1} & \phi_0 &= 0. \end{aligned} \quad (\text{A.10})$$

Inserting the boundary condition  $\bar{\eta}_N = \bar{\eta}_f$ , one gets for the full propagator

$$K(t = N\epsilon, 0) = \exp\{\bar{\eta}_f \eta_N + \phi_N\}, \quad (\text{A.11})$$

with the variables  $\eta_N$  and  $\phi_N$  defined by Eq. (A.10).

The propagator in the above form can not yet be shown to satisfy the Schrödinger equation because it hides a major pitfall. The pitfall is that it is a formal expression and has meaning only as a polynomial expansion. Due to the introduction of the time-indexed anticommuting part in the magnetic field, many terms in the polynomial expansion truncate due to the nilpotency of the Grassmann variables. However this is not a weakness, but a strength, since the truncation of polynomial expansions is the reason Grassmann variables were introduced. If the continuous limit were taken at this point the correct expansion of the exponential propagator would be lost. Expanding the propagator gives

$$K(t, 0) = e^{\bar{\eta}_f \eta_N + \phi_N} = \sum_{m=0}^{\infty} \frac{(\phi_N)^m}{m!} [1 + \bar{\eta}_f \eta_N]. \quad (\text{A.12})$$

In the expansion above the Grassmann variable  $\bar{\eta}_f$  causes a truncation.

Analogously, in the  $m^{\text{th}}$  order terms such as  $(\phi_N)^m$ , the time-indexed Grassmann parts of the magnetic field cause a truncation. That is,  $\phi_N$  is a sum of terms containing many products of Grassmann variables. Products of these coefficients have many terms that are truncated due to nilpotency of the Grassmann variables. Keeping track of the truncations in the final coefficients would be a formidable task, however doing so in the infinitesimal equations of motion is sufficient. For example, instead of calculating  $(\phi_N)^m$  by calculating  $\phi_N$  first, one can find a differential equation for  $(\phi_N)^m$  and calculate it directly. The functions that need to be calculated are thus  $(\phi_N)^m$  and  $(\phi_N)^m \eta_N$ . Adhering to the anticommutation rules one finds (up to  $O(\epsilon)$ ),

$$(\phi^m)_j = (\phi^m)_{j-1} - imB_j^* \epsilon (\phi^{m-1} \eta)_{j-1} \quad (\text{A.13})$$

$$(\phi^m \eta)_j = (1 - i\omega \epsilon) (\phi^m \eta)_{j-1} - iB_j \epsilon (\phi^m)_{j-1}. \quad (\text{A.14})$$

The above equations can now safely be taken to the continuous limit,

$$\frac{d}{dt} (\phi^m)_t = -imB^*(t) (\phi^{m-1} \eta)_t \quad (\text{A.15})$$

$$\frac{d}{dt} (\phi^m \eta)_t = -i\omega (\phi^m \eta)_t - iB(t) (\phi^m)_t, \quad (\text{A.16})$$

and used to show that the propagator satisfies the Schrödinger equation,

$$\begin{aligned} i\hbar \frac{d}{dt} \langle \bar{\eta}_f | K(t, 0) | \eta_0 \rangle &= i\hbar \frac{d}{dt} \sum_{m=0}^{\infty} \frac{1}{m!} [(\phi^m)_t + \bar{\eta}_f (\phi^m \eta)_t] \\ &= \hbar \sum_{m=0}^{\infty} \frac{1}{m!} [B^* (\phi^m \eta)_t + \bar{\eta}_f B (\phi^m)_t + \omega \bar{\eta}_f (\phi^m \eta)_t] \end{aligned} \quad (\text{A.17})$$

$$\begin{aligned}
\langle \bar{\eta}_f | H K(t, 0) | \eta_0 \rangle &= \int d\mu(\eta) \langle \bar{\eta}_f | H | \eta \rangle \langle \bar{\eta} | K(t, 0) | \eta_0 \rangle \\
&= \hbar \sum_{m=0}^{\infty} \frac{1}{m!} [B^*(\phi^m \eta)_t + \bar{\eta}_f B(\phi^m)_t + \omega \bar{\eta}_f (\phi^m \eta)_t]. \quad (\text{A.18})
\end{aligned}$$

The propagator Eq. (A.12) and Eq. (A.15-A.16) give a novel expansion of the propagator and equations for the terms in its expansion. The Schrödinger equation can be reformed from it, but in the expanded form it may be possible to apply new approximations. This issue is addressed in future work.

Having introduced and justified the introduction of the Grassmann partners, they can now be used to rewrite the propagator as a true path integral. The propagator for finite time is

$$K(t, 0) = \int \prod_{j=1}^{N-1} d\mu(\eta_j) \langle \bar{\eta}_N | e^{-\frac{i}{\hbar} H \epsilon} | \eta_{N-1} \rangle \langle \bar{\eta}_{N-1} | e^{-\frac{i}{\hbar} H \epsilon} | \eta_{N-2} \rangle \dots \langle \bar{\eta}_1 | e^{-\frac{i}{\hbar} H \epsilon} | \eta_0 \rangle. \quad (\text{A.19})$$

Due to the anti-commuting properties of the Grassmann variables, the infinitesimal propagators in the above expression could not be combined into a single exponential if a time-indexed anticommuting part were not introduced.

After their introduction the propagator becomes,

$$\begin{aligned}
K(t, 0) &= \int \prod_{j=1}^{N-1} d^2 \eta_j \exp \{ \bar{\eta}_N \eta_N \\
&\quad + \sum_{j=1}^N [-\bar{\eta}_j \eta_j + (1 - i\omega \epsilon) \bar{\eta}_j \eta_{j-1} - i\bar{\eta}_j B_j \epsilon - iB_j^* \epsilon \eta_{j-1}] \}. \quad (\text{A.20})
\end{aligned}$$

One may now evaluate this discrete path integral at the saddle point. Varying discretely, the discrete equation for the stationary path is found to be

$$\eta_j = (1 - i\omega \epsilon) \eta_{j-1} - iB_j \epsilon \quad (\text{A.21})$$

and the propagator is

$$K(t, 0) = \exp\{\bar{\eta}_N \eta_N + \sum_{j=1}^N [-(iB_j^* \epsilon) \eta_{j-1}]\}. \quad (\text{A.22})$$

Or, defining again the variable

$$\phi_j = -i \sum_{i=1}^j B_i^* \epsilon \eta_{i-1} = \phi_{j-1} - iB_j^* \epsilon \eta_{j-1}, \quad (\text{A.23})$$

and inserting the correct boundary conditions  $\bar{\eta}_N = \bar{\eta}_f$  and  $\eta_0 = \eta_i$ , one gets for the propagator

$$K(t, 0) = \exp\{\bar{\eta}_f \eta_t + \phi_t\}, \quad (\text{A.24})$$

with the variables  $\eta_N$  and  $\phi_N$  defined by Eq. (A.21) and Eq. (A.23). This is the same as the exact result previously derived. This example was handled, in the stationary path approximation, using a boson mapping in [35] and using the SU(2) representation in [33]. The result found here of exactness of the stationary path approximation agrees with the same result found in those references.

## A.2 Single mode Jaynes-Cummings

The Jaynes-Cummings Hamiltonian for a qubit interacting with a single EM field mode is

$$H = \hbar\omega_o S_+ S_- + \hbar\omega a^\dagger a + \hbar[S_+ \lambda a + a^\dagger \lambda S_-]. \quad (\text{A.25})$$

Here again it is written in a “hermitian” form in anticipation of the addition of a Grassmann part to the spin-boson coupling constant. The propagator between

initial and final coherent states is

$$K(t, 0) = \langle \bar{\eta}_t \bar{z}_t | e^{-\frac{i}{\hbar} \int_0^t H(s) ds} | \eta_0 z_0 \rangle. \quad (\text{A.26})$$

In the usual way ( $t = N\epsilon$ ) the propagator can be time sliced into a discrete time formulation. The propagator for one infinitesimal time step is (up to  $O(\epsilon)$ )

$$\begin{aligned} K(j, j-1) &= \langle \bar{\eta}_j \bar{z}_j | e^{-\frac{i}{\hbar} H\epsilon} | \eta_{j-1} z_{j-1} \rangle \\ &= \exp\{(1 - i\omega\epsilon)\bar{z}_j z_{j-1} + (1 - i\omega_o\epsilon)\bar{\eta}_j \eta_{j-1} \\ &\quad - \bar{\eta}_j(i\lambda_j\epsilon)z_{j-1} - \bar{z}_j(i\lambda_j\epsilon)\eta_{j-1}\}. \end{aligned} \quad (\text{A.27})$$

Using this equation the single infinitesimal step propagator is,

$$K(\epsilon, 0) = \langle \bar{\eta}_1 \bar{z}_1 | U_\epsilon | \eta_0 z_0 \rangle = e^{\bar{\eta}_1[\psi_1 + g_1] + \bar{z}_1[f_1 + \phi_1]} \quad (\text{A.28})$$

with the definitions,

$$\begin{aligned} g_1 &= (i\lambda_2\epsilon)z_0 & \psi_1 &= (1 - i\omega_o\epsilon)\eta_0 \\ f_1 &= (1 - i\omega\epsilon)z_0 & \phi_1 &= (i\lambda_2\epsilon)\eta_0 \end{aligned} \quad (\text{A.29})$$

The  $2\epsilon$  propagator is then computed from the above to be,

$$K(2\epsilon, 0) = \langle \bar{\eta}_2 \bar{z}_2 | U_{2\epsilon} | \eta_0 z_0 \rangle = \int d\mu(z_1) d\mu(\eta_1) \langle \bar{\eta}_2 \bar{z}_2 | U_\epsilon | \eta_1 z_1 \rangle \langle \bar{\eta}_1 \bar{z}_1 | U_\epsilon | \eta_0 z_0 \rangle \quad (\text{A.30})$$

which yields the following unwieldy expression,

$$\begin{aligned} K(2\epsilon, 0) &= e^{(1 - i\omega_o\epsilon)\bar{\eta}_2\psi_1 + (1 - i\omega\epsilon)\bar{z}_2 f_1} [1 + i\lambda\epsilon\bar{z}_2\psi_1 + (1 - i\omega_o\epsilon)\bar{\eta}_2 g_1 \\ &\quad + i\lambda\epsilon\bar{\eta}_2 f_1 + (1 - i\omega\epsilon)\bar{z}_2\phi_1 + i\lambda\epsilon\bar{z}_2 g_1 + i\lambda\epsilon\bar{\eta}_2\phi_1 \\ &\quad + i\lambda\epsilon\bar{\eta}_2\phi_1(1 - i\omega\epsilon)\bar{z}_2 f_1 - i\lambda\epsilon\bar{z}_2 g_1(1 - i\omega_o\epsilon)\bar{\eta}_2\psi_1] \end{aligned} \quad (\text{A.31})$$

At this point a time-indexed anticommuting part is given to the coupling constants such that  $\{\lambda_n, \lambda_m\} = 0$  and  $\{\lambda_n, \eta\} = \{\lambda_n, \bar{\eta}\} = 0$ . The  $2\epsilon$  propagator can be rewritten as a single exponential in the same form as the  $\epsilon$  propagator,

$$K(2\epsilon, 0) = \exp\{\bar{\eta}_2[\psi_2 + g_2] + \bar{z}_2[\phi_2 + f_2]\} \quad (\text{A.32})$$

with the definitions,

$$\begin{aligned} g_2 &= (1 - i\omega_o\epsilon)g_1 + (i\lambda_2\epsilon)f_1 & \psi_2 &= (1 - i\omega_o\epsilon)\psi_1 + (i\lambda_2\epsilon)\phi_1 \\ f_2 &= (i\lambda_2\epsilon)g_1 + (1 - i\omega\epsilon)f_1 & \phi_2 &= (i\lambda_2\epsilon)\psi_1 + (1 - i\omega\epsilon)\phi_1 \end{aligned} \quad (\text{A.33})$$

Or for greater ease of use,

$$K(2\epsilon, 0) = \exp\{\bar{\eta}_2\eta_2 + \bar{z}_2z_2\} \quad (\text{A.34})$$

with the definitions,

$$\eta_2 = (1 - i\omega_o\epsilon)\eta_1 + (i\lambda_2\epsilon)z_1 \quad (\text{A.35})$$

$$z_2 = (i\lambda_2\epsilon)\eta_1 + (1 - i\omega\epsilon)z_1. \quad (\text{A.36})$$

This process can be continued to find the propagator for any number of infinitesimal steps, with the result,

$$K(j\epsilon, 0) = \exp\{\bar{\eta}_j\eta_j + \bar{z}_jz_j\} \quad (\text{A.37})$$

and the definitions,

$$\eta_j = (1 - i\omega_o\epsilon)\eta_{j-1} + (i\lambda_j\epsilon)z_{j-1} \quad (\text{A.38})$$

$$z_j = (i\lambda_j\epsilon)\eta_{j-1} + (1 - i\omega\epsilon)z_{j-1}. \quad (\text{A.39})$$

After inserting the correct boundary conditions  $\bar{\eta}_N = \bar{\eta}_f$ ,  $\eta_0 = \eta_i$ ,  $\bar{z}_N = \bar{z}_f$ , and  $z_0 = z_i$  the propagator for time  $t = N\epsilon$  is

$$K(t = N\epsilon, 0) = \exp\{\bar{\eta}_f \eta_N + \bar{z}_f z_N\} \quad (\text{A.40})$$

with the variables  $\eta_N$ , and  $z_N$  defined by Eq. (A.38) and Eq. (A.39).

As in the previous example the propagator in the above form is only a formal expression and has meaning only as a polynomial expansion. Many terms in the polynomial expansion truncate due to the nilpotency of the Grassmann variables. Expanding the propagator gives

$$K(t, 0) = e^{\bar{\eta}_f \eta_N + \bar{z}_f z_N} = \sum_{m=0}^{\infty} \frac{(\bar{z}_f z_N)^m}{m!} [1 + \bar{\eta}_f \eta_N]. \quad (\text{A.41})$$

As before differential equations are found for the functions in the expansion of the propagator. The functions that need to be calculated are  $(z_N)^m$  and  $(z_N)^m \eta_N$ . Adhering to the anticommutation rules one finds (up to  $O(\epsilon)$ ),

$$(z^m)_j = (1 - im\omega\epsilon)(z^m)_{j-1} - im\lambda_j\epsilon(z^{m-1}\eta)_{j-1} \quad (\text{A.42})$$

$$(z^m\eta)_j = (1 - im\omega\epsilon - i\omega_o\epsilon)(z^m\eta)_{j-1} - i\lambda_j\epsilon(z^{m+1})_{j-1}. \quad (\text{A.43})$$

Or in the continuous limit,

$$\frac{d}{dt}(z^m)_t = -im\omega(z^m)_t - im\lambda(z^{m-1}\eta)_t \quad (\text{A.44})$$

$$\frac{d}{dt}(z^m\eta)_t = (-im\omega - i\omega_o)(z^m\eta)_t - i\lambda(z^{m+1})_t. \quad (\text{A.45})$$

The propagator of Eq. (A.41) can now be shown to satisfy the Schrödinger

equation.

$$\begin{aligned}
i\hbar \frac{d}{dt} \langle \bar{\eta}_f \bar{z}_f | K(t, 0) | \eta_0 z_0 \rangle &= i\hbar \frac{d}{dt} \sum_{m=0}^{\infty} \frac{(\bar{z}_f)^m}{m!} [(z^m)_t + \bar{\eta}_f (z^m \eta)_t] \quad (\text{A.46}) \\
&= \hbar \sum_{m=0}^{\infty} \frac{(\bar{z}_f)^m}{m!} \left[ (m\omega (z^m)_t + m\lambda (z^{m-1} \eta)_t) \right. \\
&\quad \left. + \bar{\eta}_f ((m\omega + \omega_o) (z^m \eta)_t + \lambda (z^{m+1})_t) \right]
\end{aligned}$$

$$\begin{aligned}
\langle \bar{\eta}_f \bar{z}_f | H K(t, 0) | \eta_0 z_0 \rangle &= \int d\mu(\eta) d\mu(z) \langle \bar{\eta}_f \bar{z}_f | H | \eta z \rangle \langle \bar{\eta} \bar{z} | K(t, 0) | \eta_0 z_0 \rangle \quad (\text{A.47}) \\
&= \hbar \sum_{m=0}^{\infty} \frac{(\bar{z}_f)^m}{m!} \left[ (m\omega (z^m)_t + m\lambda (z^{m-1} \eta)_t) \right. \\
&\quad \left. + \bar{\eta}_f ((m\omega + \omega_o) (z^m \eta)_t + \lambda (z^{m+1})_t) \right]
\end{aligned}$$

As in the previous example the propagator Eq. (A.41) and Eqs. (A.44-A.45) give a novel expansion of the propagator and equations for the terms in its expansion. However, in this case the unexpanded expression may offer an advantage when seeking the reduced dynamics. In that case the final state of the e.g. boson can be traced out using the formal exponential version of Eq. (A.41), leaving a formal expression for the reduced propagator. Equations (A.44-A.45) can then be used to find solutions for terms in the expansion of the reduced propagator.

It remains to show that the stationary path approximation yields the same exact result in this example. The propagator for finite time in this case is

$$\begin{aligned}
K(t, 0) &= \int \prod_{j=1}^{N-1} d\mu(\eta_j) d\mu(z_j) \langle \bar{\eta}_N \bar{z}_N | e^{-\frac{i}{\hbar} H \epsilon} | \eta_{N-1} z_{N-1} \rangle \\
&\quad \times \langle \bar{\eta}_{N-1} \bar{z}_{N-1} | e^{-\frac{i}{\hbar} H \epsilon} | \eta_{N-2} z_{N-2} \rangle \dots \langle \bar{\eta}_1 \bar{z}_1 | e^{-\frac{i}{\hbar} H \epsilon} | \eta_0 z_0 \rangle. \quad (\text{A.48})
\end{aligned}$$

As for the previous example the infinitesimal propagators in the above expression can be combined into a single exponential only after the introduction of a Grassmann partners to the coupling constants. The propagator is then written,

$$K(t, 0) = \int \prod_{j=1}^{N-1} d^2\eta_j d^2z_j \exp\{\bar{z}_N z_N + \bar{\eta}_N \eta_N\} \exp\left\{\sum_{j=1}^N [-\bar{z}_j z_j - \bar{\eta}_j \eta_j + (1 - i\omega\epsilon)\bar{z}_j z_{j-1} + (1 - i\omega_o\epsilon)\bar{\eta}_j \eta_{j-1} - \bar{\eta}_j(i\lambda_j\epsilon)z_{j-1} - \bar{z}_j(i\lambda_j\epsilon)\eta_{j-1}]\right\}. \quad (\text{A.49})$$

Varying discretely about the saddle point, equations for the stationary path are found to be

$$z_j = (1 - i\omega\epsilon)z_{j-1} - i\lambda_j\epsilon\eta_{j-1} \quad (\text{A.50})$$

$$\eta_j = (1 - i\omega_o\epsilon)\eta_{j-1} - i\lambda_j\epsilon z_{j-1} \quad (\text{A.51})$$

and the propagator after inserting the correct boundary conditions  $\bar{\eta}_N = \bar{\eta}_f$ ,  $\eta_0 = \eta_i$ ,  $\bar{z}_N = \bar{z}_f$ , and  $z_0 = z_i$  is

$$K(t, 0) = \exp\{\bar{\eta}_f \eta_N + \bar{z}_f z_N\}. \quad (\text{A.52})$$

with the variables  $\eta_N$  and  $\phi_N$  defined by Eqs. (A.50-A.51). This again is the same as the exact result, thereby demonstrating that the stationary path approximation is exact for the Jaynes-Cummings Hamiltonian. This specific example was computed with the stationary path approximation in [12] using a Grassmannian path integral and in [34] using the SU(2) representation. The results here agree with those found in [34], where it was also found that the stationary path approximation yielded exact results. The range of validity for the

Grassmannian path integral method in [12] was restricted to an initial bosonic vacuum state, but for that restricted range they also found the stationary path approximation to be exact.

## Appendix B

### Recursive calculation of effective action

The Hamiltonian is given in Eq. (4.1). The evaluation of the transition amplitude as a path integral begins with slicing it into infinitesimal steps. A single infinitesimal step transition amplitude for initial EMF vacuum and atomic ground state (i.e. the initial EMF and Grassmannian labels set to zero) is,

$$\begin{aligned} & \langle \mathbf{X}_1, \{\bar{z}_{1\mathbf{k}}\}, \bar{\psi}_1; t + \epsilon | \exp[-\frac{i}{\hbar} H \epsilon] | \mathbf{X}_0, \{0_{\mathbf{k}}\}, 0; t \rangle \\ &= \exp \left[ \frac{iM(\mathbf{X}_1 - \mathbf{X}_0)^2 \epsilon}{2\epsilon^2 \hbar} - i \sum_{\mathbf{k}e} \bar{\psi}_1 \bar{z}_{1\mathbf{k}} \frac{g_{1e} \epsilon}{\sqrt{\omega_{\mathbf{k}}}} \mathbf{p}_{\text{eg}} \cdot \mathbf{u}_{\mathbf{k}}^\dagger - i \sum_{\mathbf{k}l} \bar{z}_{1\mathbf{k}} \bar{z}_{1l} \frac{\lambda^2 \epsilon}{\sqrt{\omega_{\mathbf{k}} \omega_l}} \mathbf{u}_{\mathbf{k}}^\dagger \cdot \mathbf{u}_l^\dagger \right] \end{aligned} \quad (\text{B.1})$$

$$= \exp \left[ \frac{iM(\mathbf{X}_1 - \mathbf{X}_0)^2 \epsilon}{2\epsilon^2 \hbar} + A_1 + \sum_{\mathbf{k}e} \bar{\psi}_1 \bar{z}_{1\mathbf{k}} B_{1\mathbf{k}e} + \sum_{\mathbf{k}l} \bar{z}_{1\mathbf{k}} \bar{z}_{1l} C_{1\mathbf{k}l} \right] \quad (\text{B.2})$$

With the obvious definitions of  $A_1$ ,  $B_{1\mathbf{k}e}$ , and  $C_{1,\mathbf{k}l}$ . The first infinitesimal step transition amplitude, Eq. (B.1), can be used to derive the 2 infinitesimal step

amplitude:

$$\begin{aligned}
& \langle \mathbf{X}_2, \{\bar{z}_{\mathbf{k}2}\}, \bar{\psi}_2; t + 2\epsilon | \exp[-2\frac{i}{\hbar}H\epsilon] | \mathbf{X}_0, \{0_{\mathbf{k}}\}, 0; t \rangle = \\
& \int d\mu(\mathbf{X}_1) d\mu(z_1) d\mu(\psi_1) \langle \mathbf{X}_2, \{\bar{z}_{\mathbf{k}2}\}, \bar{\psi}_2; t + 2\epsilon | \exp[-\frac{i}{\hbar}H\epsilon] | \mathbf{X}_1, \{z_{1\mathbf{k}}\}, \psi_1; t + \epsilon \rangle \\
& \quad \times \langle \mathbf{X}_1, \{\bar{z}_{1\mathbf{k}}\}, \bar{\psi}_1; t + \epsilon | \exp[-\frac{i}{\hbar}H\epsilon] | \mathbf{X}_0, \{0_{\mathbf{k}}\}, 0; t \rangle \quad (\text{B.3})
\end{aligned}$$

The result is:

$$\begin{aligned}
& \langle \mathbf{X}_2, \{\bar{z}_{\mathbf{k}2}\}, \bar{\psi}_2; t + 2\epsilon | \exp[-2\frac{i}{\hbar}H\epsilon] | \mathbf{X}_0, \{0_{\mathbf{k}}\}, 0; t \rangle \\
& = \int d\mu(\mathbf{X}_1) \exp \left[ A_2 + \sum_{\mathbf{k}\epsilon} \bar{\psi}_2 \bar{z}_{2\mathbf{k}} B_{2\mathbf{k}\epsilon} \sum_{\mathbf{k}\mathbf{l}} \bar{z}_{2\mathbf{k}} \bar{z}_{2\mathbf{l}} C_{2\mathbf{k}\mathbf{l}} + \sum_{j=1}^2 \frac{iM(\mathbf{X}_j - \mathbf{X}_{j-1})^2 \epsilon}{2\epsilon^2 \hbar} \right] \\
& \quad (\text{B.4})
\end{aligned}$$

For definitions of the coefficients see Eq. (B.6) with  $n = 2$ . The 2-step transition amplitude can be generalized to an n-step transition amplitude:

$$\begin{aligned}
& \langle \mathbf{X}_n, \{\bar{z}_{n\mathbf{k}}\}, \bar{\psi}_n; t + n\epsilon | \exp[-\frac{i}{\hbar} \sum_{j=1}^n H_j \epsilon] | \mathbf{X}_0, \{0_{\mathbf{k}}\}, 0; t \rangle \\
& = \int \prod_{j=1}^n d\mu(\mathbf{X}_j) \exp \left[ A_n + \sum_{\mathbf{k}\epsilon} \bar{\psi}_n \bar{z}_{n\mathbf{k}} B_{n\mathbf{k}\epsilon} \right. \\
& \quad \left. + \sum_{\mathbf{k}\mathbf{l}} \bar{z}_{n\mathbf{k}} \bar{z}_{n\mathbf{l}} C_{n\mathbf{k}\mathbf{l}} + \sum_{j=1}^n \frac{iM(\mathbf{X}_j - \mathbf{X}_{j-1})^2 \epsilon}{2\epsilon^2 \hbar} \right] \quad (\text{B.5})
\end{aligned}$$

with the finite difference equations:

$$A_n = A_{n-1} - i\epsilon \sum_{\mathbf{k}} \frac{\lambda^2}{\omega_{\mathbf{k}}} (\mathbf{u}_{\mathbf{nk}}^\dagger \cdot \mathbf{u}_{\mathbf{nk}}) - i\epsilon \sum_{\mathbf{ke}} \frac{\bar{g}_n}{\sqrt{\omega_{\mathbf{k}}}} (\mathbf{p}_{\mathbf{ge}} \cdot \mathbf{u}_{\mathbf{nk}}) B_{n-1, \mathbf{ke}} + O(\epsilon^2) \quad (\text{B.6})$$

$$\begin{aligned} B_{n\mathbf{ke}} &= (1 - i\omega_0\epsilon - i\omega_{\mathbf{k}}\epsilon) B_{n-1, \mathbf{ke}} - i\epsilon \frac{g_n}{\sqrt{\omega_{\mathbf{k}}}} (\mathbf{p}_{\mathbf{eg}} \cdot \mathbf{u}_{\mathbf{nk}}^\dagger) \\ &\quad + i\epsilon \sum_{\mathbf{le}'} \frac{\bar{g}_n}{\sqrt{\omega_{\mathbf{l}}}} (\mathbf{p}_{\mathbf{ge}'} \cdot \mathbf{u}_{\mathbf{nl}}) B_{n-1, \mathbf{le}'} B_{n-1, \mathbf{ke}} \\ &\quad - i\epsilon \sum_{\mathbf{l}} \frac{2\lambda^2}{\sqrt{\omega_{\mathbf{k}}\omega_{\mathbf{l}}}} (\mathbf{u}_{\mathbf{nk}}^\dagger \cdot \mathbf{u}_{\mathbf{nl}}) B_{n-1, \mathbf{le}} \\ &\quad - i\epsilon \sum_{\mathbf{l}} \frac{2g_n}{\sqrt{\omega_{\mathbf{l}}}} (\mathbf{p}_{\mathbf{eg}} \cdot \mathbf{u}_{\mathbf{nl}}) C_{n-1, \mathbf{kl}} + O(\epsilon^2) \end{aligned} \quad (\text{B.7})$$

$$\begin{aligned} C_{n\mathbf{kl}} &= (1 - i\omega_{\mathbf{k}}\epsilon - i\omega_{\mathbf{l}}\epsilon) C_{n-1, \mathbf{kl}} - i\epsilon \frac{\lambda^2}{\sqrt{\omega_{\mathbf{k}}\omega_{\mathbf{l}}}} (\mathbf{u}_{\mathbf{nk}}^\dagger \cdot \mathbf{u}_{\mathbf{nl}}^\dagger) \\ &\quad - i\epsilon \sum_{\mathbf{q}} \frac{2\lambda^2}{\sqrt{\omega_{\mathbf{q}}\omega_{\mathbf{l}}}} (\mathbf{u}_{\mathbf{nl}}^\dagger \cdot \mathbf{u}_{\mathbf{nq}}) C_{n-1, \mathbf{kq}} \\ &\quad - i\epsilon \sum_{\mathbf{q}} \frac{2\lambda^2}{\sqrt{\omega_{\mathbf{q}}\omega_{\mathbf{k}}}} (\mathbf{u}_{\mathbf{nk}}^\dagger \cdot \mathbf{u}_{\mathbf{nq}}) C_{n-1, \mathbf{ql}} \\ &\quad - i\epsilon \sum_{\mathbf{qe}} \frac{2\bar{g}_n}{\sqrt{\omega_{\mathbf{q}}}} (\mathbf{p}_{\mathbf{ge}} \cdot \mathbf{u}_{\mathbf{nq}}) C_{n-1, \mathbf{lq}} B_{n-1, \mathbf{ke}} \\ &\quad - i\epsilon \sum_{\mathbf{e}} \frac{\bar{g}_n}{\sqrt{\omega_{\mathbf{l}}}} (\mathbf{p}_{\mathbf{ge}} \cdot \mathbf{u}_{\mathbf{nl}}^\dagger) B_{n-1, \mathbf{ke}} + O(\epsilon^2) \end{aligned} \quad (\text{B.8})$$

In the continuous limit those become first order differential equations with the following integral solutions:

$$\begin{aligned}
A(t + \tau) = & -i \int_t^{t+\tau} ds \sum_{\mathbf{k}} \frac{\lambda^2}{\omega_{\mathbf{k}}} (\mathbf{u}_{\mathbf{k}}^\dagger(s) \cdot \mathbf{u}_{\mathbf{k}}(s)) \\
& - i \int_t^{t+\tau} ds \sum_{\mathbf{ke}} \frac{\bar{g}}{\sqrt{\omega_{\mathbf{k}}}} (\mathbf{p}_{\text{ge}} \cdot \mathbf{u}_{\mathbf{k}}(s)) B_{\mathbf{ke}}(s) \quad (\text{B.9})
\end{aligned}$$

$$\begin{aligned}
B_{\mathbf{ke}}(t + \tau) = & -i \int_t^{t+\tau} ds \frac{g}{\sqrt{\omega_{\mathbf{k}}}} e^{-i(\omega_0 + \omega_{\mathbf{k}})(t+\tau-s)} (\mathbf{p}_{\text{eg}} \cdot \mathbf{u}_{\mathbf{k}}^\dagger(s)) \\
& + i \int_t^{t+\tau} ds \sum_{\mathbf{le}'} \frac{\bar{g}}{\sqrt{\omega_{\mathbf{l}}}} (\mathbf{p}_{\text{ge}'} \cdot \mathbf{u}_{\mathbf{l}}(s)) B_{\mathbf{le}'}(s) B_{\mathbf{ke}}(s) \\
& - i \int_t^{t+\tau} ds \sum_{\mathbf{l}} \frac{2\lambda^2}{\sqrt{\omega_{\mathbf{k}}\omega_{\mathbf{l}}}} (\mathbf{u}_{\mathbf{k}}^\dagger(s) \cdot \mathbf{u}_{\mathbf{l}}(s)) B_{\mathbf{le}}(s) \\
& - i \int_t^{t+\tau} ds \sum_{\mathbf{l}} \frac{2g}{\sqrt{\omega_{\mathbf{l}}}} (\mathbf{p}_{\text{eg}} \cdot \mathbf{u}_{\mathbf{l}}(s)) C_{\mathbf{kl}}(s) \quad (\text{B.10})
\end{aligned}$$

$$\begin{aligned}
C_{\mathbf{kl}}(t + \tau) = & -i \int_t^{t+\tau} ds \frac{\lambda^2}{\sqrt{\omega_{\mathbf{k}}\omega_{\mathbf{l}}}} (\mathbf{u}_{\mathbf{k}}^\dagger(s) \cdot \mathbf{u}_{\mathbf{l}}^\dagger(s)) \\
& - i \int_t^{t+\tau} ds \sum_{\mathbf{q}} \frac{2\lambda^2}{\sqrt{\omega_{\mathbf{q}}\omega_{\mathbf{l}}}} (\mathbf{u}_{\mathbf{l}}^\dagger(s) \cdot \mathbf{u}_{\mathbf{q}}(s)) C_{\mathbf{kq}}(s) \\
& - i \int_t^{t+\tau} ds \sum_{\mathbf{q}} \frac{2\lambda^2}{\sqrt{\omega_{\mathbf{q}}\omega_{\mathbf{k}}}} (\mathbf{u}_{\mathbf{k}}^\dagger(s) \cdot \mathbf{u}_{\mathbf{q}}(s)) C_{\mathbf{qk}}(s) \\
& - i \int_t^{t+\tau} ds \sum_{\mathbf{qe}} \frac{2\bar{g}}{\sqrt{\omega_{\mathbf{q}}}} (\mathbf{p}_{\text{ge}} \cdot \mathbf{u}_{\mathbf{q}}(s)) C_{\mathbf{lq}}(s) B_{\mathbf{ke}}(s) \\
& - i \sum_e \int_t^{t+\tau} ds \frac{\bar{g}}{\sqrt{\omega_{\mathbf{l}}}} (\mathbf{p}_{\text{ge}} \cdot \mathbf{u}_{\mathbf{l}}^\dagger(s)) B_{\mathbf{ke}}(s) \quad (\text{B.11})
\end{aligned}$$

The transition amplitude of Eq. (B.5) can be further simplified by setting the final EMF and atomic states to vacuum and ground, respectively. The transition

amplitude is then:

$$\begin{aligned} & \langle \mathbf{X}_n, \{0_{\mathbf{k}}\}, 0; t + \tau | \exp[-\frac{i}{\hbar} \int_t^{t+\tau} H ds] | \mathbf{X}_0, \{0_{\mathbf{k}}\}, 0; t \rangle \\ &= \int D\mu(\mathbf{X}(s)) \exp \left[ A(t + \tau) + \int_t^{t+\tau} ds \frac{iM\dot{\mathbf{X}}^2(s)}{2\hbar} \right] \end{aligned} \quad (\text{B.12})$$

The equations for  $B(s)$  and  $C(s)$ , Eq. (B.10) and Eq. (B.11), are Volterra type integral equations. Their solutions are infinite Born series in orders of the coupling. Approximations in the above coefficients are approximations in the basic vertex. To  $O(g^2)$ :

$$\begin{aligned} A(t + \tau) &= -i \int_t^{t+\tau} ds \sum_{\mathbf{k}} \frac{\lambda^2}{\omega_{\mathbf{k}}} [\mathbf{u}_{\mathbf{k}}^\dagger(\mathbf{X}(s)) \cdot \mathbf{u}_{\mathbf{k}}(\mathbf{X}(s))] \\ &\quad - \int_t^{t+\tau} ds \int_t^s dr \sum_{\mathbf{k}e} \frac{g^2}{\omega_{\mathbf{k}}} e^{-i(\omega_{\mathbf{k}} + \omega_0)(s-r)} [\mathbf{u}_{\mathbf{k}}(\mathbf{X}(s)) \cdot \mathbf{p}_{ge}] [\mathbf{u}_{\mathbf{k}}^*(\mathbf{X}(r)) \cdot \mathbf{p}_{eg}] \end{aligned} \quad (\text{B.13})$$

The transition amplitude with an  $O(g^2)$  vertex is thus:

$$\begin{aligned} & \langle \mathbf{X}_f; t + \tau | \exp[-\frac{i}{\hbar} \int_t^{t+\tau} H ds] | \mathbf{X}_i; t \rangle = \\ & \int D\mathbf{X} \exp \left\{ i \int_t^{t+\tau} \left[ \frac{M\dot{\mathbf{X}}^2}{2\hbar} - \sum_{\mathbf{k}} \frac{\lambda^2}{\omega_{\mathbf{k}}} \mathbf{u}_{\mathbf{k}}^*(\mathbf{X}(s)) \cdot \mathbf{u}_{\mathbf{k}}(\mathbf{X}(s)) \right. \right. \\ & \left. \left. + i \int_t^s dr \sum_{\mathbf{k}e} \frac{g^2}{\omega_{\mathbf{k}}} e^{-i(\omega_{\mathbf{k}} + \omega_0)(s-r)} [\mathbf{u}_{\mathbf{k}}(\mathbf{X}(s)) \cdot \mathbf{p}_{ge}] [\mathbf{u}_{\mathbf{k}}^*(\mathbf{X}(r)) \cdot \mathbf{p}_{eg}] \right] ds \right\} \end{aligned} \quad (\text{B.14})$$

In the above transition amplitude the polarization mode functions are dotted with the dipole vector of the atom. The direction that the atom's dipole vector takes will depend on the quantization direction chosen for the atom's internal state, but we are not free to choose a quantization direction. That is because the atom's dipole is induced by the vacuum fluctuations, and is free to

point in any direction. In that light, choosing a particular direction seems invalid. Due to the form of the dipole - EM polarization function couplings, the induced atomic dipoles in different directions do not interfere, and a set of excited states (and thus different quantization directions) can be summed over. Such a set of independent excited states will form a resolution of unity and thus give a factor of unity contribution. The above transition amplitude can then be generalized to reflect the induced dipole:

$$\begin{aligned}
& \langle \mathbf{X}_f; t + \tau | \exp[-\frac{i}{\hbar} \int_t^{t+\tau} H ds] | \mathbf{X}_i; t \rangle \\
&= \int D\mathbf{X} \exp \left\{ i \int_t^{t+\tau} \left[ \frac{M\dot{\mathbf{X}}^2}{2\hbar} - \sum_{\mathbf{k}} \frac{\lambda^2}{\omega_{\mathbf{k}}} \mathbf{u}_{\mathbf{k}}^*(\mathbf{X}(s)) \cdot \mathbf{u}_{\mathbf{k}}(\mathbf{X}(s)) \right. \right. \\
&\quad \left. \left. + i \mathbf{p}_z^2 \int_t^s dr \sum_{\mathbf{k}} \frac{g^2}{\omega_{\mathbf{k}}} e^{-i(\omega_{\mathbf{k}} + \omega_0)(s-r)} \mathbf{u}_{\mathbf{k}}(\mathbf{X}(s)) \cdot \mathbf{u}_{\mathbf{k}}^*(\mathbf{X}(r)) + O(e^4) \right] ds \right\}
\end{aligned} \tag{B.15}$$

with  $\mathbf{p}_z^2 = \langle g | \mathbf{p}_z^2 | g \rangle$  (the ground state expectation value of  $\mathbf{p}_z^2$ ).

## Appendix C

### Momentum computation

Putting in the spatial mode functions of Eq. (3.5) into the above gives the semi-classical transition amplitude in the presence of a conducting wall.

$$\begin{aligned}
K[\mathbf{X}_f; t + \tau, \mathbf{X}_i; t] &= \left( \frac{M}{2\pi i \hbar \tau} \right)^{3/2} \\
&\times \exp \left\{ \frac{iM(\mathbf{X}_f - \mathbf{X}_i)^2}{2\hbar\tau} - \frac{2i\lambda^2}{L^3} \int_t^{t+\tau} ds \sum_{\mathbf{k}} \frac{1}{\omega_{\mathbf{k}}} + O(e^4/M) \right. \\
&\quad + \frac{i\lambda^2}{L^3} \int_t^{t+\tau} ds \sum_{\mathbf{k}} \frac{\cos^2 \theta}{\omega_{\mathbf{k}}} \left[ e^{2i\mathbf{k}_z \cdot \mathbf{X}_c^0(s)} + e^{-2i\mathbf{k}_z \cdot \mathbf{X}_c^0(s)} \right] \\
&\quad - \frac{g^2 \mathbf{P}_z^2}{L^3} \int_t^{t+\tau} ds \int_t^s dr \sum_{\mathbf{k}} \frac{1}{\omega_{\mathbf{k}}} e^{-i(\omega_{\mathbf{k}} + \omega_0)(s-r) + i\mathbf{k}_{\parallel} \cdot (\mathbf{X}_c^0(s) - \mathbf{X}_c^0(r))} \\
&\quad \quad \times \left[ e^{i\mathbf{k}_z \cdot (\mathbf{X}_c^0(s) - \mathbf{X}_c^0(r))} + e^{-i\mathbf{k}_z \cdot (\mathbf{X}_c^0(s) - \mathbf{X}_c^0(r))} \right] \\
&\quad + \frac{g^2 \mathbf{P}_z^2}{L^3} \int_t^{t+\tau} ds \int_t^s dr \sum_{\mathbf{k}} \frac{\cos^2 \theta}{\omega_{\mathbf{k}}} e^{-i(\omega_{\mathbf{k}} + \omega_0)(s-r) + i\mathbf{k}_{\parallel} \cdot (\mathbf{X}_c^0(s) - \mathbf{X}_c^0(r))} \\
&\quad \quad \times \left. \left[ e^{i\mathbf{k}_z \cdot (\mathbf{X}_c^0(s) + \mathbf{X}_c^0(r))} + e^{-i\mathbf{k}_z \cdot (\mathbf{X}_c^0(s) + \mathbf{X}_c^0(r))} \right] \right\} \quad (C.1)
\end{aligned}$$

With the inclusion of the conducting boundary spatial mode functions the sums over momentum space are now over the positive half space. Despite its complicated appearance, the transition amplitude above is in a useful form for computing the evolution of the momentum expectation value. The key point is

that the transition amplitude of Eq. (C.1) is the product of several exponentials of exponentials, and contains only c-numbers. Therefore, each exponential can be expanded out into a series, the summands of all the series collected together, and the necessary integrations performed on the collected summand before redistributing the summand and resumming each exponential. That is, the individual exponentials in Eq. (C.1) can be expanded in terms such as:

$$\begin{aligned} & \exp \left\{ \frac{i\lambda^2}{L^3} \int_t^{t+\tau} ds \sum_{\mathbf{k}} \frac{\cos^2 \theta}{\omega_{\mathbf{k}}} e^{2i\mathbf{k}_z \cdot \mathbf{X}_c^0(s)} \right\} \\ &= \left[ \sum_{n=0}^{\infty} \frac{1}{n!} \left( \frac{i\lambda^2}{L^3} \right)^n \prod_{m=1}^n \int_t^{t+\tau} ds_m \sum_{\mathbf{k}_m} \frac{\cos^2 \theta_m}{\omega_{\mathbf{k}_m}} \right] e^{2i \sum_m \mathbf{k}_{mz} \cdot \mathbf{X}_c^0(s_m)} \end{aligned} \quad (\text{C.2})$$

$$\begin{aligned} & \exp \left\{ -\frac{g^2 \mathbf{P}_z^2}{L^3} \int_t^{t+\tau} ds \int_t^s dr \sum_{\mathbf{k}} \frac{1}{\omega_{\mathbf{k}}} e^{-i(\omega_{\mathbf{k}} + \omega_0)(s-r) + i\mathbf{k} \cdot (\mathbf{X}_c^0(s) - \mathbf{X}_c^0(r))} \right\} \\ &= \left[ \sum_{n=0}^{\infty} \frac{1}{n!} \left( -\frac{g^2 \mathbf{P}_z^2}{L^3} \right)^n \prod_{m=1}^n \int_t^{t+\tau} ds_m \int_t^{s_m} dr_m \sum_{\mathbf{k}_m} \frac{1}{\omega_{\mathbf{k}_m}} e^{-i(\omega_{\mathbf{k}_m} + \omega_0)(s_m - r_m)} \right] \\ & \quad \times e^{i \sum_m \mathbf{k}_m \cdot (\mathbf{X}_c^0(s_m) - \mathbf{X}_c^0(r_m))} \end{aligned} \quad (\text{C.3})$$

The resulting collected summand is,

$$\begin{aligned}
\text{Summand}(\{n\}) = \exp \left\{ 2i \sum_{m_1=1}^{n_1} \mathbf{k}_{m_1 z} \cdot \mathbf{X}_c^0(s_{m_1}) - 2i \sum_{m_2=1}^{n_2} \mathbf{k}_{m_2 z} \cdot \mathbf{X}_c^0(s_{m_2}) \right. \\
+ i \sum_{m_3=1}^{n_3} (\mathbf{k}_{m_3||} + \mathbf{k}_{m_3 z}) \cdot (\mathbf{X}_c^0(s_{m_3}) - \mathbf{X}_c^0(r_{m_3})) \\
+ i \sum_{m_4=1}^{n_4} (\mathbf{k}_{m_4||} - \mathbf{k}_{m_4 z}) \cdot (\mathbf{X}_c^0(s_{m_4}) - \mathbf{X}_c^0(r_{m_4})) \\
+ i \sum_{m_5=1}^{n_5} \mathbf{k}_{m_5||} \cdot (\mathbf{X}_c^0(s_{m_5}) - \mathbf{X}_c^0(r_{m_5})) \\
+ i \sum_{m_5=1}^{n_5} \mathbf{k}_{m_5 z} \cdot (\mathbf{X}_c^0(s_{m_5}) + \mathbf{X}_c^0(r_{m_5})) \\
+ i \sum_{m_6=1}^{n_6} \mathbf{k}_{m_6||} \cdot (\mathbf{X}_c^0(s_{m_6}) - \mathbf{X}_c^0(r_{m_6})) \\
\left. - i \sum_{m_6=1}^{n_6} \mathbf{k}_{m_6 z} \cdot (\mathbf{X}_c^0(s_{m_6}) + \mathbf{X}_c^0(r_{m_6})) \right\} \quad (\text{C.4})
\end{aligned}$$

$$= \exp \left\{ \text{ic}(\{\mathbf{n}\}) \cdot (\mathbf{X}_f - \mathbf{X}_i) + \text{ib}(\{\mathbf{n}\}) \cdot \mathbf{X}_i \right\} \quad (\text{C.5})$$

with definitions

$$\begin{aligned}
\text{c}(\{\mathbf{n}\}) = & 2 \sum_{m_1=1}^{n_1} \mathbf{k}_{m_1 z} \frac{s_{m_1}}{\tau} - 2 \sum_{m_2=1}^{n_2} \mathbf{k}_{m_2 z} \frac{s_{m_2}}{\tau} \\
& + \sum_{m_3=1}^{n_3} (\mathbf{k}_{m_3||} + \mathbf{k}_{m_3 z}) \frac{s_{m_3} - r_{m_3}}{\tau} + \sum_{m_4=1}^{n_4} (\mathbf{k}_{m_4||} - \mathbf{k}_{m_4 z}) \frac{s_{m_4} - r_{m_4}}{\tau} \\
& + \sum_{m_5=1}^{n_5} \mathbf{k}_{m_5||} \frac{s_{m_5} - r_{m_5}}{\tau} + \sum_{m_5=1}^{n_5} \mathbf{k}_{m_5 z} \frac{s_{m_5} + r_{m_5}}{\tau} \\
& + \sum_{m_6=1}^{n_6} \mathbf{k}_{m_6||} \frac{s_{m_6} - r_{m_6}}{\tau} - \sum_{m_6=1}^{n_6} \mathbf{k}_{m_6 z} \frac{s_{m_6} + r_{m_6}}{\tau} \quad (\text{C.6})
\end{aligned}$$

and

$$\text{b}(\{\mathbf{n}\}) = 2 \sum_{m_1=1}^{n_1} \mathbf{k}_{m_1 z} - 2 \sum_{m_2=1}^{n_2} \mathbf{k}_{m_2 z} + 2 \sum_{m_5=1}^{n_5} \mathbf{k}_{m_5 z} - 2 \sum_{m_6=1}^{n_6} \mathbf{k}_{m_6 z} \quad (\text{C.7})$$

The momentum expectation value is then,

$$\begin{aligned}
\mathbf{P}(t + \tau) = & \frac{\hbar}{N} \sum_{\{n, n'\}} \Delta(\{n, n'\}) \int \frac{d\mathbf{P}_f}{(2\pi)^3} \mathbf{P}_f \int d\mathbf{X}_i d\mathbf{X}'_i d\mathbf{X}_f d\mathbf{X}'_f \Psi(\mathbf{X}_i) \Psi^*(\mathbf{X}'_i) \\
& \times \exp \left\{ -i\mathbf{P}_f \cdot \mathbf{X}_f + i\mathbf{P}_f \cdot \mathbf{X}'_f \right\} \\
& \times \exp \left\{ i\mathbf{c}(\{\mathbf{n}\}) \cdot (\mathbf{X}_f - \mathbf{X}_i) + i\mathbf{b}(\{\mathbf{n}\}) \cdot \mathbf{X}_i \right. \\
& \quad \left. - i\mathbf{c}(\{\mathbf{n}'\}) \cdot (\mathbf{X}'_f - \mathbf{X}'_i) - i\mathbf{b}(\{\mathbf{n}'\}) \cdot \mathbf{X}'_i \right\} \quad (\text{C.8})
\end{aligned}$$

The momentum expectation value, the normalization factor, and other moments of the momentum operator can be computed with the generating function:

$$\begin{aligned}
Z(\mathbf{J}) = & \sum_{\{n, n'\}} \Delta(\{n, n'\}) \int \frac{d\mathbf{P}_f}{(2\pi)^3} \int d\mathbf{X}_i d\mathbf{X}'_i d\mathbf{X}_f d\mathbf{X}'_f \Psi(\mathbf{X}_i) \Psi^*(\mathbf{X}'_i) \\
& \times \exp \left\{ -i\mathbf{P}_f \cdot \mathbf{X}_f + i\mathbf{P}_f \cdot \mathbf{X}'_f + i\mathbf{P}_f \cdot \mathbf{J} \right\} \\
& \times \exp \left\{ i\mathbf{c}(\{\mathbf{n}\}) \cdot (\mathbf{X}_f - \mathbf{X}_i) + i\mathbf{b}(\{\mathbf{n}\}) \cdot \mathbf{X}_i \right. \\
& \quad \left. - i\mathbf{c}(\{\mathbf{n}'\}) \cdot (\mathbf{X}'_f - \mathbf{X}'_i) - i\mathbf{b}(\{\mathbf{n}'\}) \cdot \mathbf{X}'_i \right\} \quad (\text{C.9})
\end{aligned}$$

from which:

$$\mathbf{P}(t + \tau) = \left. \frac{\hbar}{iZ(0)} \frac{dZ(\mathbf{J})}{d\mathbf{J}} \right|_{\mathbf{J}=0} \quad (\text{C.10})$$

The factor  $\Delta(\{n, n'\})$  is the summation measure. The initial wavefunction is taken to be a Gaussian centered at  $(\mathbf{R}, \mathbf{P}_0)$  with the standard deviations  $(\sigma, 1/\sigma)$ . This choice allows the possibility that the atom is slowly moving toward the wall. Slowly, in this case, means adiabatically such that the external motion is much

slower than internal time scales.

$$\Psi(\mathbf{X}_i) = \left( \frac{1}{\sqrt{\pi\sigma^2}} \right)^{3/2} \exp \left\{ - \frac{(\mathbf{X}_i - \mathbf{R})^2}{2\sigma^2} + i\mathbf{P}_0 \cdot \mathbf{X}_i \right\} \quad (\text{C.11})$$

In the limits  $M \rightarrow \infty$  and  $\sigma \rightarrow 0$  such that  $\frac{\mathbf{P}_0}{M} \rightarrow \mathbf{V}$  and  $\sigma^2 M \rightarrow \infty$  the generating function is:

$$\begin{aligned} Z(\mathbf{J}) = \exp \left\{ \frac{i\lambda^2}{L^3} \int_t^{t+\tau} ds \sum_{\mathbf{k}} \frac{\cos^2 \theta}{\omega_{\mathbf{k}}} e^{i\mathbf{k}_z \cdot \mathbf{J}} \left[ e^{2i\mathbf{k}_z \cdot (\mathbf{R} + \mathbf{V}s)} - \text{c.c.} \right] \right. \\ \left. - \frac{g^2 \mathbf{p}_z^2}{L^3} \int_t^{t+\tau} ds \int_t^s dr \sum_{\mathbf{k}} \frac{1}{\omega_{\mathbf{k}}} \left[ e^{-i(\omega_{\mathbf{k}} + \omega_0)(s-r) + i\mathbf{k} \cdot \mathbf{V}(s-r)} + \text{c.c.} \right] \right. \\ \left. + \frac{g^2 \mathbf{p}_z^2}{L^3} \int_t^{t+\tau} ds \int_t^s dr \sum_{\mathbf{k}} \frac{\cos^2 \theta}{\omega_{\mathbf{k}}} e^{i\mathbf{k}_z \cdot \mathbf{J}} \right. \\ \left. \left[ e^{-i(\omega_{\mathbf{k}} + \omega_0)(s-r) + i\mathbf{k}_z \cdot (2\mathbf{R} + \mathbf{V}(s+r-2t)) + i\mathbf{k}_{\parallel} \cdot \mathbf{V}(s-r)} + \text{c.c.} \right] \right. \\ \left. - \frac{\mathbf{J}^2}{4\sigma^2} + i\mathbf{J} \cdot \mathbf{P}_0 + O(e^4/M) + O(\sigma^2) \right\} \quad (\text{C.12}) \end{aligned}$$

Finally, in the limits  $M \rightarrow \infty$  and  $\sigma \rightarrow 0$  the momentum expectation value is:

$$\begin{aligned} \mathbf{P}(t + \tau) = \mathbf{P}_0 - \frac{2i\lambda^2 \hbar}{L^3} \sum_{\mathbf{k}} \frac{\mathbf{k}_z \cos^2 \theta}{\omega_{\mathbf{k}}} \int_t^{t+\tau} ds e^{-2i\mathbf{k}_z \cdot (\mathbf{R} + \mathbf{V}s)} \\ + \frac{g^2 \mathbf{p}_z^2 \hbar}{L^3} \sum_{\mathbf{k}} \frac{\mathbf{k}_z \cos^2 \theta}{\omega_{\mathbf{k}}} \int_t^{t+\tau} ds \int_t^s dr e^{-i\mathbf{k}_z \cdot (2\mathbf{R} + \mathbf{V}(s+r-2t))} \\ \left[ e^{-i(\omega_{\mathbf{k}} + \omega_0)(s-r)} - e^{i(\omega_{\mathbf{k}} + \omega_0)(s-r)} \right] \quad (\text{C.13}) \end{aligned}$$

## Appendix D

### Calculational details of qubit in a thermal bath

#### D.1 Approximated functional solutions

Eqs. (4.14-4.19) are two sets of coupled differential equations. One set being the pair of equations

$$\dot{F}[m_k] = -i \sum_q m_q \omega_q F[m_k] + i \sum_{lp} m_l \bar{\lambda}_l G_p[m_k - \delta_{kl}] \quad (\text{D.1})$$

$$\dot{G}_p[m_k] = -i(\omega_o + \sum m \omega) G_p[m_k] + i \lambda_p F[m_k + \delta_{kp}] \quad (\text{D.2})$$

and the remaining four equations comprising the other set. This solution method for this pair in the low temperature and weak coupling limits will be sketched out in this appendix. The solutions for the other set in the same limits will follow a similar sequence. First, given the initial conditions

$$F[m_k](t=0) = 1 \quad (\text{D.3})$$

$$G_p[m_k](t=0) = 0 \quad (\text{D.4})$$

the Laplace transforms of the above equations are

$$z\tilde{F}[m_k](z) - 1 = -i \sum_q m_q \omega_q \tilde{F}[m_k](z) + i \sum_{lp} m_l \bar{\lambda}_l \tilde{G}_p[m_k - \delta_{kl}](z) \quad (\text{D.5})$$

$$z\tilde{G}_p[m_k](z) = -i(\omega_o + \sum m\omega) \tilde{G}_p[m_k](z) + i\lambda_p \tilde{F}[m_k + \delta_{kp}](z). \quad (\text{D.6})$$

The second equation can be rearranged into

$$\tilde{G}_p[m_k](z) = \frac{i\lambda_p \tilde{F}[m_k + \delta_{kp}](z)}{z + i(\omega_o + \sum m\omega)}, \quad (\text{D.7})$$

which can be substituted back into Eq. (D.5) to give

$$\left( z + i \sum_q m_q \omega_q \right) \tilde{F}[m_k](z) = 1 + i \sum_{lp} \frac{im_l \bar{\lambda}_l \lambda_p \tilde{F}[m_k - \delta_{kl} + \delta_{kp}](z)}{z + i(\omega_o - \omega_l + \sum m\omega)}. \quad (\text{D.8})$$

In this expression the low temperature approximation is applied by setting  $p = l$  in the summation of the RHS. The justification is that the summation on the RHS will be peaked about  $\omega_l = \omega_o$  such that the greatest contribution from  $\tilde{F}[m_k - \delta_{kl} + \delta_{kp}](z)$  will be for  $\omega_l = \omega_o$ . However, at low temperatures those frequencies will not be populated. As a result the vacuum will be annihilated, unless  $\delta_{kp} = \delta_{kl}$ , which will cause the major contribution from the  $p$  summation to be from  $p = l$ . Applying this approximation, Eq. (D.8) can be rewritten as

$$\tilde{F}[m_k](z) = \left( z + i \sum_q m_q \omega_q + \sum_l \frac{m_l \lambda_l^2}{z + i(\omega_o - \omega_l + \sum m\omega)} \right)^{-1}. \quad (\text{D.9})$$

The zero<sup>th</sup> order pole of  $\tilde{F}[m_k](z)$  is at  $z = -i \sum m\omega$ . Evaluating the reaction term at this point,

$$\begin{aligned} \lim_{z \rightarrow -i \sum m\omega} \left( \sum_l \frac{m_l \lambda_l^2}{z + i(\omega_o - \omega_l + \sum m\omega)} \right) &= \lim_{z \rightarrow 0} \left( \sum_l \frac{m_l \lambda_l^2}{z + i(\omega_o - \omega_l)} \right) \\ &= \sum_l \frac{m_l \lambda_l^2}{\omega_l} \left( \delta(\omega_o - \omega_l) + P \frac{1}{\omega_o - \omega_l} \right) \\ &= \frac{\Gamma m_o}{2} + i\Delta. \end{aligned} \quad (\text{D.10})$$

gives the second order shift in the pole of a real part and a frequency shift. After absorbing the frequency shift in a renormalization of the frequency, the second order pole is  $z = -i \sum m\omega - \frac{\Gamma m_o}{2}$  with the definitions

$$m_o = \sum_{\omega_l = \omega_o} m_l \quad (\text{D.11})$$

The desired functional can be calculated as in inverse Laplace transform of Eq. (D.9) at the second order pole to give

$$F[m_k](t) = \exp \left\{ -\frac{\Gamma m_o}{2} t - i \sum m\omega t \right\}. \quad (\text{D.12})$$

The other functional in the pair can be calculated by integrating Eq. (4.15)

$$G_l[m_k - \delta_{kl}](t) = i \frac{\lambda}{\sqrt{\omega_l}} \frac{1 - \exp \left\{ -\frac{\Gamma m_o}{2} t - i \sum m\omega t \right\}}{\frac{\Gamma m_o}{2} + i(\omega_l - \omega_o)} e^{i(\omega_l - \omega_o - \sum m\omega)t}. \quad (\text{D.13})$$

Following similar calculations the rest of the functionals are found to be

$$\Psi^f[m_k](t) = \exp \left\{ -\frac{\Gamma(m_o + 1)}{2}t - i(\omega_o + \sum m\omega)t \right\} \quad (\text{D.14})$$

$$\Psi_l^g[m_k - \delta_{kl}](t) = \frac{\lambda \exp \left\{ -\frac{\Gamma}{2}t - i(\omega_o + \sum m\omega)t \right\}}{\sqrt{\omega_l}(\omega_l - \omega_o - i\frac{\Gamma m_o}{2})} \left[ e^{i(\omega_l - \omega_o)t} - e^{-\frac{\Gamma m_o}{2}t} \right] \quad (\text{D.15})$$

$$\Psi_q^f[m_k](t) = \frac{\lambda \exp \left\{ -\frac{\Gamma m_o}{2}t - i(\omega_o + \sum m\omega)t \right\}}{\sqrt{\omega_q}(\omega_q - \omega_o - i\frac{\Gamma}{2})} \left[ e^{-\frac{\Gamma}{2}t} - e^{i(\omega_q - \omega_o)t} \right] \quad (\text{D.16})$$

$$\begin{aligned} \Psi_{ql}^g[m_k - \delta_{kl}](t) &= \frac{\lambda^2 \exp \left\{ -i(\omega_o + \omega_q - \omega_l + \sum m\omega)t \right\}}{\sqrt{\omega_q}\sqrt{\omega_l}} \\ &\quad \times \frac{\exp \left\{ -\frac{\Gamma}{2}t + i(\omega_q - \omega_o)t \right\} - 1}{(\omega_q - \omega_o) + i\frac{\Gamma}{2}} \\ &\quad \times \frac{1 - \exp \left\{ -\frac{\Gamma m_o}{2}t - i(\omega_l - \omega_o)t \right\}}{(\omega_l - \omega_o) - i\frac{\Gamma m_o}{2}} \end{aligned} \quad (\text{D.17})$$

## D.2 Computation of density matrix elements

The solutions of Eqs. (D.12-D.17) can be substituted into Eqs. (4.24-4.27) to evaluate the reduced density matrix elements in the limits of low temperature and weak coupling. The reduced density matrix elements in that form are summations over all distributions  $\{m_k\}$ . The  $\rho_{10}(t)$  matrix element will be demonstrated below as a representative calculation. The evaluation of the other summations follow along similar lines. From Eq. (4.26), the off-diagonal density matrix element is

$$\rho_{10}(t) = \rho_{10} \sum_{\{m_k\}} \left( \Psi^f[m_k] + \sum_l m_l \Phi_{ll}^g[m_k - \delta_{kl}] \right) \bar{F}'[m_k] e^{-\beta \sum m\omega}. \quad (\text{D.18})$$

First, from Eqs. (D.12-D.17) the functional in parentheses can be determined to be

$$\Psi^f[m_k] + \sum_l m_l \Phi_{ll}^g[m_k - \delta_{kl}] = \exp \left\{ -\frac{\Gamma(m_o + 1)}{2} t - i(\omega_o + \sum m\omega)t \right\}, \quad (\text{D.19})$$

so that the off-diagonal matrix element becomes

$$\rho_{10}(t) = \rho_{10} \sum_{\{m_k\}} \exp \left\{ -\frac{\Gamma(2m_o + 1)}{2} t - i\omega_o t \right\} e^{-\beta \sum m\omega}. \quad (\text{D.20})$$

Denoting by primes those terms for which  $\omega_k = \omega_o$  and double primes those for which  $\omega_k \neq \omega_o$ , the summand can be rewritten with the substitution

$$m_o = \sum'_k m_k,$$

$$\rho_{10}(t) = \rho_{10} e^{\frac{\Gamma}{2}t - i\omega_o t} \sum_{\{m_k\}} \exp \left\{ -\Gamma t \sum'_k m_k - \beta \omega_k \sum m_k \right\} \quad (\text{D.21})$$

$$= \rho_{10} e^{\frac{\Gamma}{2}t - i\omega_o t} \sum_{\{m_k\}} \prod'_k \exp \{ -(\Gamma t + \beta \omega_o) m_k \} \prod''_k \exp \{ -\beta \omega_k m_k \}. \quad (\text{D.22})$$

The summation over distributions can be more clearly written as

$$\sum_{\{m_k\}} = \left[ \prod_k \sum_{m_k=0}^{\infty} \right] = \left[ \prod'_k \sum_{m_k=0}^{\infty} \right] \left[ \prod''_k \sum_{m_k=0}^{\infty} \right], \quad (\text{D.23})$$

so that Eq. (D.22) becomes

$$\rho_{10}(t) = \rho_{10} e^{\frac{\Gamma}{2}t - i\omega_o t} \left[ \prod'_k \sum_{m_k=0}^{\infty} \exp\{-(\Gamma t + \beta\omega_o)m_k\} \right] \left[ \prod''_k \sum_{m_k=0}^{\infty} \exp\{-\beta\omega_k m_k\} \right] \quad (\text{D.24})$$

$$= \rho_{10} e^{\frac{\Gamma}{2}t - i\omega_o t} \left[ \prod'_k \frac{1}{1 - \exp\{-(\Gamma t + \beta\omega_o)\}} \right] \left[ \prod''_k \frac{1}{1 - \exp\{-\beta\omega_k\}} \right] \quad (\text{D.25})$$

$$= \rho_{10} e^{\frac{\Gamma}{2}t - i\omega_o t} \exp \left\{ - \sum'_k \ln [1 - e^{-(\Gamma t + \beta\omega_o)}] - \sum''_k \ln [1 - e^{-\beta\omega_k}] \right\} \quad (\text{D.26})$$

$$= \rho_{10} e^{\frac{\Gamma}{2}t - i\omega_o t} \exp \left\{ - \sum'_k \ln \left[ \frac{1 - e^{-(\Gamma t + \beta\omega_o)}}{1 - e^{-\beta\omega_o}} \right] - \sum''_k \ln [1 - e^{-\beta\omega_k}] \right\} \quad (\text{D.27})$$

$$= \rho_{10} e^{\frac{\Gamma}{2}t - i\omega_o t} \left( \frac{1 - e^{-\beta\omega_o}}{1 - e^{-(\Gamma t + \beta\omega_o)}} \right) \exp \left\{ - \sum''_k \ln [1 - e^{-\beta\omega_k}] \right\} \quad (\text{D.28})$$

The factor at the end is removed by normalization of the reduced matrix element by its  $\Gamma = 0$  value. The final result for the off-diagonal matrix element is

$$\rho_{10}(t) = \rho_{10} e^{\frac{\Gamma}{2}t - i\omega_o t} \left( \frac{1 - e^{-\beta\omega_o}}{1 - e^{-(\Gamma t + \beta\omega_o)}} \right) \quad (\text{D.29})$$

with  $\Gamma/2$  the zero temperature decoherence rate. The rest of the reduced density matrix elements are given in Chapter 4.

## Appendix E

### COM functional integration

The position path integral which needs to be evaluated is:

$$\begin{aligned} & \int D\mathbf{X} \exp \left[ -\frac{iM}{2} \int_0^t ds \dot{\mathbf{X}} \right] \\ & \times \exp \left[ -i \int_0^t ds \sum_{\mathbf{k}} \bar{g}_{\mathbf{k}}(\mathbf{X}(s)) e^{-i\omega_{\mathbf{k}}(t-s)} \bar{z}_{f\mathbf{k}} \eta(s) \right. \\ & \quad \left. - \int_0^t ds \int_0^s dr \sum_{\mathbf{k}} g_{\mathbf{k}}(\mathbf{X}(s)) \bar{g}_{\mathbf{k}}(\mathbf{X}(r)) e^{-i\omega_{\mathbf{k}}(s-r)} \bar{\eta}(s) \eta(r) \right] \end{aligned} \quad (\text{E.1})$$

which can be expanded and truncated to:

$$\begin{aligned} & \int D\mathbf{X} \exp \left[ -\frac{iM}{2} \int_0^t ds \dot{\mathbf{X}} \right] \\ & \times \left[ 1 - i \int_0^t ds \sum_{\mathbf{k}} \bar{g}_{\mathbf{k}}(\mathbf{X}(s)) e^{-i\omega_{\mathbf{k}}(t-s)} \bar{z}_{f\mathbf{k}} \eta(s) \right. \\ & \quad \left. - \int_0^t ds \int_0^s dr \sum_{\mathbf{k}} g_{\mathbf{k}}(\mathbf{X}(s)) \bar{g}_{\mathbf{k}}(\mathbf{X}(r)) e^{-i\omega_{\mathbf{k}}(s-r)} \bar{\eta}(s) \eta(r) \right] \end{aligned} \quad (\text{E.2})$$

There are thus three correlation functions which need to be computed.

First the spatial mode functions must be chosen in order to specify the targeted correlation functions. For an electromagnetic field in free space (no cavity or boundaries)

$$g_{\mathbf{k}}(\mathbf{X}) = \frac{\lambda}{\sqrt{\omega_{\mathbf{k}}}} \exp(i\mathbf{k} \cdot \mathbf{X}), \quad (\text{E.3})$$

the correlations functions are:

$$\int_{\mathbf{X}_{i,0}}^{\mathbf{X}_{f,t}} D\mathbf{X} \exp\left[-\frac{iM}{2} \int_0^t d\tau \dot{\mathbf{X}}(\tau)\right] = \left(\frac{M}{2\pi it}\right)^{3/2} \exp\left[\frac{iM}{2t}(\mathbf{X}_f - \mathbf{X}_i)^2\right] \quad (\text{E.4})$$

$$\begin{aligned} & \int_{\mathbf{X}_{i,0}}^{\mathbf{X}_{f,t}} D\mathbf{X} \exp\left[\mathbf{i}\mathbf{k} \cdot \mathbf{X}(s) - \frac{iM}{2} \int_0^t d\tau \dot{\mathbf{X}}(\tau)\right] \\ &= \left(\frac{M}{2\pi it}\right)^{3/2} \exp\left[\frac{iM}{2t}(\mathbf{X}_f - \mathbf{X}_i)^2 + \mathbf{i}\frac{s}{t}\mathbf{k} \cdot (\mathbf{X}_f - \mathbf{X}_i) - \frac{i}{2M} \frac{s(t-s)}{t} \mathbf{k}^2\right] \end{aligned} \quad (\text{E.5})$$

$$\begin{aligned} & \int_{\mathbf{X}_{i,0}}^{\mathbf{X}_{f,t}} D\mathbf{X} \exp\left[-\mathbf{i}\mathbf{k} \cdot \mathbf{X}(s) + \mathbf{i}\mathbf{k} \cdot \mathbf{X}(r) - \frac{iM}{2} \int_0^t d\tau \dot{\mathbf{X}}(\tau)\right] \\ &= \left(\frac{M}{2\pi it}\right)^{3/2} \exp\left[\frac{iM}{2t}(\mathbf{X}_f - \mathbf{X}_i)^2 - \mathbf{i}\frac{s-r}{t}\mathbf{k} \cdot (\mathbf{X}_f - \mathbf{X}_i) \right. \\ & \quad \left. - \frac{i}{2M} \frac{(t-(s-r))(s-r)}{t} \mathbf{k}^2\right] \end{aligned} \quad (\text{E.6})$$

Substituting these expressions back into the Eq.(5.10) gives for the transition amplitude:

$$\begin{aligned} K(t, 0) = & \int D\bar{\eta}D\eta e^{i\omega_0 t/2} \left(\frac{M}{2\pi it}\right)^{3/2} \\ & \times \exp\left[\bar{\eta}_f \eta(t) - \int_0^t (\bar{\eta}\dot{\eta} + i\omega_0 \bar{\eta}\eta) ds\right] \exp\left[\frac{iM}{2t}(\mathbf{X}_f - \mathbf{X}_i)^2\right] e^{-i\omega_{\mathbf{k}}(s-r)} \\ & \times \left[1 - \mathbf{i} \int_0^t ds \sum_{\mathbf{k}} \frac{\lambda}{\sqrt{\omega_{\mathbf{k}}}} \exp\left[\mathbf{i}\frac{s}{t}\mathbf{k} \cdot (\mathbf{X}_f - \mathbf{X}_i) - \frac{i}{2M} \frac{s(t-s)}{t} \mathbf{k}^2\right] e^{-i\omega_{\mathbf{k}}(t-s)} \bar{z}_{f\mathbf{k}} \eta(s) \right. \\ & \left. - \int_0^t ds \int_0^s dr \sum_{\mathbf{k}} \frac{\lambda^2}{\omega_{\mathbf{k}}} \exp\left[-\mathbf{i}\frac{s-r}{t}\mathbf{k} \cdot (\mathbf{X}_f - \mathbf{X}_i) \right. \right. \\ & \quad \left. \left. - \frac{i}{2M} \frac{(t-(s-r))(s-r)}{t} \mathbf{k}^2\right] \bar{\eta}(s)\eta(r)\right] \end{aligned} \quad (\text{E.7})$$

# BIBLIOGRAPHY

- [1] Shresta S, Hu B L, and Phillips N G, Phys. Rev. A in preparation, quant-ph/0302004.
- [2] Shresta S, Dragulescu A, Anastopoulos C, and Hu B L, University of Maryland Physics Preprint 03-012.
- [3] Shresta S and Hu B L, Phys. Rev. A 68, 012110 (2003).
- [4] H. B. G. Casimir and D. Polder, Phys. Rev. 73, 360 (1948).
- [5] C. I. Sukenik, M. G. Boshier, D. Cho, V. Sandoghar, and E. A. Hinds, Phys. Rev. Lett. 70 5 560 (1993).
- [6] A. Landragin, J. -Y. Courtois, G. Labeyrie, N. Vansteenkiste, C. I. Westbrook, and A. Aspect, Phys. Rev. Lett. 77 8 1464 (1996).
- [7] Yu. B. Ovchinnikov, I. Manek, and R. Grimm, Phys. Rev. Lett. 79 2225 (1997); M. Hammes, D. Rychtarik, and R. Grimm, C. R. Acad. Sci. Paris, t. 2 IV 625 (2001); S. K. Sekatskii, B. Reido, and G. Dietler, Opt. Comm. 195 197 (2001); P. Domokos and H. Tirsch, Europhys. Lett. 54 305 (2001);

- J. P. Burke Jr., S. -T. Chu, G. W. Bryant, C. J. Williams, and P. S. Julienne, Phys. Rev. A 65 043411 (2002).
- [8] G. Birkl, F. B. J. Buchkremer, R. Dumke, and W. Ertmer, Opt. Comm. 191 67 (2001).
- [9] J. Denschlag, G. Umshaus, and J. Schmiedmayer, Phys. Rev. Lett. 81 737 (1998).
- [10] C. Cohen-Tannoudji, *Atomic Motion in Laser Light* eds. J. Dalibard, J. M. Ramond, and J. Zinn-Justin Les Houches, Session LIII, 1990 (Elsevier Science 1991).
- [11] Carmichael H J *Statistical Methods in Quantum Optics 1: Master equations and Fokker-Planck Equations* (Springer Berlin, 1999).
- [12] C. Anastopoulos and B. L. Hu, Phys. Rev. A 62, 033821 (2000).
- [13] J. P. Barnes and W. S. Warren, Phys. Rev. A 60 4363 (1999).
- [14] J. Gea-Banacloche, Phys. Rev. A 65 022308 (2002).
- [15] S. J. van Enk and H. J. Kimble, Quant. Inf. and Comp. 2 1 (2002).
- [16] W. H. Louisell, *Quantum Statistical Properties of Radiation* (J Wiley and Sons, 1973).
- [17] D. F. Walls and G. J. Milburn, *Quantum Optics* (Springer Verlag, Berlin, 1994).

- [18] C. Cohen-Tannoudji, J. Dupont-Roc, and G. Grynberg, *Atom-Photon Interactions: Basic Processes and Applications* (J Wiley and Sons, 1992).
- [19] O. Scully and M. Suhail Zubairy, *Quantum Optics* (Cambridge University Press, Cambridge, 1997).
- [20] C.W. Gardiner and P. Zoller, *Quantum Noise* (Springer Verlag, Berlin, 2000).
- [21] N. G. van Kampen, *Stochastic Processes in Physics and Chemistry* (Elsevier Science B. V., Amsterdam, 2003).
- [22] F. Haake, *Z. Physik* 223 353 (1969).
- [23] A. O. Caldeira and A. J. Leggett, *Ann. Phys.* 149 374 (1983).
- [24] K. Lindenberg and B. West, *Phys. Rev. A* 30 568 (1984).
- [25] H. Grabert, P. Schramm, and G. -L. Ingold, *Phys. Rep.* 168 115 (1988).
- [26] H. Kleinert, *Path Integrals in Quantum Mechanics, Statistics, and Polymer Physics* (World Scientific, Singapore, 1990).
- [27] L. S. Schulman, *Techniques and Applications of Path Integration* (J. Wiley and Sons, New York, 1981).
- [28] I. M. Gelfand and A. M. Yaglom, *J. Math Phys.* 1 48 (1960).

- [29] Y. Ohnuki and T. Kashiwa *Coherent States of fermi operators and the path integral* eds. J. Klauder and B. Skagerstam Coherent states: applications in physics and mathematical physics (Singapore: World Scientific 1978).
- [30] K. E. Cahill and R. J. Glauber, Phys. Rev. A 59 2 1538 (1999).
- [31] A. Perelomov *Generalized coherent states and their applications* (Berlin: Springer 1986).
- [32] W.-M. Zhang, D. H. Feng, and R. Gilmore, Rev. Mod. Phys. 62 867 (1990).
- [33] A. Alscher and H. Grabert, J. Phys. A 32 4907 (1999).
- [34] A. Alscher and H. Grabert, Euro. Phys. D 14 127 (2001).
- [35] T. Boudjeda, T. F. Hammann and Kh. Nouicer, J. Math. Phys. 36 4 1602 (1995).
- [36] V. R. Vieira, Phys. Rev. B 39 7174 (1989).
- [37] V. V. Smirnov, J. Phys. A 32 1285 (1999).
- [38] P. W. Milonni, *The Quantum Vacuum: An Introduction to Quantum Electrodynamics* (Academic Press, 1994).
- [39] G. Barton, Proc. R. Soc. Lond A 410, 141 (1987).
- [40] J. M. Wylie and J. E. Sipe, Phys. Rev. A 30, 1185 (1984).
- [41] S. -T. Wu and C. Eberlein, Proc. R. Soc. Lond A 455, 2487 (1999).

- [42] P. W. Milonni, Phys. Rev. A 25, 1315 (1982).
- [43] N. D. Birrell and P. C. W. Davies *Quantum Fields in Curved Space*  
(Cambridge, 1982).
- [44] L. Parker and S. A. Fulling, Phys. Rev. D 9, 341 (1974).
- [45] B. L. Hu, Phys. Rev. D 9, 3263 (1974).
- [46] S. A. Fulling, L. Parker, and B. L. Hu, Phys. Rev. D 10, 3905 (1974).
- [47] R. Passante, G. Compagno, and F. Persico, Phys. Rev. A 31, 2827 (1985);  
R. Passante, G. Compagno, and F. Persico, Fortschr. Phys. 51, 219 (2003).
- [48] G. Compagno and D. Valenti, J. Phys. B: At. Mol. Opt. Phys. 32, 4705  
(1999).
- [49] G. Compagno and D. Valenti, Phys. Rev. A 65, 032106 (2002).
- [50] G. Compagno, R. Passante and F. Persico, *Atom-Field Interactions and  
Dressed Atoms* (Cambridge University, Cambridge, 1995).
- [51] C. Baxter, M. Babiker, and R. Loudon, J. Mod. Opt. 37, 685 (1990); C.  
Baxter, M. Babiker, and R. Loudon, Phys. Rev. A 47, 1278 (1993); V. E.  
Lembessis, C. Baxter, M. Babiker, and R. Loudon, Phys. Rev. A 48, 1594  
(1993).
- [52] Martin Wilkens, Phys. Rev. A 47 671; Martin Wilkens, Phys. Rev. A 48  
570.

- [53] L. G. Boussiakou, C. R. Bennett, and M. Babiker, *Phys. Lett.* 89, 123001 (2002).
- [54] A. J. Leggett, S. Chakravarty, A. T. Dorsey, M. P. A. Fisher, A. Garg, and W. Zwerger, *Rev. Mod. Phys.* 59, 1 (1987).
- [55] G. S. Agarwal, *Phys. Rev. A* 4, 1778 (1971); G. S. Agarwal, *Phys. Rev. A* 7, 1195 (1973).
- [56] K. Zaheer and M. S. Zubairy, *Phys. Rev. A* 37, 1628 (1988).
- [57] C. Cohen-Tannoudji and W. D. Phillips, *Physics Today* 43 10, 33 (1990).
- [58] W. D. Phillips, *Rev. Mod. Phys.* 70, 21 (1998).
- [59] C. Cohen-Tannoudji, *Rev. Mod. Phys.* 70, 707 (1998).
- [60] G. K. Brennen, C. M. Caves, P. S. Jessen, and I. H. Deutsch, *Phys. Rev. Lett.* 82, 1060 (1999).
- [61] T. Calarco, H. -J. Briegel, D. Jaksch, J. I. Cirac, and P. Zoller, *Fortschr. Phys.* 48 9-11, 945 (2000).
- [62] I. H. Deutsch and G. K. Brennen, *Fortschr. Phys.* 48 9-11, 925 (2000).
- [63] G. J. Milburn, *Fortschr. Phys.* 48 9-11, 957 (2000).
- [64] D. Jaksch, H. -J. Briegel, J. I. Cirac, C. W. Gardiner, and P. Zoller, *Phys. Rev. Lett.* 82, 1975 (1999).

- [65] G. Brennen, I. H. Deutsch, and C. J. Williams, Phys. Rev. A 65, 022313 (2002).
- [66] J. F. Poyatos, J. I. Cirac, and P. Zoller, Fortschr. Phys. 48 9-11, 785 (2000).
- [67] B. Dubetsky and P. R. Berman, Phys. Rev. A 53, 390 (1996).
- [68] M. Wilkens, Z. Bialynicka-Birula, and P. Meystre, Phys. Rev. A 45, 477 (1992).
- [69] W. Ren and H. J. Carmichael, Phys. Rev. A 51, 752 (1995).
- [70] D. W. Vernooy and H. J. Kimble, Phys. Rev. A 56, 4287 (1997).
- [71] Robert Graham, Daniel F. Walls, and Peter Zoller, Phys. Rev. A 45, 5018 (1992).
- [72] A. Anderson and J. J. Halliwell, Phys. Rev. D 48, 2753 (1993); C. Anastopoulos and J. J. Halliwell, Phys. Rev. D 51, 6870 (1995); C. Anastopoulos, Phys. Rev. E 53, 4711 (1996).
- [73] R. P. Feynman and A. R. Hibbs, *Quantum Mechanics and Path Integrals* (McGraw-Hill, New York, 1965) ; R. P. Feynman and F. L. Vernon, Ann. Phys. 24, 118 (1963).
- [74] J. Schwinger, J. Math. Phys. 2 (1961) 407; L. V. Keldysh, Zh. Eksp. Teor. Fiz. 47 , 1515 (1964) [Engl. trans. Sov. Phys. JEPT 20, 1018 (1965)]. G. Zhou, Z. B. Su, B. Hao and L. Yu, Phys. Rep. 118, 1 (1985); Z. Su, L. Y.

Chen, X. Yu and K. C. Chou, Phys. Rev. B37, 9810 (1988). E. Calzetta and B. L. Hu, Phys. Rev. D40, 656 (1989).

[75] M. Weissbluth, *Photon-Atom Interactions* (Academic Press, San Diego, 1988).

[76] B. W. Shore, P. Meystre, and S. Stenholm, J. Opt. Soc. Am. B 8, 903 (1991).

[77] B. Lev, Y. Lassailly, L. Chungsook, A. Scherer, and H. Mabuchi, App. Phy. Lett. 83, 395 (2003).

[78] P. Grangier, G. Reymond, N. Schlosser, Fortschr. Phys. 48 859-874 (2000).

